



## Micro fabrication of biodegradable polymer drug delivery devices

**Nagstrup, Johan**

*Publication date:*  
2013

*Document Version*  
Publisher's PDF, also known as Version of record

[Link back to DTU Orbit](#)

*Citation (APA):*  
Nagstrup, J. (2013). *Micro fabrication of biodegradable polymer drug delivery devices*. Technical University of Denmark.

---

### General rights

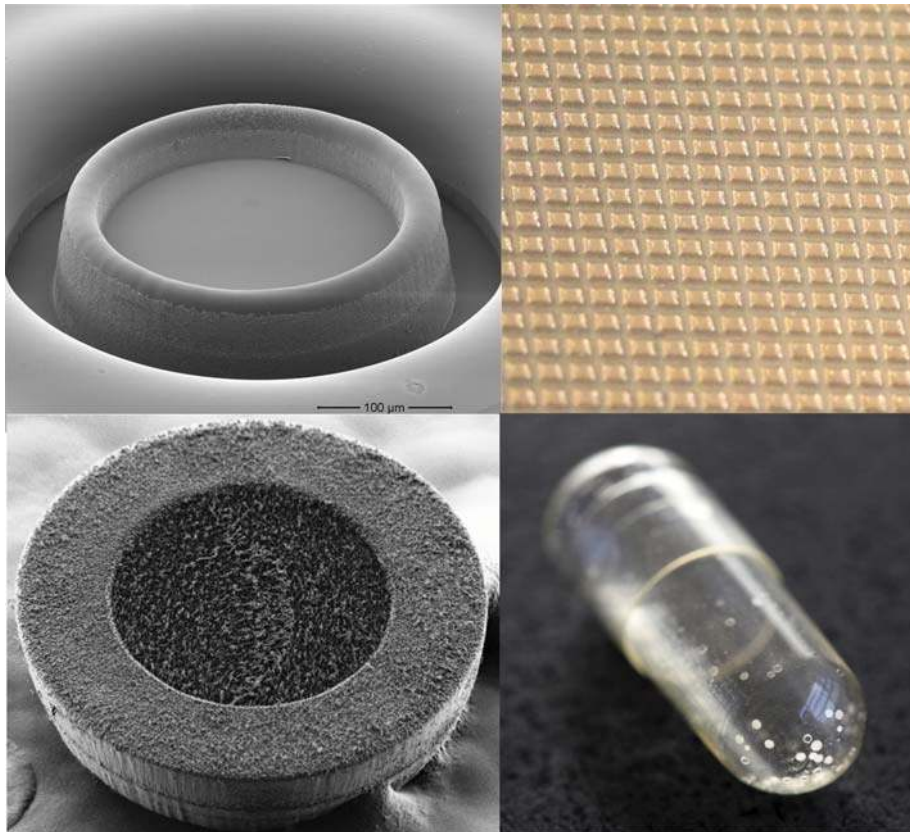
Copyright and moral rights for the publications made accessible in the public portal are retained by the authors and/or other copyright owners and it is a condition of accessing publications that users recognise and abide by the legal requirements associated with these rights.

- Users may download and print one copy of any publication from the public portal for the purpose of private study or research.
- You may not further distribute the material or use it for any profit-making activity or commercial gain
- You may freely distribute the URL identifying the publication in the public portal

If you believe that this document breaches copyright please contact us providing details, and we will remove access to the work immediately and investigate your claim.

Ph.D Thesis

# Micro fabrication of biodegradable polymer drug delivery devices.



Johan Nagstrup

January 2013

DTU Nanotech - Department of Micro- and Nanotechnology  
Technical University of Denmark



## Abstract

The pharmaceutical industry is presently facing several obstacles in developing oral drug delivery systems. This is primarily due to the nature of the discovered drug candidates. The discovered drugs often have poor solubility and low permeability across the gastro intestinal epithelium. Furthermore, they are often degraded before they can be absorbed. The result is low bioavailability of the drugs. To overcome these challenges, better drug delivery systems need to be developed. Recently, micro systems have emerged as promising candidates to solve the challenges of poor solubility, low permeability and degradation. These systems are for the majority based on traditional materials used in micro technology, such as SU-8, silicon, poly(methyl methacrylate). The next step in developing these new drug delivery systems is to replace classical micro fabrication materials with biodegradable polymers. In order to successfully do this, methods for fabricating micro structures in biodegradable polymers need to be developed.

The goal of this project has been to develop methods for micro fabrication in biodegradable polymers and to use these methods to produce micro systems for oral drug delivery. This has successfully been achieved by fabrication of micro container systems made of poly(L-lactic acid) and polycaprolactone.

To achieve this, polymer solutions have been developed using the theory of Hansen's solubility parameters. The solutions are used to fabricate polymer films by spin coating, which are used in the fabrication of micro devices for oral drug delivery. Films consisting of both polymer and pharmaceuticals have also been developed by spin coating. A deep reactive ion etch producing sloped sidewalls for stamp production has been developed. The sloped sidewalls ensure a successful separation of stamp and film after patterning. Large scale methods for filling of micro reservoirs based on embossing, screen printing and solvent casting have been developed.

In vitro drug release experiments on both type of micro devices have been performed. The experiments show that most of the drug is released from the developed devices. Additionally, it has been shown that it is possible to control the release of drug by adding polymeric coatings.



## Dansk resumé

Den farmaceutiske industri står i øjeblikket over for flere forhindringer, når de udvikler medicin administreret oralt, primært på grund af typen af lægemiddelkandidaterne. Lægemidlerne er ofte svært opløselige og har en lav permeabilitet i gastrointestinalt epithel. Desuden nedbrydes de ofte, før de bliver absorberet. Resultatet er en lav biotilgængelighed af lægemidlerne. For at overvinde disse udfordringer, er det nødvendigt at udvikle medicineringssystemer.

For nylig er mikrosystemer kommet frem som kandidater til at løse problemerne. Størstedelen af disse systemer er baseret på materialer, der ofte anvendes i mikroteknologi, såsom SU-8, silicium, poly(methyl methacrylate). Det næste skridt i udviklingen af nye medicineringssystemer er at erstatte klassiske mikrofabrikationsmaterialer med bionedbrydelige polymerer. For at kunne gøre dette, skal der udvikles metoder til at fremstille mikrostrukturer i bionedbrydelige polymerer.

Målet med dette projekt har været at udvikle metoder til mikrofabrikation af bionedbrydelige polymerer og at anvende disse metoder til at fremstille systemer, der kan bruges til oral medicinering. Dette er opnået ved fremstilling af mikrocontainere lavet af poly(L-lactid acid) og polycaprolactone. Endvidere er et mikrosystem baseret på stablede lag af polymer og lag af polymer blandet med medicin fremstillet.

For at fremstille mikrosystemerne, er polymeropløsninger blevet udviklet ud fra Hansens teori om opløselighedsparametre. Opløsningerne bruges til fremstilling af polymerfilm ved spin-coating. Disse film benyttes ved fremstilling af mikrosystemer til oral medicinering. En film, som består af både af polymer og lægemiddel, er desuden også blevet udviklet ved spin-coating.

Dybe reaktive ion ætse, der producerer skrå sidevægge til stempel produktionen, er blevet udviklet. De skrånende sidevægge sikre en vellykket adskillelse af stempel og film efter stempeling. Metoder til fyldning af mikroreservoirer er blevet udviklet. Disse er baseret på prægning, silketryk og solvent støbning.

Der er udført in vitro lægemiddelfrigivelsesforsøg på begge mikrosystemer. Disse viser, at næsten al lægemidlet frigives fra systemerne. Endvidere har det vist sig, at det er muligt at kontrollere frigivelsen af lægemidlet ved tilsætning af polymerbelægninger.

## Preface

This thesis is carried out at DTU Nanotech, Department of Micro and Nanotechnology, at the Technical University of Denmark, DTU. The thesis is carried out in the Nanoprobes group under the supervision of Professor Anja Boisen and Assistant Professor Stephan Sylvest Keller. The project started on the 1st of December 2009 and was finished on the 31st of January 2013.

Kongens Lyngby, January 31st 2013

---

Johan Nagstrup

DTU Nanotech - Department of Micro- and Nanotechnology  
Technical University of Denmark  
DTU - Building 345 east  
DK-2800 Kongens Lyngby  
Denmark

## Acknowledgements

I would like to thank my supervisors Professor Anja Boisen and Associate Professor Stephan Sylvest Keller for guidance, support and feedback. I would like to acknowledge Professor Kristoffer Almdal for his help on several topics and especially his help on polymer related topics, Professor Thomas Rades and Associate Professor Anette Müllertz for their support on pharmaceutical topics. Thanks to the laboratory technicians and process specialists at Danchip, especially process specialist Jonas Michael Lindhard for his help with DRIE and SEM related questions. I would like to thank the entire NAMEC team for a great working environment and support during the thesis. Finally I would like to thank the rest of the Nanoprobes group for guidance on different subjects and a lot of good times.





# Contents

<b>1</b>	<b>Introduction</b>	<b>1</b>
1.1	NAMEC project & vision . . . . .	1
1.2	Device . . . . .	2
1.3	Goal of the PhD . . . . .	3
1.4	Model drug . . . . .	3
1.5	Review of existing research . . . . .	3
1.6	Novelty . . . . .	6
1.7	Thesis outline . . . . .	7
<b>2</b>	<b>Polymers</b>	<b>9</b>
2.1	Solubility theory . . . . .	9
2.2	Biopolymers . . . . .	13
2.3	Solutions . . . . .	14
2.4	Polymer films . . . . .	15
2.5	Summary . . . . .	18
<b>3</b>	<b>Polymer drug matrix</b>	<b>19</b>
3.1	Solvent-polymer-drug interaction . . . . .	19
3.2	Drug matrix characterization . . . . .	23
3.3	Summary . . . . .	27
<b>4</b>	<b>Stamps</b>	<b>29</b>
4.1	Fabrication . . . . .	29
4.2	SU-8 stamps . . . . .	30
4.3	Silicon . . . . .	32
4.4	Nickel . . . . .	34
4.5	Stamp comparison . . . . .	35
4.6	DRIE process development . . . . .	36
4.7	summary . . . . .	41
<b>5</b>	<b>Micro containers</b>	<b>43</b>
5.1	SU-8 micro containers . . . . .	43
5.2	Biodegradable polymer containers . . . . .	46
5.3	Fabrication technologies . . . . .	46

5.4	Comparison of methods . . . . .	48
5.5	Hot embossing . . . . .	49
5.6	PLLA containers . . . . .	50
5.7	PCL containers . . . . .	53
5.8	Summary . . . . .	54
<b>6</b>	<b>Container filling</b>	<b>57</b>
6.1	Embossing . . . . .	57
6.2	Screen printing . . . . .	60
6.3	Solvent casting . . . . .	62
6.4	Comparison . . . . .	65
6.5	Summary . . . . .	66
<b>7</b>	<b>Drug delivery</b>	<b>67</b>
7.1	Dissolution . . . . .	67
7.2	Drug matrix . . . . .	70
7.3	Micro containers . . . . .	73
7.4	UV imager experiment . . . . .	75
7.5	Summary . . . . .	77
<b>8</b>	<b>Conclusion</b>	<b>79</b>
<b>9</b>	<b>Outlook</b>	<b>83</b>
	<b>Bibliography</b>	<b>85</b>
	<b>Appendices</b>	<b>92</b>

# Chapter 1

## Introduction

Oral delivery is often the preferred route of drug administration since it provides good compliance for the patients and no need for health professionals. However, the pharmaceutical industry is presently facing several obstacles when developing oral delivery systems, primarily due to the nature of the discovered drug candidates. Generally drug candidates can be divided into two categories; small molecules and biological compounds. The discovered active small molecules often have a poor solubility and a low permeability across the gastro intestinal (GI) epithelium. Biological compounds, like proteins and nucleic acids, are degraded in the GI tract and have a poor permeability. Both types of compounds therefore require development of special drug delivery systems to reach a satisfactory oral bioavailability.

Traditionally, oral drug delivery is based on compressed tablets and capsules. Recently, micro and nano particles as well as micro systems have emerged as possible drug carriers that can solve the challenges described above [1, 2]. The aim of the project is to develop and improve such micro systems for drug delivery. The PhD study is carried out as part of a larger consortium, NAnoMEChanical sensors and actuators, fundamentals and new directions (NAMEC) - a VKR Centre of Excellence, working on micro systems for oral drug delivery among other technologies such as sensors. The main collaborators for the oral drug delivery project consist of engineers from the Department of Micro and Nanotechnology (DTU Nanotech), at the Technical University of Denmark and pharmacists from the Department of Pharmaceutics and Analytical Chemistry at the University of Copenhagen (KU Farma). The following sections will explain the vision of the NAMEC drug delivery project as well as introduce the collaborating parties and the main tasks set forth for each party.

### 1.1 NAMEC project & vision

The main goal of the drug delivery project in NAMEC is to realize and characterize micro systems for oral administration of drug. It is the vision of this project to develop a general drug delivery system that can deal with the challenges described above no matter which kind of drug the system carries. The system should have a protective shell around the

drug to protect the drug from degradation in the stomach. Technologies controlling the release should be developed to control the release kinetics such as time and position. The system should adhere to the intestinal epithelial surface and release the drug unidirectional across the epithelial cell surface to increase the drug uptake. Ideally, this should prevent drug from passing through the gastrointestinal tract without being absorbed. Formulations aiding the dissolution and enhancing the permeability across the gastrointestinal epithelium should be developed. Additionally, the devices should be easy to swallow to increase patient compliance.

## 1.2 Device

A device capable of performing the tasks described above is sketched in figure 1.1. The aim is to keep the device as simple as possible. This means that no electronics will be involved in the system. Furthermore, the system should consist of materials approved for oral drug delivery. As a guideline, materials approved by the food and drug administration (FDA)<sup>1</sup> should be used in order to minimize authorization procedures. The device consists of a container with the purpose of protecting the drug in the GI tract. Preferably, the container should be made in biodegradable polymers which are approved by the FDA. For this purpose poly(L-lactic acid)(PLLA) and polycaprolactone (PCL) are chosen. Besides the container, the device consists of a membrane or coating that should enable drug to be released at a specific time and/or place in the GI tract. Additionally, the device should enhance the solubility and the permeability of the active pharmaceutical ingredient (API) and thereby enhance bioavailability. This is to be obtained by improved drug formulations and by having a mucoadhesive device, which attaches to the intestine wall and performs a unidirectional release of the API across the intestine wall. The mucoadhesion can be obtained by polymeric coatings[3] or by chemical surface modifications[4]. As for the drug formulation, several options exist that can enhance the solubility and permeability, such as lipid based formulations [5], supersaturating drug delivery systems [6], solid dispersions

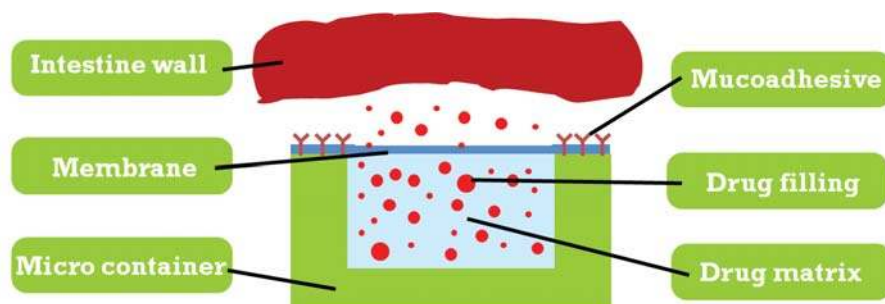


Figure 1.1: Diagram showing the different parts of the drug delivery system.

---

<sup>1</sup>The FDA is the American government agency, whom authorizes compounds for use in foods and drugs.

[7], amorphous drug formulations[8] and nano crystalline formulations [9]. In determining the size of the device the following consideration are made. The size of the device should allow for easy swallowing as this can be a problem for patients. Generally, people can detect particles with a size of a few hundred microns in the mouth [10]. Thus it can be an advantage to keep the size of the device below a few hundred microns. In terms of drug delivery, the bigger the device is, the fewer devices are needed for a dose. An estimate of micro devices needed for an erythropoietin dose of 0.03mg is found to be 230.000 [11], assuming a device measuring 40  $\mu\text{m}$  in diameter and 6.2  $\mu\text{m}$  in height. Thus, having larger devices could reduce this number significantly. Little is known about mucoadhesion of micro devices and the effect of size on this property. It is likely that the device would be dragged along by intestinal fluids if it sticks too far out of the mucus layer. Additionally, there is the issue of handling the devices, which become significantly easier the larger the devices are. With these factors in mind, it is decided to fabricate micro container prototypes with a characteristic length of 300  $\mu\text{m}$ .

The development of the drug delivery device is divided into work packages consisting of; (1) micro container fabrication, which is my work package, (2) lid and coatings, (3) mucoadhesion, (4) filling of micro containers, drug matrix and (5) drug formulation. The DTU Nanotech personnel is responsible for the container fabrication, the container filling as well as the lid and coatings while the KU Farma personnel is responsible for mucoadhesion, drug matrix as well as drug formulations.

### 1.3 Goal of the PhD

This section lists the goals set forth at the beginning of the PhD. The goals are based on the vision and the device described above and the first work package.

- Develop fabrication methods for micro structuring of biodegradable polymers.
- Fabrication of micro containers in biodegradable polymers.
- Develop methods that can be up scaled for large scale production.

### 1.4 Model drug

Pharmaceutical active ingredients are often divided into four categories classifying them by solubility and permeability [12]. For the class 1 drugs, both the permeability and solubility is high, while both are low for the class 4 drugs. Class 2 has a high permeability and low solubility and vice versa for class 3 drugs. As a model drug, a class four drug is chosen as it represents the challenges facing most newly developed drugs [13]. The choice of drug is furosemide. The drug is used for treating edema and hypertension cite [14, 15].

### 1.5 Review of existing research

This section presents the most relevant research concerning micro devices for oral drug delivery. In terms of size, micro devices for oral drug delivery position themselves between

conventional tables and research fields such as micro- and nano-particles, vesicles, micelles etc. These research fields represent alternative technologies to the micro devices and will not be covered here. The research field concerning micro devices similar to the one described in section 1.1 emerged a little more than a decade ago. The first micro system matching the vision described in section 1.1 is found in a patent dating 01/06/2000 and published 03/12/2002. The patent idea is published in an article by Martin and Grove [1]. Both have since demonstrated the idea by realizing silicon micro particles [16, 17]. Since then, several research groups around the world have worked within the field of micro devices for oral drug delivery. A number of reviews [18, 19, 20, 21, 22] outline most of the work carried out and the future potential. To give an overview of the current state of the art, the work of four research groups are highlighted in the following paragraphs and summarized in table 1.1 and figure 1.2.

The group of Tejal Desai at University of California, San Francisco has carried out a lot of research on mucoadhesive micro devices for oral drug delivery and their work represents the state of the art within the field. Several micro systems have been realized and optimized during the past decade. Their first devices where micro wells fabricated in silicon using standard silicon technology [26]. The structures had a height of  $2\ \mu\text{m}$  with a  $1\ \mu\text{m}$  deep reservoir and a width of 50 to  $150\ \mu\text{m}$ . Improved bioadhesion was shown by chemically modifying the device surface and attaching lectin. In vitro experiments on CaCo-2 cells showed improved bioadhesion. Desai et al. have later improved these devices several times. Micro devices with multiple drug reservoirs have been fabricated [4]. Devices have been realized in poly(methyl methacrylate) (PMMA)[27], poly(lactic-co-glycolic acid) (PLGA), gelatine and SU-8.[28]. Devices have typical feature size of 50-200  $\mu\text{m}$  in width and height of 5-10  $\mu\text{m}$ . Testing of drug release and bioadhesion of these devices is done in vitro [29, 30]. The latest work describes bioadhesive micro devices with multiple reservoirs made in PMMA [23]. The device has three compartments containing three different types of drug and measures 200  $\mu\text{m}$  in width and 7.5  $\mu\text{m}$  in height. The compartments measure 60  $\mu\text{m}$  and are 5  $\mu\text{m}$  deep. In vitro drug release was tested in a CaCo-2 cell setup. Figure 1.2(a) shows an image of the latest device published.

The group of Joseph DiSimone at University of North Carolina has developed a fabrication method, Particle Replication In Non-wetting Templates (PRINT), which is used to produce micro and nano particles for drug delivery. The method enables the fabrication of individual particles. The non-wetting technology avoids the creation of a residual layer that usually connects particles made by embossing. Figure 1.2(b) shows a schematic of the PRINT technology. Particles have been fabricated with sizes ranging from 200 nm to 7  $\mu\text{m}$  [31, 32, 24, 33]. The particles have been fabricated in many different materials such as poly(ethylene glycol) (PEG), Poly(L-lactic acid) (PLLA) and PLGA and tested in vitro and in vivo.

The group of Kanji Takada at Kyoto Pharmaceutical University has made devices for oral drug delivery consisting of solvent cast layers of ethyl cellulose, cellulose and a pH sensitive coating, such as Eudragit<sup>®</sup> or HP-55<sup>®</sup>. The layers are stacked upon each other

and merged to one piece by heating. The devices are cut out in squares of 3 by 3 mm and are 115  $\mu\text{m}$  high. [34, 35, 25]. The latest work follows the same principles and includes membranes made of polycaprolactone (PCL) and poly lactide acid (PLA) polymers [36]. The devices are round with a diameter of 1.85 mm and a height of 0.15 mm. In vitro and in vivo characterization is presented. The micro device is shown in figure 1.2(c).

The group of James L. Lee at Ohio State University has done considerable research within the field of micro devices for drug delivery [11, 37, 38]. They have fabricated micro wells ranging in size from 2-10  $\mu\text{m}$  in height and 30-80  $\mu\text{m}$  in width. Figure 1.2(d) shows the

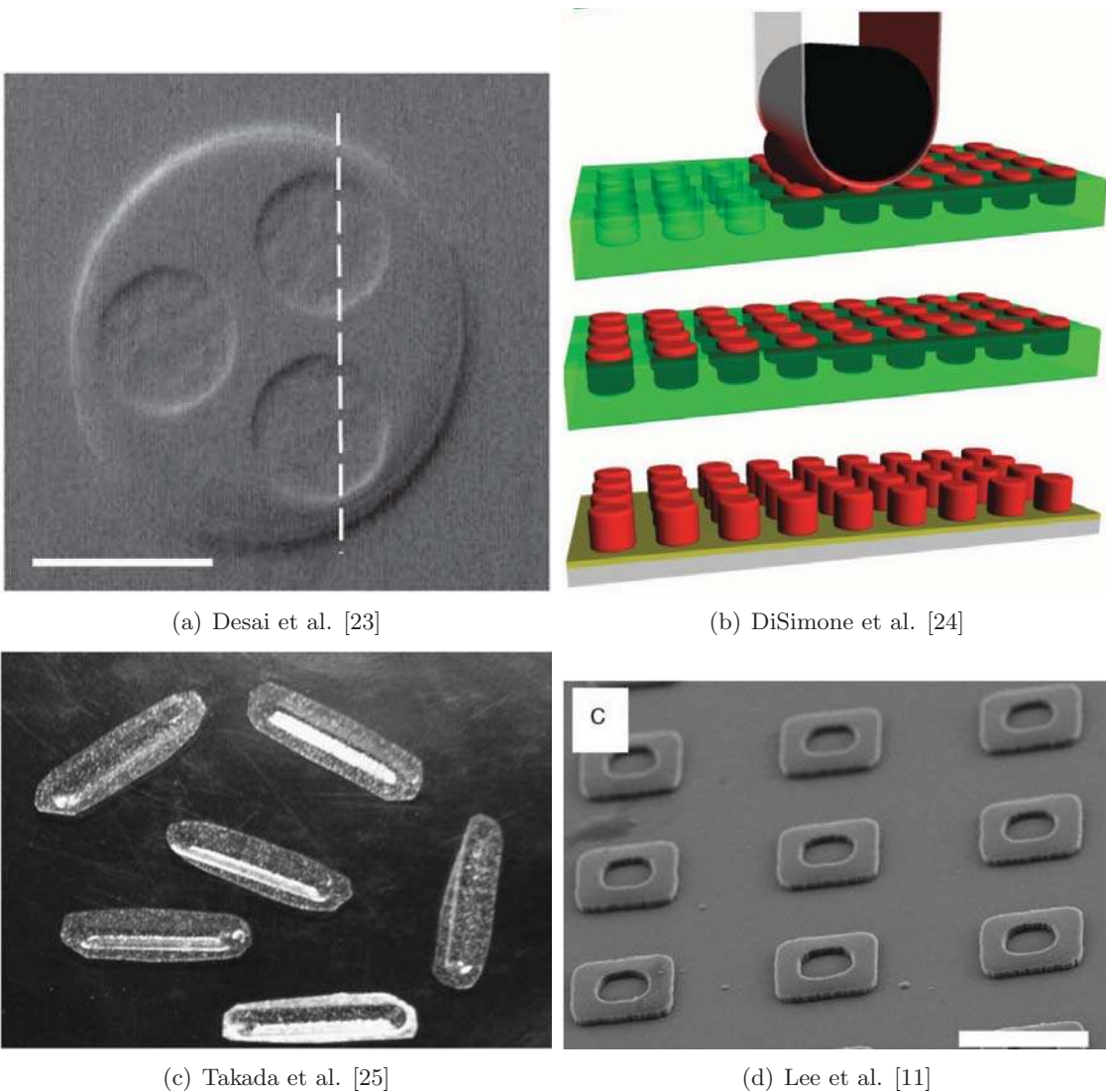


Figure 1.2: The figure shows the state of the art devices fabricated by selected groups and a schematic of the PRINT technology.



Table 1.1: Comparison of micro systems developed for oral drug delivery similar to what is described in US patent number: 6355270 B1.

Group	Material	Size Height/width	Demonstration level	Process type
Desai et al	Silicon SU-8 PMMA PLGA	1-10 $\mu$ m/ 50-200 $\mu$ m	In vitro	Lithography molding
Takada et al.	cellulose Eudragit <sup>®</sup> HP-55 <sup>®</sup> PCL PLA	115-185 $\mu$ m/ 1.85-3mm	In vitro In vivo	Solvent casting
Lee et al. Micro wells:	PEGMA PEGDMA PLGA Chitosan	2-10 $\mu$ m/ 30-80 $\mu$ m	In vitro	Molding soft lithogr- pahy lithography
mm Containers	PCL	1.5mm/ 4.5mm	In vivo	Molding
DeSimone et al.	PLLA PLGA PEG	200nm-7 $\mu$ m/ 200nm-7 $\mu$ m	In vitro In vivo	PRINT <sup>®</sup>

fabricated micro wells. The micro devices are realized in PEGMA, PEGDMA, PLGA and Chitosan. The micro devices range from simple wells to self folding micro containers. Other research performed by the same group includes containers with sizes of 1.8 mm height and 4.5 mm width made in PCL [2, 39] and similar devices made in gels [40]. The demonstration level of drug delivery includes the use of animal intestines in experiments as well as animal tests.

## 1.6 Novelty

The novelty of this work consists of the following; fabrication of micro systems in biodegradable polymers that are approved by FDA. Development of large scale fabrication of micro systems for drug delivery by hot embossing of biodegradable polymers. The development of methods for large scale filling of micro containers.

## 1.7 Thesis outline

This section presents an overview of the chapters in the thesis and a short summary of the content of the individual chapters. The thesis is divided into ten chapters plus appendices. The first appendix is a list of scientific contributions made during the PhD study. Following this is published work, then a list of polymers considered for the project and data sheets for PCL and PLLA. Lastly process recipes and process data are included. Each chapter starts with a short introduction and ends with a summary of the most important findings.

**Chapter 2 - Polymers** The chapter describes the theory of solubility used for making solutions. It highlights characteristics of the most used polymers. Finally, it describes the spin coating method used for film deposition along with spin curves for PCL and PLLA.

**Chapter 3 - Drug matrix** This chapter describes the development of a drug matrix consisting of PCL and furosemide. The chapter shows how Hansen's solubility parameters can be used for complex systems with multiple compounds. Furthermore, the drug matrix is characterized by microscopy and X-ray diffraction.

**Chapter 4 - Stamps** This chapter explains the fabrication of the different stamps made in the project. The stamps are later used for embossing of polymers. Stamps in three different materials are made; SU-8, silicon and nickel. Finally, a deep reactive ion etch process is developed to tune the slope of the side walls.

**Chapter 5 - Micro containers** The fabrication of the different micro containers is described in this chapter along with an introduction to hot embossing. Micro containers are made in SU-8, PLLA and PCL.

**Chapter 6 - Filling** The filling of the different micro containers is shown in this chapter. Three different methods for filling are tested and compared.

**Chapter 7 - Drug delivery** In vitro drug release from the drug matrix along with the drug release from micro containers are described in this chapter. The drug release is tested mainly by  $\mu$ -dissolution. A control experiment using a UV-imager is made.

**Chapter 8 - Conclusion** The conclusion summarizes the most important results obtained in the thesis.

**Chapter 9 - Outlook** The outlook highlights possible directions for future development of micro devices for drug delivery.



## Chapter 2

# Polymers

This chapter covers the theory of solubility, the characteristics of the most used polymers in this project, preparation of biopolymer solutions and film fabrication by spin coating. In this project a lot of emphasis is on the fabrication of biodegradable micro containers made in poly-L-lactide acid (PLLA) and polycaprolactone (PCL) which are approved by the FDA. These polymers will be covered in depth in this chapter while less frequently used polymers and materials will be covered to some degree.

### 2.1 Solubility theory

This section contains the solubility theory used throughout the project in the development of solutions for various purposes. First, an introduction to Hansen's solubility parameters (HSP) is given and the thermodynamic theory behind HSP is presented. The parameter space and solubility concept of HSP is explained. Once the concepts of HSP are established an example of its use in choosing solvent(s) for a given polymer is presented. Furthermore, considerations of solubility of systems with multiple components are given.

#### 2.1.1 Introduction

The theory of solubility is a complex matter and several different approaches exist. Flory-Huggins are among the first to derive a solubility theory. The Flory-Huggins solubility theory is based on change in Gibbs free energy. The solubility is defined by the interaction parameter  $\chi$  [41]. The approach to solubility that will be addressed in this chapter is the one of Hildebrand and Hansen. The theory is based on the cohesive energy. The Hildebrand parameter  $\delta$  is an interaction parameter like Flory-Huggins. The theory is applicable to associated solutions and is based on the principle of "like dissolve like". Thus, materials with similar  $\delta$  parameters are likely to be miscible.

Hansen solubility parameters (HSP) expand the Hildebrand solubility parameter  $\delta$  into three parameters, creating a three dimensional parameter space. The use of three parameters offers a more accurate treatment of solubility than that of Hildebrand. Although HSP improves the theory of Hildebrand, limitations apply to the theory as molecular shape and size are not taken into account. HSP is an empirical approach to solubility

and thus material parameters have to be determined in order to use HSP. Luckily many people have worked with HSP and thus HSP parameters can be found for more than 2000 compounds[42]. If a specific compound of interest is not cataloged with HSP data, the reader is referred to [43] for details on how to obtain HSP data.

For further information on the different solubility theories, see [43, 41, 44].

### 2.1.2 Parameter space & solubility

Hansens solubility parameters use cohesive energy to predict solubility. The cohesive energy can be divided into three components, the non polar atomic interactions  $E_D$ , the permanent dipole- permanent dipole molecule interactions  $E_P$  and the hydrogen bonding interaction  $E_H$ . The total cohesive energy is given by:

$$E_{cohesive} = E_D + E_P + E_H \quad (2.1)$$

Dividing with the molar volume, one arrives at the Hildebrand and Hansen parameters  $\delta$  [ $\text{MPa}^{\frac{1}{2}}$ ]:

$$\frac{E_{cohesive}}{V_{mol}} = \delta^2 = \delta_D^2 + \delta_P^2 + \delta_H^2 \quad (2.2)$$

The three parameters determine the coordinate of a compound in Hansen space. The parameters can either be found experimentally, see [43] or they can be calculated using various models included in HSPiP[42]. The coordinate is the center of the Hansen solubility sphere. The radius of the sphere is determined via experiments. The material in question is immersed in a series of test solvents with different HSP coordinates. By determining whether or not the material dissolves, the solvent is given a score of either 1 if it dissolves (good) or 0 if it does not dissolve (bad). The distance between the sphere center coordinate and the test solvents is then calculated using the following formula:

$$R_a^2 = 4(\delta_{D1} - \delta_{D2})^2 + (\delta_{P1} - \delta_{P2})^2 + (\delta_{H1} - \delta_{H2})^2 \quad (2.3)$$

An interaction radius  $R_0$  is defined such that; solvents lying outside the interaction radius are considered bad solvents (score 0) and solvents lying inside the interaction radius are considered good solvents (score 1). By iteration of the test solvents, the interaction radius  $R_0$  is determined. The uncertainty of  $R_0$  depends on the number of test solvents and their HSP coordinates. For easy recognition of good and bad solvents, the RED number is introduced as the ratio of distance between a solvent and the sphere center and the interaction radius:

$$RED = R_a/R_0 \quad (2.4)$$

If the RED number is below 1 the affinity of the solvent is good and if the RED number is above 1, the affinity of the solvent is bad. Thus, a solvent with a coordinate outside the sphere will not dissolve the compound while a solvent inside will dissolve it. Figure 2.1 shows a two dimensional representation of the sphere concept. In practise the uncertainty inherent from the calculation of HSP data give rise to a grey area for solvents with a RED number close to 1. Solvents just outside the sphere might dissolve the material and vice versa.

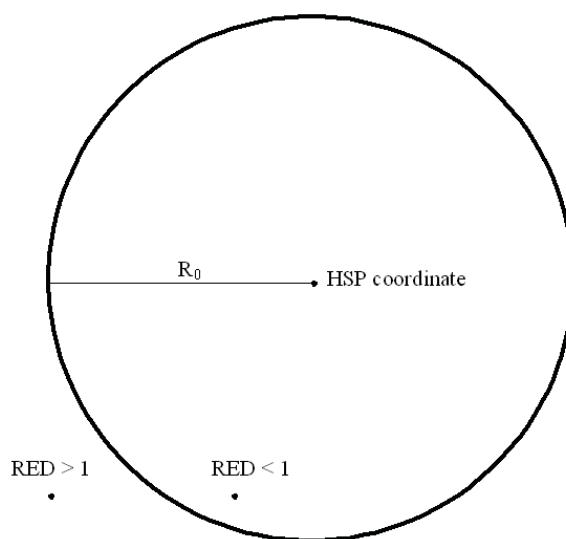


Figure 2.1: Two dimensional schematic of the Hansen sphere concept. Solvents with a RED number above 1 are outside the sphere and categorized as bad solvents. Solvents inside the sphere are considered good.

### 2.1.3 Example - choosing a solvent for polycaprolactone

The following is an example of how to use HSP to select a solvent for polycaprolactone (PCL). Table 2.1 shows a set of selected solvents and their corresponding HSP data [45]. It is seen that Dioxolane and Methylene dichloride have a RED number below 1 and are good candidates for dissolving PCL. Ethyl acetate is just at the border of the interaction radius and might interact with PCL by either dissolving or swelling PCL.

From experiments it is known that methylene dichloride is a good solvent for PCL. Ethyl acetate swells the PCL, but does not dissolve it and neither acetone nor 2-propanol dissolve PCL. Depending on the application of the solution some solvents might be favored over others. I.e. in the case of spincoating it can be an advantage to have a solvent which does not evaporate fast at room temperature and thus baking of the resist is needed to solidify it. Toxicity could be another important factor to consider when choosing a solvent. HSP does not help to make those decisions, it only provides a selection of possible solvents.

### 2.1.4 Multiple component systems

When dealing with multiple component systems several cases arise. The following example outlines some of the possibilities and limitations of HSP as a tool. For the ease of drawing and explaining, the following example will be sketched in two dimensions, though remember that HSP is a three dimensional parameter space. Figure 2.2 shows a situation with two compounds (spheres 1 and 2) and three different solvents (black dots). If one wants to dissolve both compounds one needs a solvent that matches the overlapping area (volume). In this example that fits with solvent 1. In the situation that no solvent lies

Table 2.1: The table shows the HSP data for a selected set of solvents for polycaprolactone. The table is sorted by the RED number. It is seen that Dioxolane and Methylene dichloride have a RED number below 1 and thus are good candidates for dissolving PCL.

Solvents	$\delta_d$	$\delta_p$	$\delta_h$	RED
1,3-Dioxolane	18.1	6.6	9.3	0.48
Methylene Dichloride	17	7.3	7.1	0.78
Ethyl Acetate	15.8	5.3	7.2	1.02
Vinyl Acetate	16	7.2	5.9	1.22
Methyl Acetate	15.5	7.2	7.6	1.26
p-Xylene	17.8	1.0	3.1	1.71
Acetone	15.5	10.4	7.0	1.79
Toluene	18	1.4	2.0	1.9
2-Propanol	15.8	6.1	16.4	2.17

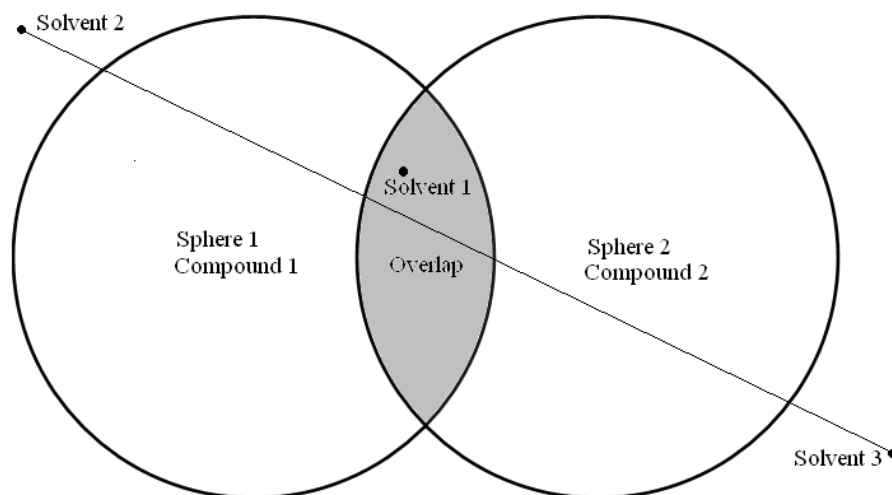


Figure 2.2: 2d schematic of a multiple compound HSP system. Sphere 1 and 2 represent two different compounds. The grey area shows the overlapping HSP areas of compound 1 and 2. Solvent 1, 2 and 3 represents different solvents. The line between solvent 2 and 3 shows the possible HSP values when mixing the solvents.

in the overlapping (volume), choosing two solvents on opposite sides of the overlapping spheres will dissolve the material if mixed in the right way. The combined HSP values of a solvent system are linearly additive and thus it is possible to achieve HSP values on a straight line connecting two solvents in HSP space. To dissolve a two component system one has to match the solvent(s) HSP values to the overlapping sphere volumes of the given compounds. The line between solvent 2 and solvent 3 shows the possible HSP values when a combination of the solvents are mixed. In this example, a mix around half and half of each solvent, will give a value inside the overlapping region of sphere 1 and

sphere 2, thus dissolving both compounds. The trick of mixing solvents to match a specific HSP value is valid for a single compound as well. When mixing solvents it is important to take the boiling point into account. For example solvent 1 evaporates fast while solvent 2 evaporates slowly. The solvent mixture will alter its composition over time if it is allowed to evaporate. Thus the HSP values of the system will change when the ratio of solvent change. If the system is delicate and responds fast to the change in solvent ratio, one of the components might go out of solution while the other will remain in solution. Depending on the application of the blend this can either be a feature or an issue.

### 2.1.5 HSP remarks

The strength of HSP lies in the large amount of data available to the user. Data can be found in Hansen's solubility parameters, a users handbook[43] or on the web[42]. It can be of great help to use the HSPiP program, which has all data available in data sheets and tools to help you with calculations and comparisons. It should be noted that HSP values are affected by temperature, which the theory does not include. Thus, data obtained at room temperature might be significantly different if used at extreme temperatures. Molecular size and shape are not considered and can play a role in solubility. Regardless of its limits, HSP can be of great help when choosing solvents, as it provides the user with a selection of possible solvents to use.

## 2.2 Biopolymers

This section contains relevant physical and chemical properties for the two polymers, PCL and PLLA. Both polymers belong to the polyester family and their structures are shown in figure 2.3. Both polymers are categorized as biopolymers [46] and they are both biodegradable, though only PLLA is a biobased polymer while PCL is a fossil fuel based polymer. PLLA can be produced from different organic materials such as corn starch and sugarcane. PCL is made from  $\epsilon$ -caprolactone which is cyclic ester. The two biopolymers

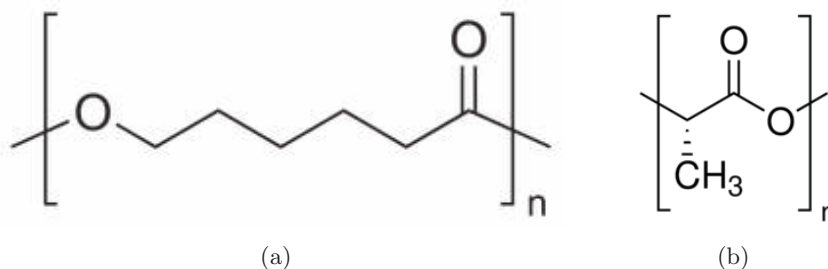


Figure 2.3: Structural formula of a) polycaprolactone and b) polylactic acid.

are selected for their good properties for fabrication and both polymers are successfully used in the fabrication of films [47, 48, 49] and various drug delivery systems as well as for scaffolds for tissue engineering [50] [51]. Although both polymers are used for similar purposes their properties are quite different. Table 2.2 lists the physical properties for



Table 2.2: List of properties for chosen biopolymers based on peer reviewed literature. Density ( $\rho$ , in g/cm<sup>3</sup>), tensile properties: tensile strength ( $\sigma$ , in MPa), tensile modulus (E, in GPa) and ultimate strain ( $\epsilon$ , in %), glass transition temperature ( $T_g$ , in °C) and melting point ( $T_m$ , in °C) [52]

Properties	Limits	Polymers		
		PLA	PLLA	PCL
$\rho$ (g/cm <sup>3</sup> )	Upper	1.21	1.24	1.11
	Lower	1.25	1.30	1.146
$\sigma$ (MPa)	Upper	21	15.5	20.7
	Lower	60	150	42
E (GPa)	Upper	0.35	2.7	0.21
	Lower	3.5	4.14	.44
$\epsilon$ (%)	Upper	2.5	3	300
	Lower	6	10	1000
$T_g$ (°C)	Upper	45	55	-60
	Lower	60	65	-65
$T_m$ (°C)	Upper	150	170	58
	Lower	162	200	65

PCL, PLA and the specific L configuration of PLA referred to as PLLA. The table shows the polymer density ( $\rho$ , in g/cm<sup>3</sup>), tensile strength ( $\sigma$ , in MPa), tensile modulus (E, in GPa) and ultimate strain ( $\epsilon$ , in %), glass transition temperature ( $T_g$ , in °C) and melt point ( $T_m$ , in °C). The suppliers datasheets for PLLA and PCL used in the project can be found in appendix D & E. When comparing PCL to PLLA it is clear that they are very different polymers. For fabrication purposes such as hot embossing the  $T_g$  is an important parameter. While PCL has a very low  $T_g$  around -60 °C, PLLA has a  $T_g$  of around 60 °C. Coupled with the differences in young's modulus and ultimate strain, PLLA stands out as a firm polymer while PCL is a rubbery polymer at room temperature. The use of these two different polymers provides a versatile basis for future development of diverse micro systems and fabrication techniques.

## 2.3 Solutions

In order to work with the polymers and fabricate films, the polymer granulates need to be dissolved in a solvent. Figure 2.4 shows the granulates before dissolution, while dissolving and the final solution. The dissolution of the polymer can take from minutes to a couple of days depending on the polymer and the concentration of polymer in the solution. Table 2.3 shows a list of solvents and whether they dissolve our model drug furosemide and the polymers poly(acrylic acid) (PAA), PCL and PLLA. The amount of material dissolved is 0.5 g for the drug and 1 g for the polymers in 10 ml of solvent. The amount of material a solvent can dissolve is of importance when preparing solutions for spin coating. The more viscous a solution is the thicker a film can be produced. Dichloromethane (DCM) is a good

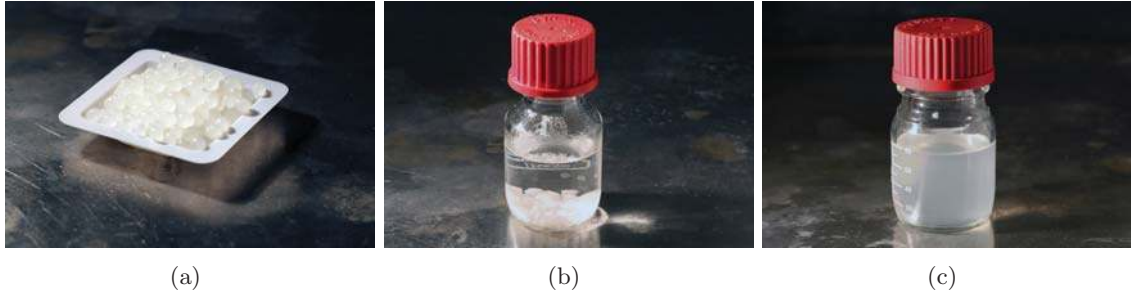


Figure 2.4: The figure shows the polymer as received a), while dissolving b) and in solution c). In this case it is PLLA in DCM 25wt%.

Table 2.3: Solubility of polymers and furosemide medicine. 10 ml of solvent used.

solvents	Furosemide 0.5 g	PAA 1 g	PCL 1 g	PLLA 1 g
Acetone	Soluble	Slightly Soluble	Not Soluble	Not Soluble
Dichloromethane	Not Soluble	N A	Soluble	Soluble
Ethanol	Not Soluble	Soluble	Not Soluble	Not Soluble
Isopropanol	Not Soluble	Soluble	N A	N A
DMSO	Soluble	Soluble	N A	N A
Water	Not Soluble	Soluble	Not Soluble	Not Soluble

solvent for both PCL and PLLA. Solutions containing up to 30 wt% of polymer (to solvent) are prepared for both polymers. For highly concentrated solutions, the dissolution process is accelerated by heating the solution to 50 °C during the dissolution. The solution is cooled to room temperature when the dissolution process is complete. Further information on solutions and in particular multi component solutions is given in chapter 3, while the applied theory is covered in section 2.1.

## 2.4 Polymer films

The following section describes how the polymer films used in the project are fabricated and how different fabrication techniques are used to tune the adhesion of the polymer films to the substrates. The majority of the polymer film fabrication is done by spin coating. Other methods such as solvent casting and sheet extrusion have been used to a small extend to fabricate polymer film. The PLLA sheets are fabricated by collaborators at DTU RISØ, while the solvent casting is performed in our own lab. Both techniques are used to a little extend as spin coated films have performed better for our processes. Spray coating is used in the project for film deposition. That work is carried out by colleagues in the group. For this reason spin coating is the only method described in this section.

### 2.4.1 Spin coating

Spin coating is a fabrication technique that is widely used for deposition of thin films, especially in the micro electronics industry. The film thickness varies greatly from tens of nanometers [53] to hundreds of micro meters [54]. The spin coating process is a well documented and well established technique. The process is described here, though for further details on theory the reader is referred to [55] [56]. Figure 2.5 shows the spin coating process. First, a solution is dispensed on the center of a substrate. The substrate is then rotated at high rotation per minute (RPM). The centrifugal force pushes the solution from the center to the edge of the substrate, where excess solution is spun off the substrate. The thickness of the film is inversely proportional to the spin speed and time. After spinning the film is dried. The subsequent procedure after spin coating is highly dependent on the spun solution. It might be drying at room temperature or baking at elevated temperature. This is highly dependent on the solvent(s) used in the spin coated solution. Furthermore, heating steps can be used to facilitate cross linking. In our case, the films are either degassed at room temperature or on a hotplate, depending on the solution and the wanted film adhesion. The procedure can be repeated to stack layers of spin coated films on top of each other. Experiments with different solutions and spin

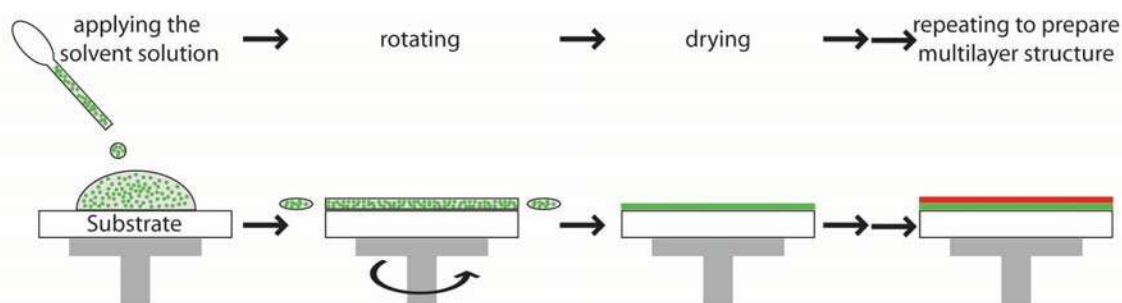


Figure 2.5: Main process steps in the spin coating process. [57] First, solution is applied to the substrate. Then the substrate is rotated. The rotation distributes the solution uniformly on the substrate creating a film. After rotation the film is dried. The process can be repeated to stack layers.

speed are performed to obtain spin curves relating spin speed to film height. Figure 2.6 shows the spin curves for solutions of PLLA with a weight percent (wt%) of 25 and 30 and for a PCL solution with a wt% of 25. The solvent used in both cases is DCM. The spin time is kept constant at 50 sec. It is seen that PCL and PLLA have similar spin curves. The 30 wt% solution is difficult to spin and often an uneven result is obtained, hence the large error bars. Figure 2.7 shows spin curves for a solution of PLLA with a wt% of 15 and 20. The spin curves shown in figure 2.6 are made with the first batch of polymers received, while the spin curves in figure 2.7 are made with the second batch of polymers received. There is a small difference in the thickness of the polymer films created with the two batches. A 20 wt% solution with the second batch produces almost similar film thicknesses as a 25 wt% solution of the first batch. The reason for this is unknown though

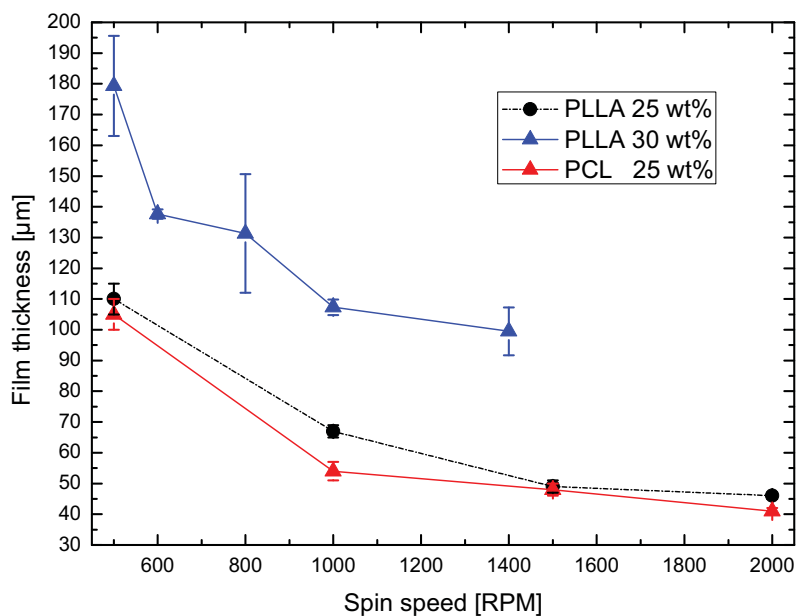


Figure 2.6: Graph showing spin curves for PLLA and PCL solutions in DCM. Solutions with a polymer weight percent of 25 and 30 are tested. It is seen that the PCL and PLLA have similar spin curves for similar weight percent solution.

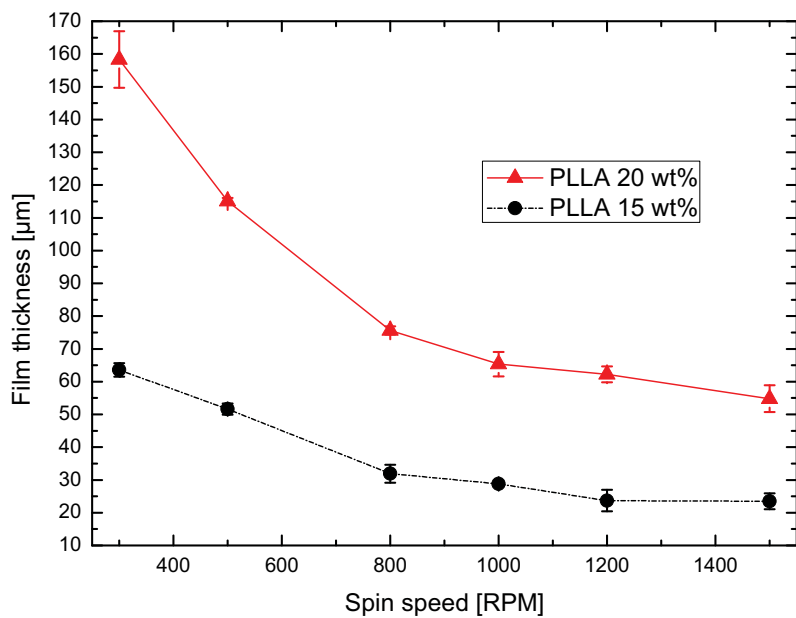


Figure 2.7: The figure shows spin curves for PLLA in DCM. Solutions with a polymer weight percent of 15 and 20 are tested.

it is likely due to a difference in molecular weight. The spin curves serve as a guideline for polymer film fabrication. The polymer film is later used to fabricate micro containers by hot embossing, see chapter 5.

### 2.4.2 PLLA film on silicon wafer - procedure

This paragraph describes the procedure used for a successful spin coating of PLLA. Furthermore, the possible post spinning treatments that can be used to tune the adhesion of the polymer to the substrate are explained.

In order to reproduce film thickness and to get a uniform and smooth surface it is recommended to use fresh solutions every time and not to use the last 10% of solution. The reason for this is that some of the solvent will evaporate from the solution when using it and thus the solution will thicken. The wafer should be rotating while the solution is dispensed on the wafer. When the silicon wafer is coated, the wafer is left to degas for 24 H. This is done in order to minimize the content of solvent left in the film. If the wafer is heated right after spin coating, bubbles of trapped solvent will create a very uneven surface. Depending on the desired adhesion, the following steps can vary. If a good adhesion is wanted, the wafers should receive a heat treatment. The wafers should be heated on a hotplate at 220 °C for a minimum of 15 min. When removing the wafers, they should be placed on a poor heat conductor i.e. cleanroom paper. If the temperature decreases too fast, stress will be induced in the film from the difference in thermal expansion between the substrate and polymer. This can cause peeling of the polymer film. If the PLLA film contains bubbles these can be removed by extending the heating time to i.e. 1 hour. A weak adhesion of the film to the silicon wafer is obtained by not heating the substrate. If left for several days up to weeks, the adhesion will diminish and result in the polymer peeling off. This can be a desired option if you want to release the film from the substrate after complete processing.

## 2.5 Summary

In this chapter Hansen's theory of solubility is introduced. Examples of its use to choose a solvent for PCL are shown and its applications in multiple component systems are described. The two biodegradable polymers (PCL, PLLA) mainly used in the project are introduced along with their properties. It is shown how to prepare films, by dissolving the polymers in organic solvent and spin coating the solutions on silicon substrates. Furthermore, the polymer film adhesion to the substrate can be tuned by heat treatment after spin coating.

## Chapter 3

# Polymer drug matrix

The idea is to have a versatile film consisting of polymer and drug, that is applicable to many applications such as filling of micro containers, see section 6.1. This chapter describes the development of the polymer drug matrix used in the project for filling of micro containers via a hot embossing technique. The polymer drug matrix is developed with the following conditions in mind; 1) The furosemide should preferably be in the amorphous state, to facilitate a fast dissolution of the otherwise poorly soluble drug. 2) The matrix should contain as much drug as possible, thus maximizing the amount of active ingredient per volume. 3) The distribution of the polymer and drug should be uniform. First, an overview of the solvent-polymer-drug interaction is presented along with the two methods used for fabricating polymer drug films; solvent casting and spin coating. Second, the developed polymer drug matrix is characterized. The drug dissolution from the polymer drug matrix is characterized with a Pion  $\mu$  dissolution UV profiler and the results from these experiments can be found in the drug release chapter 7.

### 3.1 Solvent-polymer-drug interaction

To achieve the properties above, it is of great importance to understand the interaction of the polymer, the drug and the solvents, as it affects the final product as well as the possible methods of fabrication. To achieve a homogenous film a good blend of the polymer and the drug is needed. Two different techniques are tested for the fabrication of the drug matrix; solvent casting and spin coating. Other techniques for fabricating films exist such as molding, thermoforming and extrusion, but these have not been investigated in this project. Hot melt extrusion is widely used in the plastic industry as well as the pharmaceutical industry and is a good example of how to mass produce polymer drug films [58, 59]. Two approaches for achieving a homogenous distribution of polymer and drug have been considered. 1) Either the polymer and drug should be miscible and thus phase separation can be avoided. 2) The solvent should evaporate immediately upon film formation, thus freezing the material in place, similar to quench cooling. The first approach requires that the materials are miscible. According to HSP this means that they should be alike, thus having similar HSP values. The second requirement is that they can be dissolved in the

Table 3.1: Table of HSP values for selected solvents, polymers and model drug furosemide. All values are from the HSP database 3.1.2 [45] unless otherwise noted in the table. Note that the database is constantly updated and values might change.

Material	$\delta_d$	$\delta_p$	$\delta_h$	R	Dist. Furo	Dist furo fit
Furosemide	20.6	12.6	12.9		0	
Furosemide fit calc. <sup>a</sup>	16.92	13.41	8.66	4.5		0
PCL	17.7	5.0	8.4	8.0	10.57	8.56
PLA	18.6	9.9	6.0	10.7	8.42	5.54
Acrylic acid <sup>b</sup>	11.33	8.08	5.22		20.57	12.85
DCM	17.3	8.2	8.8		8.88	5.27
DMSO	18.4	16.4	10.2		6.41	4.48
Acetone	15.5	10.4	7.0		11.99	4.46

<sup>a</sup> Calculated HSP values for furosemide based on own experiments, (DCM DMSO Acetone, isopropanol, ethanol,(water))

<sup>b</sup> HSP Values from [60]

Table 3.2: Table showing solvent composition for dissolution of selected materials in solutions of DCM/DMSO and DCM/Acetone. The table shows the optimal composition of solvents based on HSP calculations for the specific solvents and materials as well as the optimal composition based on lab tests. The numbers are given in volume.

Material	Solvent composition for dissolution	
	DCM / DMSO	DCM / Acetone
HSP optimization		
Furosemide	14/86	0/100
PLLA	71/29	100/0
PCL	100/0	100/0
PAA	99/1	1/99 <sup>a</sup>
Lab tests		
PAA + furosemide	32/68	N/A
PCL + furosemide	50/50	50/50 - 25/75
PLLA + furosemide	70/30 - 50/50 <sup>a</sup>	N/A

<sup>a</sup> Denotes poor solubility

<sup>b</sup> Lower than 70% dcm = Dissolve only smaller amounts of PLLA

same solvent, thus their solubility radii must have shared volume in HSP space. Looking at the HSP parameters for furosemide and polymers in table 3.1, all three polymer have a greater distance between them and furosemide than the solubility radius  $R$ . This is equal to a RED number above one, meaning that they are not alike. Based on the HSP values phase separation of the materials is expected. Therefore, the first option is unlikely and the second option is considered for the fabrication of a homogenous film. HSP is used to determine if the drug and polymer can be dissolved in the same solution. To be dissolved in the same solution the solubility spheres of the compounds must overlap and thus share a volume in Hansen space. This case is described in section 2.1.4 of the polymer theory. A blend of solvents is used in order to dissolve both furosemide and polymer. Table 3.2 shows solvent composition for dissolution of the frequently used materials in this project in blends of DCM/Dimethyl sulfoxide (DMSO) and DCM/Acetone. The table shows the optimal composition of solvents based on HSP calculations for the specific solvents and materials as well as the optimal composition based on lab experience.

Based on the HSP knowledge gathered, solutions containing furosemide and polymers are developed, especially with PCL as it is easy to work with in terms of molding. The melting point of furosemide is 203-206 °C [61]. The low melting point of PCL (60 °C) enables the furosemide PCL compound to be shaped while the furosemide remains intact. Experiments involving both solvent casting and spin coating have been conducted. Based upon initial experiments, spin coating gives the best results. For solvent casting either phase separation and/or rough surfaces are observed. Furthermore, it is difficult to obtain films in order of tens of microns in thickness. Generally, thicker films are produced by solvent casting. Due to these circumstances it was decided to focus on development of spin coated polymer drug films. Figure 3.1 shows three images of spin coated solutions with different ratios of furosemide to PCL and with different blends of DMSO, DCM and acetone. The main guidelines for mixing of solvents are shown in table 3.2 for furosemide and the polymer PCL, PAA and PLLA. Figure 3.1(a) shows a film where DCM, DMSO and acetone are used as solvents. The solution consists of 20 ml acetone, 10 ml DCM, 5 ml DMSO, 2 g furosemide and 3 g PCL. DMSO evaporates slowly while DCM and acetone evaporate fast. This results in the PCL going fast out of solution while the furosemide remains in solution in the DMSO. The furosemide concentrates at the top of the film resulting in an inhomogeneous film. Figure 3.1(b) and figure 3.1(c) show two films where DCM and acetone are used as solvents. The film shown in figure 3.1(b) is clearly inhomogeneous and exhibits phase separation while the film shown in figure 3.1(c) is homogeneous. The difference in the films is clearly visible, although the solutions are only slightly different. The solutions consist of the following ratios between acetone:DCM, furosemide:PCL and combined weight percent of furosemide and PCL. Solution of 3:1, 1:3 and 16.2 wt% for figure 3.1(b) and 2:1, 1:4 and 17.2 wt% for figure 3.1(c). The difference in acetone to DCM ratio is a consequence of the difference in the amount of furosemide for the solutions and is needed in order to properly dissolve all the furosemide. The solutions used for spin coating of films are summarized in table 3.3.

The film shown in figure 3.1(c) represents the highest amount of furosemide achieved in a PCL film while still having a homogeneous material. The solution used for the film



Table 3.3: Table showing the solutions used for the spin coating of films shown in figure 3.1.

Figure	Solvents [ml]	Furosemide [g]	PCL [g]
3.1(a)	DCM/DMSO/Acetone 20/10/5	2	3
3.1(b)	DCM/Acetone 10/30	1.5	4.5
3.1(c)	DCM/Acetone 10/20	1	4

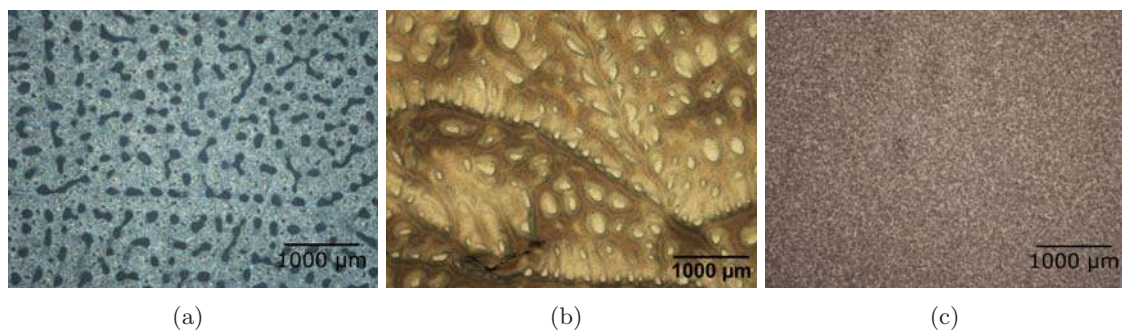


Figure 3.1: The figure shows three images of spin coated solutions containing furosemide and polycaprolactone. a) shows a film where DCM, DMSO and acetone are used as solvents. DMSO evaporates slowly while DCM and acetone evaporate fast. This results in the PCL quickly going out of solution while the furosemide remains in solution in the DMSO. The furosemide concentrates at the top of the film in a highly non uniform film. b) and c) show two films where DCM and acetone is used as solvent. The ratio of furosemide to PCL is 1:3 for b) with a 16.2 wt% solution, while it is 1:4 for c) with a 17.2 wt% solution. The film shown in b) exhibits clear phase separation while the materials are well distributed in c).

shown in figure 3.1(c) has been used for filling of micro containers. Figure 3.2 shows an example of a PCL furosemide blend, where the amount of furosemide is higher than 20 %. While it is possible to achieve a relatively homogenous film by spin coating, heating of the polymer film results in spherulites formation. If the furosemide precipitates out of the PCL matrix forming spherulites or if the PCL forms spherulites is uncertain. There are two situations that likely can occur; 1) the furosemide acts as a filler in the polymer and thus the furosemide acts as a nucleation site for the formation of PCL spherulites. 2) the furosemide forms crystals when heated to 100 °C and thus furosemide precipitates out of drug matrix. The first case has not been observed for PCL furosemide films with 20% furosemide or less, which suggest that the second case is observed.

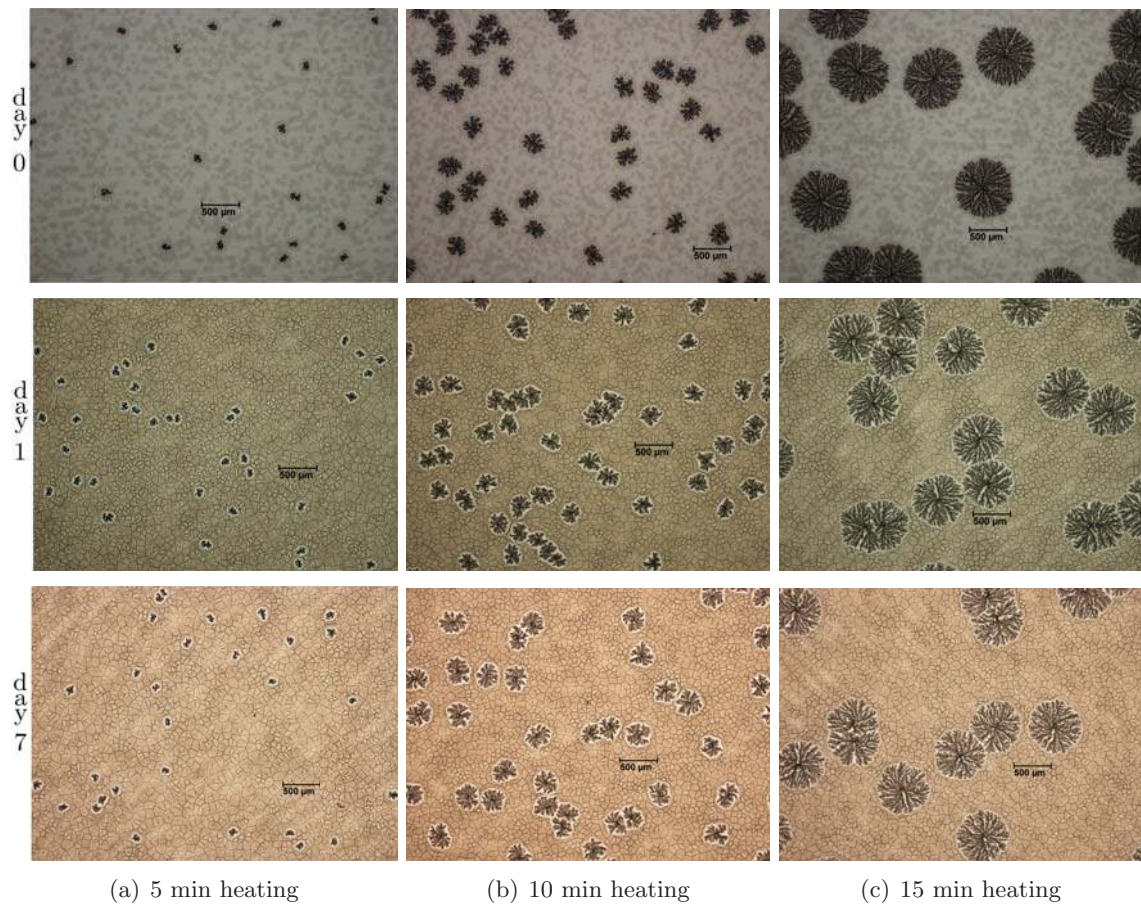


Figure 3.2: Optical microscope images of spin coated solution of furosemide and polycaprolactone. Column (a), (b) and (c) shows films that have been annealed on a hotplate at 100 °C for 5,10 and 15 minutes respectively. The top row shows images right after the annealing. The middle row 1 day after annealing and the bottom row 7 days after annealing.

## 3.2 Drug matrix characterization

A set of experiments based on the optimized polymer drug matrix seen in figure 3.1(c) is conducted. A total of six different batches are used to evaluate the effect of heat treatment (Room temperature, 60 °C for 10,30,60 min, 100 °C for 60 min.) and pressure treatment (embossing 60 °C for 60 min at 1.9MPa) on the drug release and conformation of the polymer- drug films. The objective is to evaluate the stability of the PCL furosemide drug matrix during processing. This section will describe the experiment and all the results except for the drug release which is covered in chapter 7.

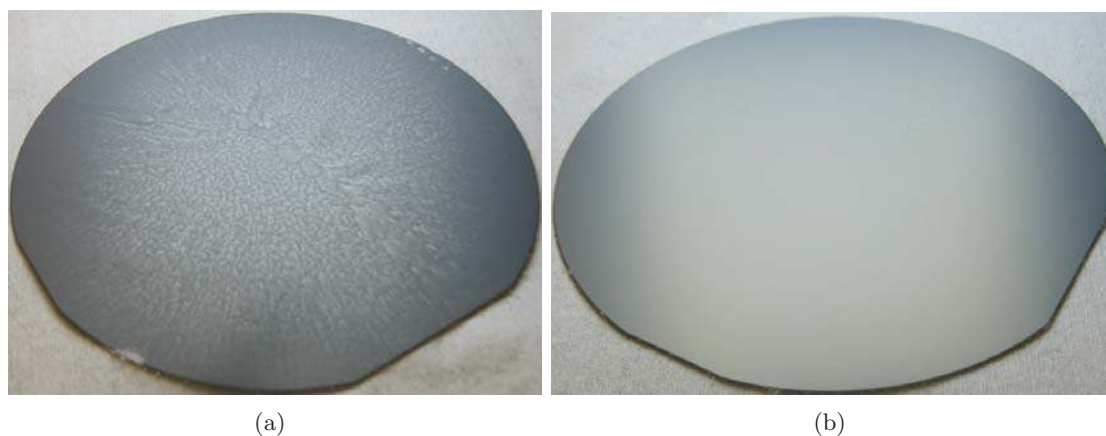


Figure 3.3: The figure shows spin coatings of a solution consisting of 2 g of furosemide, 8 g of PCL, 40 ml of acetone and 20 ml of DCM on silicon wafer. It illustrates the importance of dispensing the solution in the center of the wafer and in a swift manner. a) shows an unsuccessful attempt while b) shows a successful spin coating process.

### 3.2.1 Experiment and Methods

The polymer-drug films are fabricated by spin coating of a solution consisting of 2g of furosemide, 8g of PCL, 40ml of acetone and 20ml of DCM on silicon wafers with a fluorocarbon anti-sticking coating [62]. The polymer-drug solution is dispensed on the silicon wafers rotating at 200 RPM. The wafers are then accelerated at 2000 RPM/s to rotate at 1000 RPM for 60 s. The resulting film thickness is 15  $\mu\text{m}$  measured after 48 hours of degassing in a fume hood. Thicker films can be fabricated by repeating the spin coating process. Figure 3.3 shows silicon wafers spin coated as described above. The solution dispensing needs to be swift and precise in the center of the wafer. Otherwise, the spin coating results in an inhomogeneous film as shown in figure 3.3(a). If the spin coating is performed properly, the result is a smooth and homogeneous film with a slightly opaque look as seen in figure 3.3(b). The heating of the films is done using a hotplate and the subsequent cooling is done by placing them on a metal table at room temperature. The films reach room temperature within a few seconds. The films are heated to 60 °C for periods of 10, 30 and 60 min and to 100 °C for 1 hour. The pressure is applied using an EVG NIL imprinter capable of exerting a pressure of 1.9 MPa. The films are pressed for 60 min at 1.9 MPa at a temperature of 60 °C. For characterization, the films are cut into discs with a diameter of 9 mm using a carbon dioxide laser. For ease of handling the films are placed on carbon pads (Agar scientific, carbon tabs). The polymer drug morphology is studied by optical images and x-ray diffraction. For the x-ray diffraction an X'Pert PRO X-ray diffractometer (PANalytical, Almelo, The Netherlands) is used with the following settings; 45 kV; 40 mA, starting angle of  $5^\circ 2\theta$  and an end angle of  $35^\circ 2\theta$ .

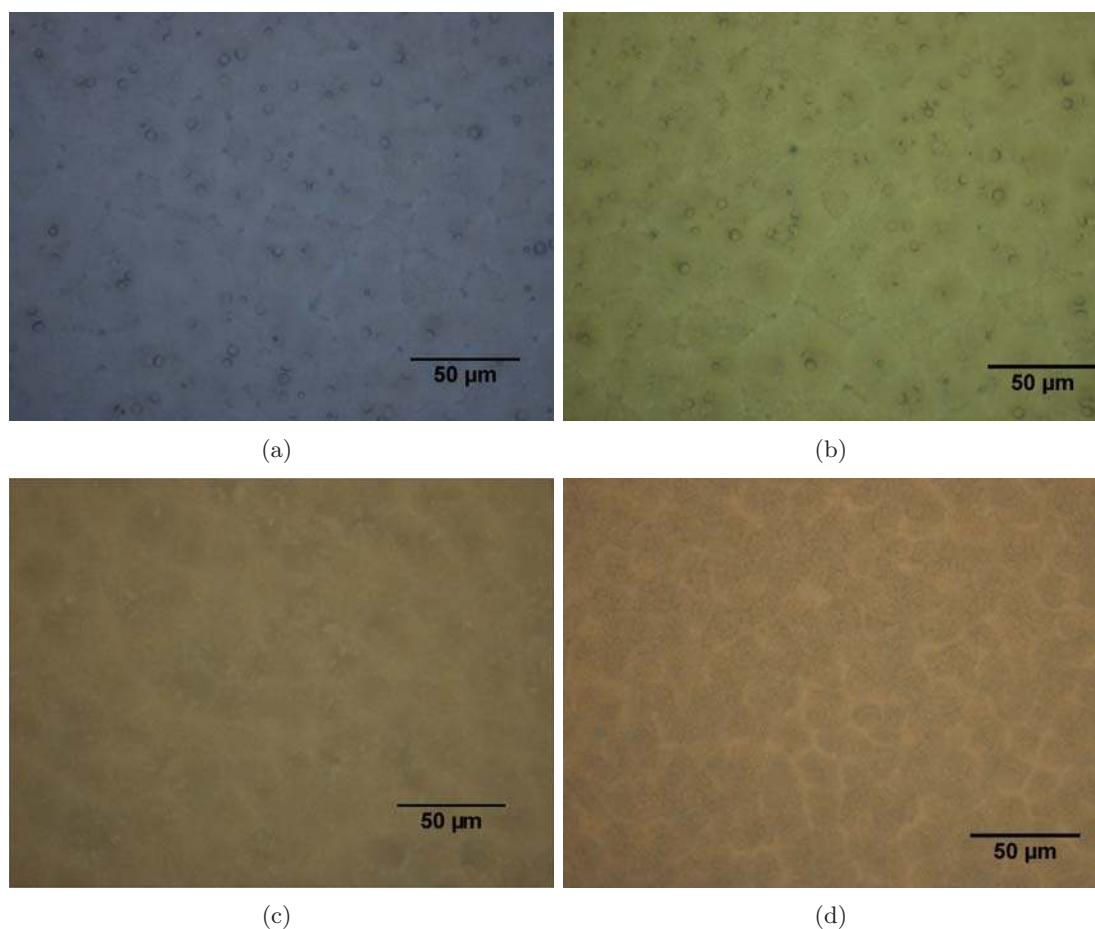


Figure 3.4: Optical images at 50x magnification showing the drug matrix. a) with no treatment, it is seen that the film is porous. b) with 60 °C for 1 hour, still with porous structures. c) embossed at 60 °C, 1.9 MPa for 1 hour, film without porous and a smooth surface. d) heated at 100 °C for 1 hour, film without porous and a smooth surface.

### 3.2.2 Results and discussion

A total of six different batches are used to test the effect of heat and pressure treatment on the morphology of the polymer- drug films. Figure 3.4 shows optical inspection by microscope with a magnification of 50 times. Figure 3.4(a) shows the fabricated film without any treatment. Figure 3.4(b) shows the film after annealing at 60 °C for 1 hour. Figure 3.4(c) shows the film after embossing at 60 °C for 1 hour with a pressure of 1.9MPa. Figure 3.4(d) shows the film after annealing at 100 °C for 1 hour. The figures reveal that the film contains porous structures with a pore size around 5-10 μm after spin coating. The experiments show that it is possible to remove the porous structure by embossing or annealing of the film above the melting point of the polymer. Heating at 60 °C does not remove or reduce the porous structures while heating at 100 °C does. The film changes



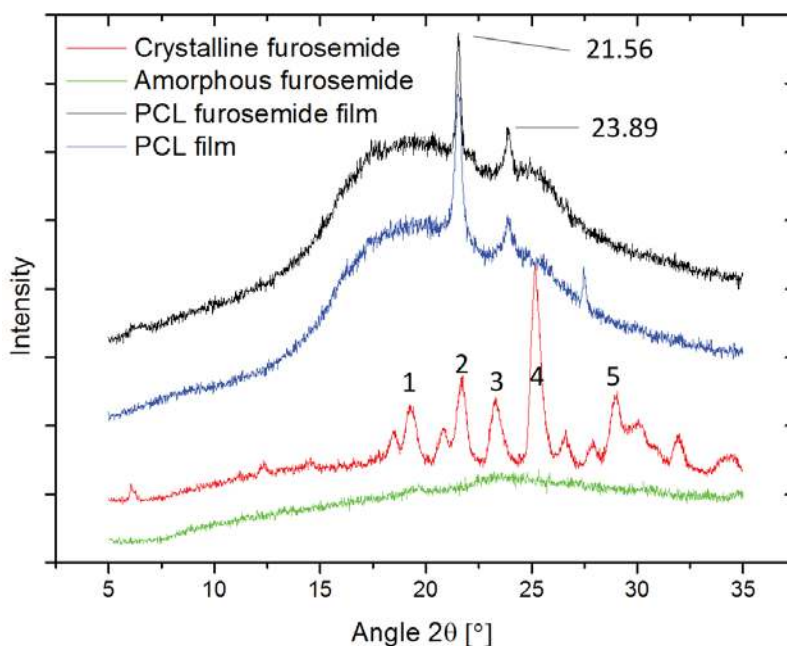


Figure 3.5: Graph showing the x-ray diffraction data obtained for; crystalline furosemide, spray dried amorphous furosemide, a spin coated PCL film and the spin coated drug matrix. Both the drug matrix and PCL film have a carbon pad as support substrate for handling. The curves are offset for a clear peak visualization.

color when heat treated. The untreated film appears blue due to the blue wafer substrate, whereas the heat treated films occur more opaque. The optical images show that grain boundaries become more apparent after annealing and this change in the polymer structure can account for the change in optical appearance.

The morphology of the furosemide and polycaprolactone is studied using X-ray diffraction (XRD). Figure 3.5 shows the XRD spectra of crystalline and amorphous furosemide powder along with the pure polymer film and the drug matrix. The amorphous furosemide does not show any characteristic peaks, as expected. The crystalline furosemide shows five characteristic peaks at  $19.26^\circ$ ,  $21.74^\circ$ ,  $23.3^\circ$ ,  $25.18^\circ$ , and  $29.05^\circ$ . This matches well with other reported data on crystalline furosemide [63, 61], though with a slight upward shift in the  $2\theta$  angle. The most distinct peak (nr. 4) is reported at  $24.7^\circ$ - $24.8^\circ$  and is found at  $25.18^\circ$  in figure 3.5. The PCL film shows two peaks at  $21.56^\circ$  and  $23.89^\circ$ . This matches the peaks reported for semi crystalline PCL at  $21.4^\circ$  and  $23.6^\circ$  [64]. The PCL furosemide drug matrix shows two peaks matching the peaks found for PCL exactly. This shows that furosemide is in an amorphous state after the drug matrix is spin coated. A reason for this could be that the spin coating process acts as a quenching of the furosemide and thus hinders crystallization. Figure 3.6(a) shows the XRD curves obtained for the samples that are embossed and heat treated at  $60^\circ\text{C}$ . The spectra obtained show peaks at the characteristic semi-crystalline PCL peaks as observed with the non treated film. It seems that the heat treatment at  $60^\circ\text{C}$  does not affect the morphology of the drug matrix.

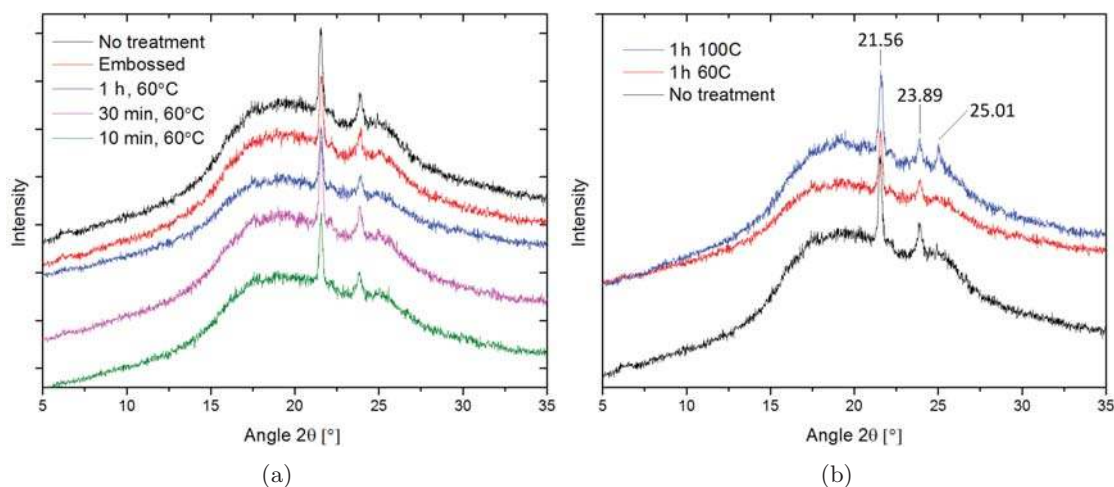


Figure 3.6: Graphs showing the x-ray diffraction data obtained for different treatments of the drug matrix. Drug matrix samples heated on a hotplate at; 60 °C for 10,30,60 minutes, 100 °C for 60 minutes and embossed at 60 °C for 60 min at 1.9 MPa. The non treated drug matrix is plotted as reference. The curves are offset for a clear peak visualization.

This corresponds to the observations made with the optical microscopy inspection. The addition of pressure in form of the embossing process does not alter this result. Figure 3.6(b) shows the spectra obtained for the sample heated at 100 °C. An additional peak at 25.01 is observed. The peak matches well with the most pronounced peak observed for the crystalline furosemide in figure 3.5. It is likely that the elevated temperature facilitates the formation of crystalline furosemide in the drug matrix. Crystallization of amorphous furosemide is reported to occur at temperature 80-100 °C [63]. The results obtained from the XRD and the microscopy suggest that the furosemide is amorphous and that it does not change during processing with temperature of 60 °C. For processing at temperatures of 100 °C furosemide crystallinity is observed. The results indicate that the morphology of the furosemide can be tuned by heat treating the drug matrix.

### 3.3 Summary

On the basis of HSP a polymer drug matrix is developed. The matrix consists of furosemide and PCL. The compounds are dissolved in organic solvents, DCM and Acetone to form a solution which can be spin coated to form films. For fabrication of a homogeneous film the highest possible content of furosemide in PCL is 20%. If the content of furosemide is higher, there is a high risk of phase separation during spin coating. X-ray diffraction shows that the furosemide is in amorphous form after spin coating and remains in this form after heat- and pressure treatments at 60 °C. For heat treatments at 100 °C crystalline furosemide is observed.



# Chapter 4

## Stamps

This chapter covers all the stamps fabricated in this project, from fabrication process to durability. Many stamps have been fabricated in the project in three different materials, SU-8, silicon and nickel. First, the fabrication processes are described along with the design, then a comparison of the stamps is given along with recommendations. The development of deep reactive ion etches (DRIE) enabling the fabrication of nickel and silicon stamps is then described.

### 4.1 Fabrication

The following sections contain a description of the processes used for fabricating stamps while the detailed process flows for each stamp fabrication can be found in appendix G, H, I. The stamps are fabricated at the DTU Danchip cleanroom facilities. The techniques used for the fabrication are; photolithography, wet and dry etching, metal deposition by evaporation and sputtering, electro plating, cutting and dicing. For knowledge on theory and principles of the techniques the reader is referred to [55, 65, 56].

#### 4.1.1 Design

The design of the stamp is based on previous experience with nano imprint lithography (NIL) and work carried out in the Nanoprobes group, where NIL was used to fabricate arrays of polymer cantilever chips [66]. The stamps are to be used in a hot embossing process of thick polymer films. The less material that needs to be displaced in order to obtain the wanted shape, the faster the embossing will be. For this reason it is chosen to have the stamp structures "stick out" of the stamp surface, as this will result in the least amount of material displaced in the hot embossing process. For information on the hot embossing technique the reader is referred to [67]. Figure 4.1 shows the stamp design. The stamp is divided in 16 squares, each square with 20 by 20 individual units. With each square containing 400 units, the total amount of units is 6400. Thus the stamp design enable the fabrication of 6400 containers. Figure 4.1(b) shows an individual unit. It consists of two parts, an inner disc and an outer ring structure. There are three important parameters for this unit. 1) The diameter of inner disk, which translates into the inner



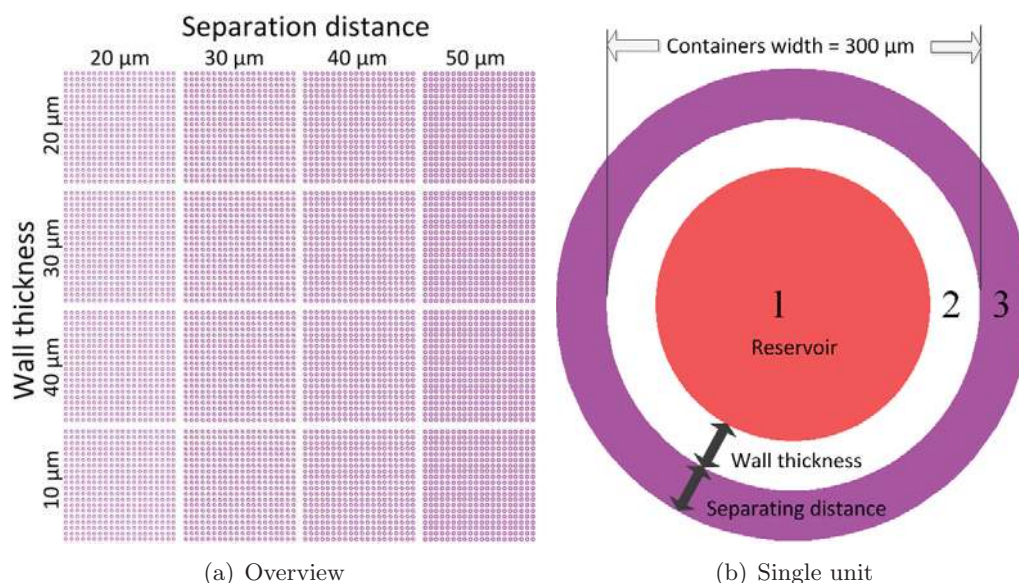


Figure 4.1: The figure shows the design layout. a) shows how the 16 squares with the various design parameters are placed. b) shows a single unit design. 1, the inner diameter of the micro container, 2, the width of the container wall and 3, the separation distance of the container to the surrounding polymer film.

diameter of a micro container, 2) the distance between the disc and ring structure, which corresponds to the width of the micro container wall and 3) the outer ring structure, which is the distance that the micro container is separated from the polymer film surrounding the micro container. This design is referred to as the cookie cutter design. The total width of the containers is kept constant at  $300 \mu\text{m}$ . The wall thickness is varied  $10\text{-}20\text{-}30\text{-}40 \mu\text{m}$  and thus the inner diameter varies  $220\text{-}240\text{-}260\text{-}280 \mu\text{m}$ . The separation distance to the polymer film is varied  $20\text{-}30\text{-}40\text{-}50 \mu\text{m}$ . The variations in design are chosen to test how thin the sidewalls can be while still maintaining their stability and to test if the thickness of the cookie cutter affect the wall formation.

## 4.2 SU-8 stamps

SU-8 is a negative epoxy photoresist that is widely used in micro and nanotechnology. It was originally developed by IBM in 1989 [68]. The SU-8 stamps are fabricated on silicon wafers, working as a stabilizing support substrate for the SU-8 structures that are made by photolithography. The main components of the stamp are two thick layers of SU-8. The thickness of the first layer determines the depth of the micro containers, while the second layer determines the bottom thickness of the micro container. Figure 4.2 shows the major steps in the fabrication of the SU-8 stamps. First, a layer of SU-8 is spin coated and soft baked on a hotplate. Second, the SU-8 layer is illuminated through a mask to pattern the SU-8 followed by a post exposure bake on a hotplate. Third, a

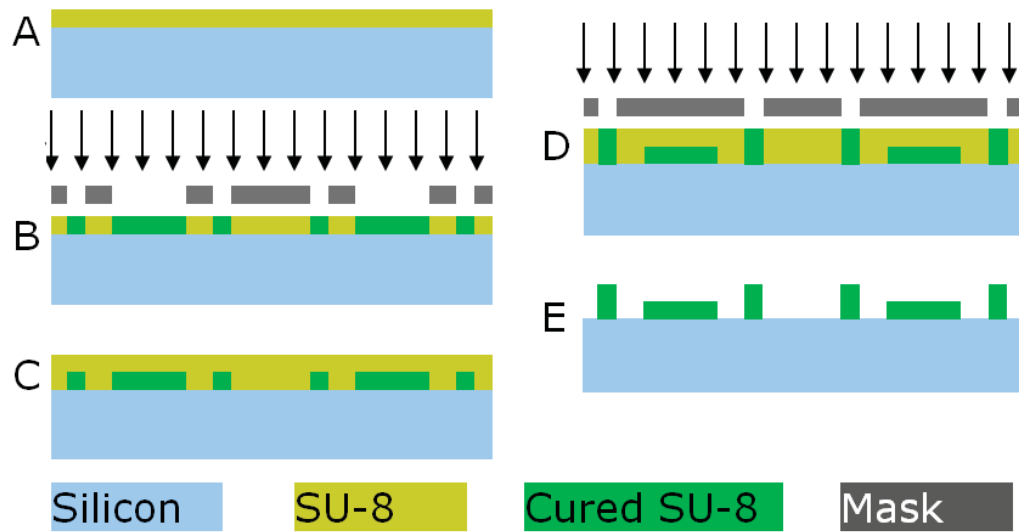


Figure 4.2: Schematic showing the five major steps in the fabrication of SU-8 stamps. A, a layer of SU-8 is spin coated and soft baked on a hotplate. B, the SU-8 layer is illuminated through a mask to pattern the SU-8 followed by a post exposure bake on a hotplate. C, another layer of SU-8 is spincoated and baked. D, the SU-8 is illuminated again through a mask to pattern the second SU-8 layer. E, both layers of SU-8 are developed in PGMEA.

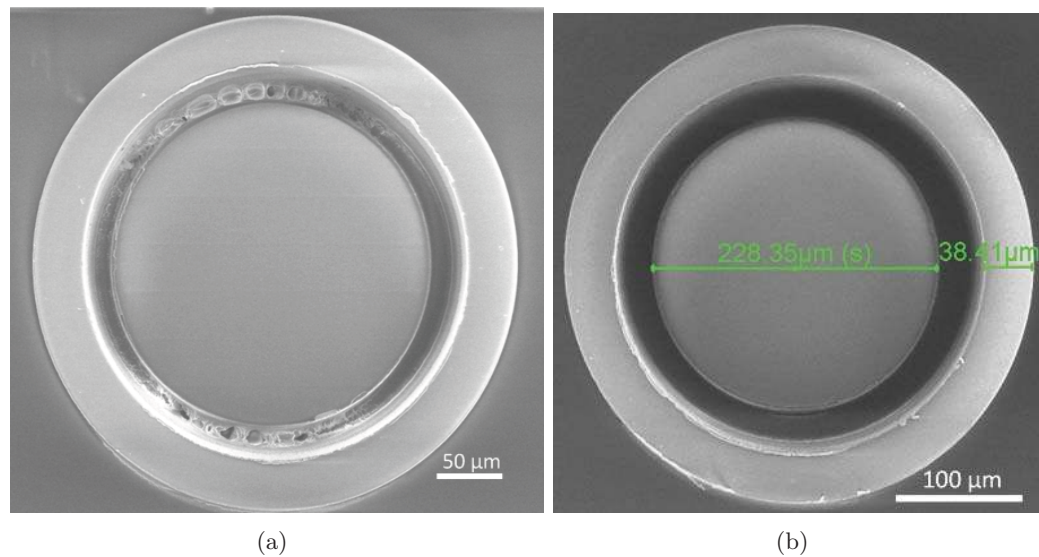


Figure 4.3: SEM images of SU-8 stamps. a) shows a stamp that is overexposed and where SU-8 residues remain in the trench defining the container wall. b) shows a stamp fabricated with the optimized process recipe. The result is a well defined structure with vertical sidewalls.

second SU-8 layer is spincoated and baked. Fourth, the second SU-8 layer is patterned by photolithography. Fifth, both layers of SU-8 are developed in propylene glycol methyl ether acetate (PGMEA). The tricky part of the fabrication is to find the right exposure dose for the SU-8. In the optimal case, the process produces vertical sidewalls which is a requirement for a successful embossing process. To achieve this, the SU-8 receives a high exposure dose, to ensure that the lower part of the film cross links properly. To avoid heating of the upper part of the SU-8 film, the exposure is done in intervals with 30 s cooling cycles between each exposure. Figure 4.3 shows SEM images of single SU-8 stamp units. Figure 4.3(a) shows a case where the top part of the first SU-8 layer received such a high exposure dose that the inner disk is connected to the outer ring structure. Small residual structures remain in the trench. Figure 4.3(b) shows the optimized stamp process, where vertical sidewalls and well defined structures are achieved. The details of the optimized process are found in appendix G. The unit shown in figure 4.3(b) has the following design parameters; 220  $\mu\text{m}$  inner diameter, 40  $\mu\text{m}$  wall thickness, 30  $\mu\text{m}$  separation distance. It is seen that the actual sizes of the SU-8 structures are larger and that the SU-8 is overexposed by roughly 4  $\mu\text{m}$ .

### 4.3 Silicon

Figure 4.4 shows the process for fabricating stamps in silicon wafers. The process is composed of four main components; deposition and patterning of two layers of masking material and two subsequent DRIE etches. The process starts by defining the first etch mask in aluminium. Photoresist is spin coated, patterned by positive photolithography followed by development. An aluminium layer is deposited by e-beam evaporation followed by a liftoff process to make the first etch mask pattern. This is step A-D in figure 4.4. The second etch mask is defined in photoresist by a negative photolithography step. Step E-G show spin coating of photoresist, photolithography and development. The wafer is now ready for the two etching processes. The depth of the first etch determines the height of the container walls, while the second determines the container bottom thickness. Step H-I shows the first DRIE process and the removal of the photoresist etch mask by plasma asher. The DRIE process is an anisotropic process that allows for etching in one direction. This process effectively trims down the wafer except where the etch masks protect the wafer. By having two etch masks it is possible to obtain two different heights for the structures defining the outline of the container and the inner part of the container. Step J shows the last DRIE process, where the container bottom thickness is defined. A detailed process flow can be found in appendix H. Figure 4.5 shows the fabricated silicon stamps. The unit shown in figure 4.5(b) has the following design parameters; inner diameter of 220  $\mu\text{m}$ , wall thickness of 40  $\mu\text{m}$  and separation distance of 30  $\mu\text{m}$ . It is seen that the fabrication of the silicon stamp is within a couple of  $\mu\text{m}$  from the design parameters.

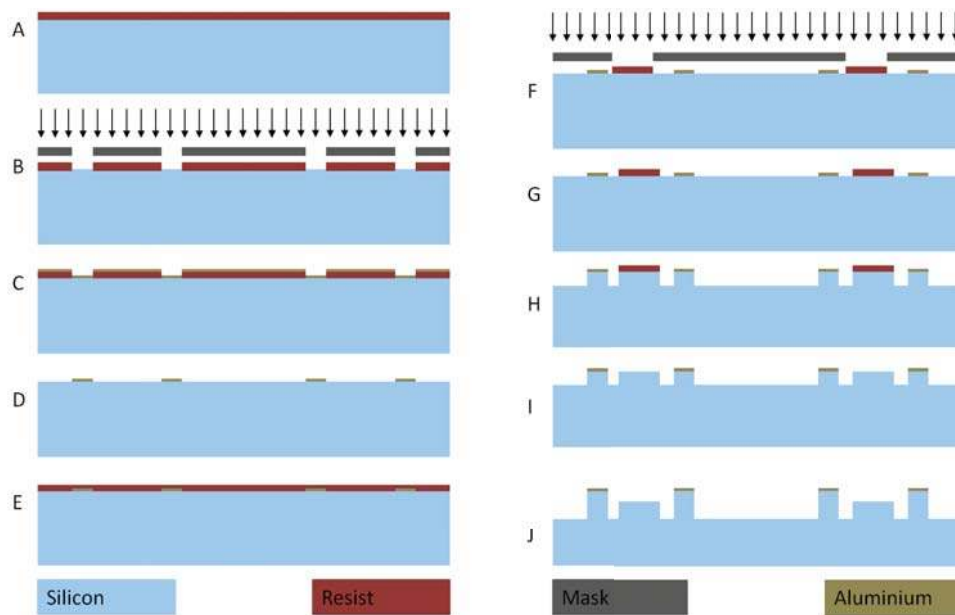


Figure 4.4: Schematic showing the major steps in the fabrication of silicon stamps. A) Deposition of resist by spin coating. B) Patterning by positive photolithography. C) deposition of aluminium by thermal and e-beam evaporation. D) Lift-off of excess aluminium. E) Deposition of resist by spin coating. F-D) Patterning by negative photolithography. H) Anisotropic etch by DRIE process. I) Removal of photoresist by plasma asher. J) Anisotropic etch by DRIE process.

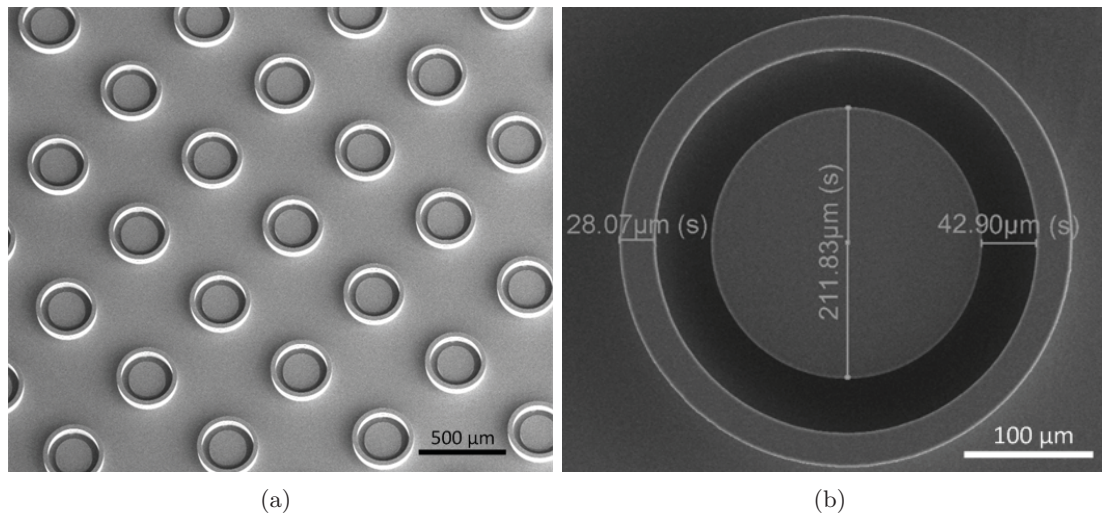


Figure 4.5: SEM images of silicon stamp. a) shows an overview of the stamp with several units. b) shows a single unit and the measured design parameters.

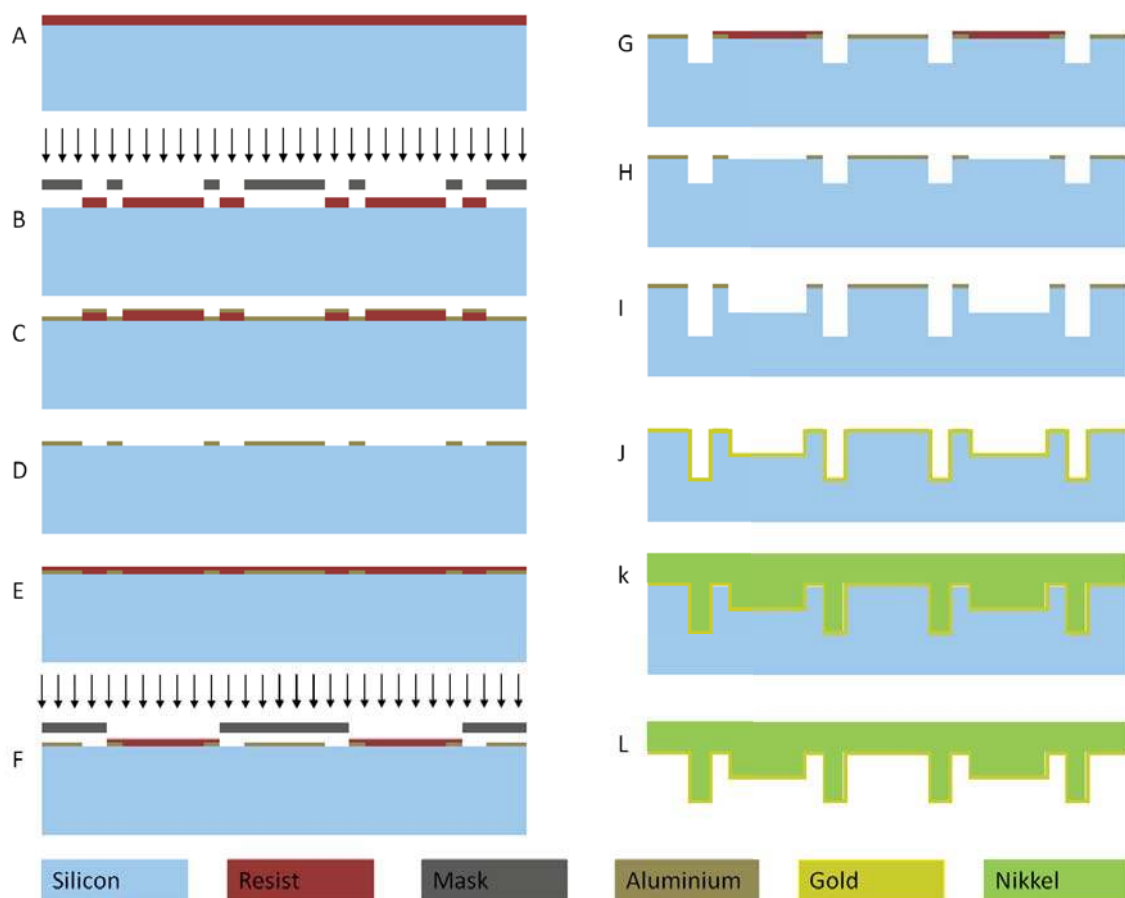


Figure 4.6: Schematic showing the major steps in the fabrication of nickel stamps. A) Deposition of resist by spin coating. B) Patterning by negative photolithography. C) deposition of aluminium by thermal and e-beam evaporation. D) Lift-off of excess aluminium. E) Deposition of resist by spin coating. F) Patterning by negative photolithography. G) Anisotropic etch by DRIE process. H) Removal of photoresist by plasma ash. I) Anisotropic etch by DRIE process. J) Deposition of gold by sputtering. K) Electroplating of nickel. L) Silicon removal by KOH etching.

## 4.4 Nickel

The fabrication of nickel stamps resembles the fabrication of the silicon stamps, as it includes two etch masks and two DRIE steps. The difference is that the silicon acts as a mold rather than as the stamp itself. For this reason the structures are etched into the substrate instead of sticking out. Once the silicon mold is fabricated a seed layer is deposited on the entire surface of the mold and nickel is electroplated on top of it. The mold is then removed by etching it.

Figure 4.6 shows the entire nickel stamp process. First, the aluminium etch mask is deposited and patterned by photolithography of a photoresist followed by a liftoff process,



step A-D. Second, the photoresist mask is spun and patterned by photolithography, step E-F. Third, DRIE process and removal of photoresist etch mask, step G-H. Fourth, second DRIE process. The silicon mold is now complete and the electro plating of the nickel can start. A gold seed layer is sputtered on the entire mold surface and the mold is submerged in a nickel plating bath, step J-K. Once the electro plating is complete, the wafer is rinsed in water and submerged into a KOH bath, where the silicon is etched away. Occasionally, a heightened edge arises from the electro plating process which is removed by cutting away the outer 1 cm of the nickel stamp. This marks the end of the fabrication and the stamp is ready for use after rinse in water.

## 4.5 Stamp comparison

As described stamps in three materials, SU-8, silicon and nickel are produced. SU-8 stamps are good for prototyping as they are fast to produce and many can be produced rapidly with a simple photolithography process. The downside of the SU-8 stamps are that they quickly build up a significant amount of flaws during the embossing process. This can for example be delamination of single or multiple units during the release of the stamp after embossing or minor deformations. The addition of an anti-sticking coating only provides a minor prolongation of the lifetime of the SU-8 stamps. Adding a thin SU-8 layer below the two layers containing the structures decreases the delamination of structures. Generally, the SU-8 stamps can be used for 5-10 experiments. Silicon is a strong material and is widely used for stamps in the NIL industry. The fabrication of the silicon stamps is longer than for SU-8 and not as suitable for a large production as it contains several single wafer processes. Especially the deposition of aluminium and the DRIE processes are time consuming. Unfortunately, the silicon stamps turned out to be very fragile and cracking of stamps during the separation of stamp and embossed film occurred frequently, contrary to expectations. The reason for the cracking is believed to be caused by the relative large amount of silicon removed during the DRIE process, exposing defects and/or creating them in the silicon wafer. Cracking of the silicon wafers is not observed for the support wafers used for the SU-8 stamps and thus the processing of the silicon must weaken the strength of the material. Due to the cracking problem, the silicon stamps perform poorly and can generally only be used for 1-2 experiments. A better and stronger solution than both the silicon and the SU-8 is desired for stable and repeatable container embossing process. For this reason the attention is turned to nickel which is a very strong material without the brittle properties of silicon. It is used in industry for replication of DVD's among other processes requiring a very high throughput and thus durability. It incorporates well in the developed silicon technology used for the silicon stamp and nickel can be deposited / grown by electroplating on a seed layer. The fabrication process of a nickel stamp resembles the silicon stamp process with an extra deposition of a seed layer followed by electro plating and removal of the silicon mold. Thus the process is more time consuming, though the final result is a highly durable stamp with precision of silicon fabrication technology. The strength of the nickel stamps depends on the speed of the electro plating process. The slower the deposition of nickel is, the more

Table 4.1: Comparison of SU-8, silicon and nickel stamps. Precision denotes deviation of the actual fabricated structures from the mask design.

Material	Precision	Fabrication time	Anti-sticking coating	Durability
SU-8	+4 $\mu\text{m}$	< 1 week	Minimal improvement	< 5-10 experiments
Silicon	+2 $\mu\text{m}$	< 2 weeks	Minimal improvement	< 2 experiments
Nickel	+3 $\mu\text{m}$	< 3 weeks	Not needed	>50 experiments

dense and stiff the nickel will be. The deposition of 500  $\mu\text{m}$  nickel can be done in 4 hours, though it is recommended to do this over a 12-24 hours period to achieve a denser and more stiff nickel. This lowers the risk of stamp deformation in the final cutting process. The nickel stamps fabricated remain without noteworthy faults after many embossing experiments. Table 4.1 summarizes the three different stamp materials and their respective performances. The precision describes the difference between fabricated structure size and mask design. Some of the processes will inevitably result in a different size than that of the mask design and is by no means a measure of a bad process. The information provides a basis to design structures of desired dimensions if one are to follow the given processes. The fabrication time provides a realistic time frame for fabrication of the stamps at the Danchip cleanroom facilities. Faster fabrication is possible, though delays often occur due to machine use and service. Anti-sticking coatings developed by Keller et al. [62] and from a "Applied Microstructures MVD 100 system" are tested for the SU-8 and silicon stamps. The coatings improve the separation process after embossing, but do not extend the lifetime of the stamps significantly. The durability summarizes the number of experiments that one can expect from the given stamps. For the nickel stamp this number could very well be significantly higher as no faults are observed after extensive use. For hot embossing experiments similar to the ones performed in this project with thick films it is advised to use nickel stamps as they are the most robust stamps and can be fabricated with the same precision as the silicon and SU-8 stamps.

## 4.6 DRIE process development

The deep reactive ion etch processes used in the stamp fabrication are important for the functionality of the stamps. The etch must produce structures where the sidewall is either vertical or with a slope that allows the stamp to be separated from the embossed polymer film without compressing the polymer in the separation. Figure 4.7 shows a graphical representation of this. Figure 4.7(a) shows a situation where separation of the stamp is easy, as the tips of the stamp are narrower than the base structure. Figure 4.7(b) shows the opposite situation where the tips are wider than the base structure. To separate the stamp from the film, the film will be compressed during separation or the film will rupture if separation is even possible. Situation (a) is referred to as positive sidewall slope and situation (b) as negative sidewall slope. Two DRIE processes are developed to accommodate positively sloped sidewalls. The standard mode of operation for DRIE

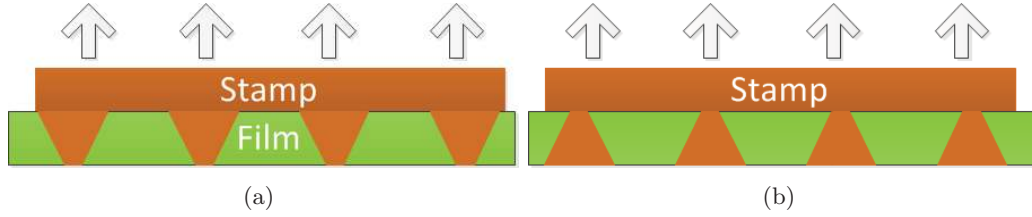


Figure 4.7: a) shows an example of sloped sidewalls on a stamp that allows for separation. b) shows an example of sloped sidewalls acting as hooks, not allowing for separation.

Table 4.2: DRIE process parameters used in the SPTS Pegasus DRIE tool at Danchip to obtain positively sloped sidewalls. Dep denotes the passivation deposition and etch denotes the etching cycle for the Bosch process. - denotes parameters changing throughout the process with the start and the end value. The Bosch process is run at 0 °C while the continuous process is run at 10 °C.

Process Name	Mode	Pressure [mTorr]	Coil/Platen Power [W]	Gas flow [sccm]	Cycle time [s]
JNA-D4	Bosch	dep 20 etch 26	dep 2000 / 0 etch 2500 / 35	$C_4F_8$ : 150 $SF_6$ : 275 $O_2$ : 5	dep 2 etch 2.4
Stamp etch	Continuous	230-90	2800 / 170-215	$SF_6$ : 180 $O_2$ : 160 $Ar$ : 160	N/A

tools at Danchip are Bosch processes<sup>1</sup> where time multiplexed etching alternates between two modes. One mode where an isotropic etch removes silicon and another mode where a passivation layer is deposited. The passivation layer is repeatedly removed in the bottom by ion etching/bombardment, while the passivation on the sidewalls remains intact. In this way an anisotropic etch is achieved. In collaboration with Danchip a Bosch process is developed to achieve positively sloped sidewalls on a SPTS Pegasus DRIE etch tool. The optimized Bosch process parameters are shown in table 4.2 along with a continuous process developed at a later stage. First, a description of the Bosch process is given with focus on the fabricated silicon structures used as molds for nickel stamps.

Figure 4.8 shows the structures produced with the Bosch DRIE process (JNA-D4). Figure 4.8(a) and figure 4.8(b) show reoccurring fabrication issues. Silicon pillars appear in the regions where the silicon is supposed to be etched away. The silicon pillars are believed to be an artifact of relatively equal ratio of etching to passivation time. Figure 4.8(c) shows a cross sectional view of a silicon mold broken approximately along the center. It is seen that the sidewalls are vertical in the upper part while they are positively sloped in the bottom. Increasing the etching cycle time produces vertical to slightly negatively sloped sidewalls.

<sup>1</sup>Process developed and patented by Robert Bosch GmbH i.e. United States Patent 6531068 and United States Patent 5501893 among others.



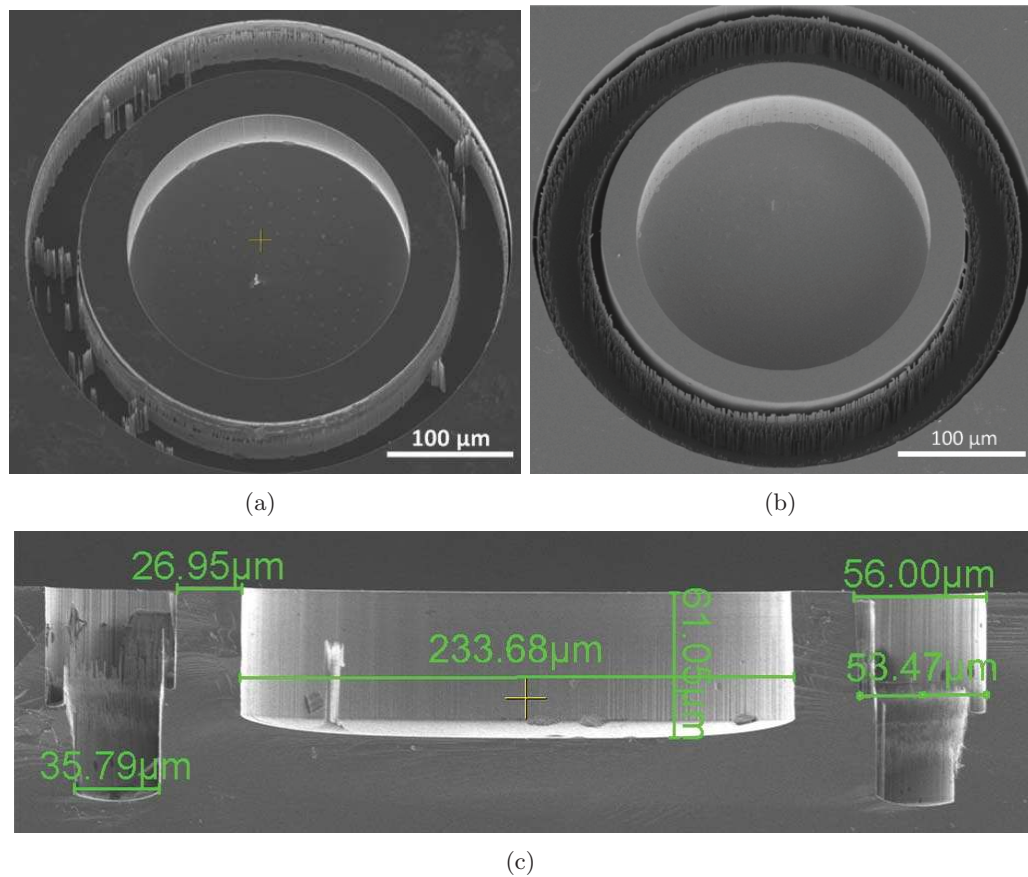


Figure 4.8: The figure shows SEM images after the second DRIE process in the fabrication of a silicon mold for electroplating of the nickel stamps. a) and b) shows typical issues observed after the DRIE process. a) shows sparsely scattered silicon pillars. b) shows silicon pillars mainly along the side of the deep trench. c) shows a cross-sectional view of a unit with the following design dimensions, inner diameter  $240 \mu\text{m}$ , wall width  $30 \mu\text{m}$ , separation distance  $50 \mu\text{m}$ .

As the silicon pillars have a large surface area they are easy to remove in an isotropic wet polysilicon etch. Figure 4.9 shows the etching of the same pillars at 0, 7 and 15 minutes of etch time. If the DRIE process produces profound scallops a trick to remove these is to oxidize the silicon and subsequently remove the silicon oxide. This will smoothen the surface. Using the Bosch process, well functioning nickel stamps are produced and used extensively. The process however has some drawbacks as shown in figures 4.8, 4.9 and a new DRIE process is developed. The new DRIE process does not utilize the Bosch concept. It is a continuous etch inspired by Li et al. [69] where DRIE etched via holes for three dimensional MEMS packaging are investigated. The optimized process parameters are listed in table 4.2 and figure 4.10 shows some of the results of the optimization. The process is run at a varying pressure. It starts as high as machine tolerances allow at 230

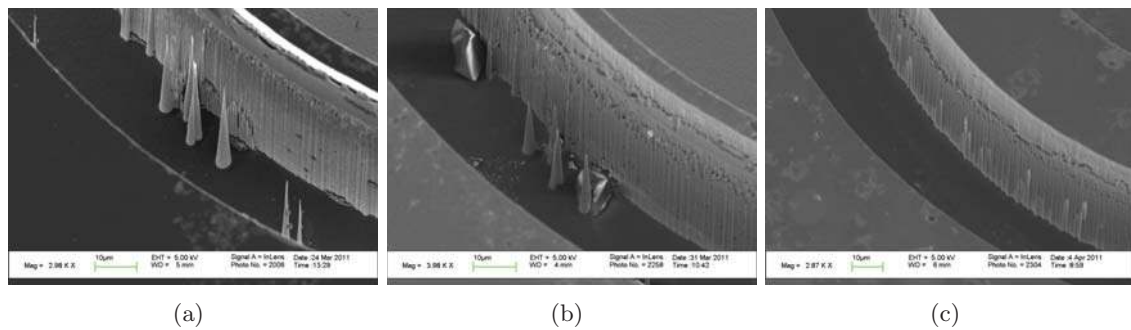


Figure 4.9: The figure shows SEM images of the same spot on a wafer after isotropic silicon etch for a) 0 minutes, b) 7 minutes, c) 15 minutes.

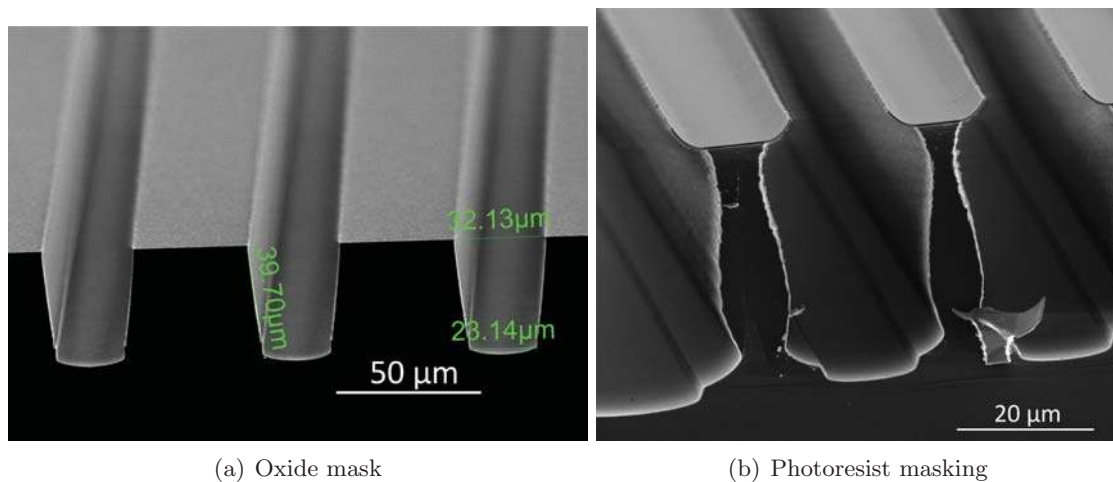


Figure 4.10: SEM images comparing the results of etching with an oxide mask and a photoresist mask.

mTorr and is then decreased to 90 mTorr linearly for the duration of the process. The coil power is kept constant at 2800 W while the platen power is varied linearly 170-215 W. The linear variations create positively sloped sidewalls as shown in figure 4.10(a). Figure 4.10 shows the difference between the use of a hard masking material such as aluminium and oxide and the use of photoresist as masking material when etching for an extensive period of time. Photoresist as masking material only works for short periods of etching and is successfully used for fabrication of stamps following the process described for the nickel stamp. Figure 4.11 shows a silicon mold fabricated with the continuous DRIE process. Figure 4.11(a) shows a silicon mold and figure 4.11(b) shows a zoom of the wall of that silicon mold. It is clear that the wall has a positive slope. Furthermore, no silicon pillars are produced with this DRIE process. Figure 4.11(c) shows a confocal microscopy scan of a silicon mold and figure 4.11(d) shows the data measured from that scan. The figures clearly show the container structure and the measurement shows that the height of the container is 87  $\mu\text{m}$  with a bottom thicknesses of 13-14  $\mu\text{m}$ . Figure 4.12(a) shows the mask

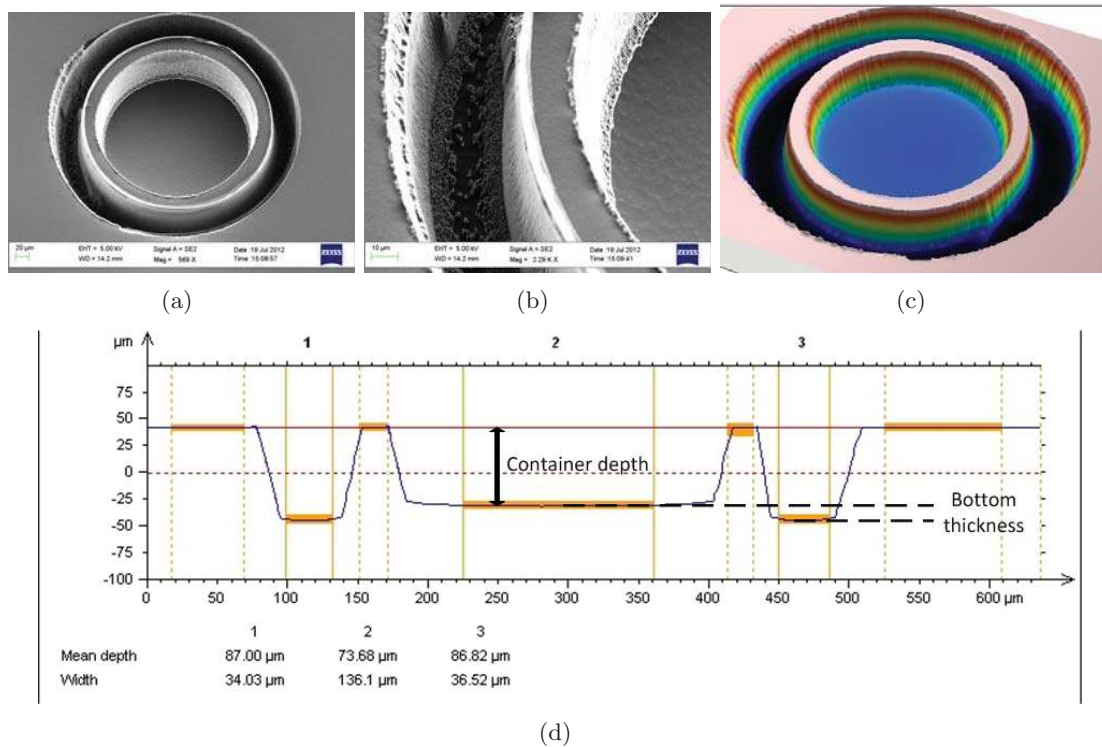


Figure 4.11: The figure shows SEM images of a silicon mold fabricated with the stamp etch process and a confocal microscopy scan of a silicon mold and the data obtained. It is seen that the sidewalls are positively sloped. The confocal microscopy scan shows that the bottom thickness of the container is roughly 13-14  $\mu\text{m}$  and that the reservoir depth is 73-74  $\mu\text{m}$ .

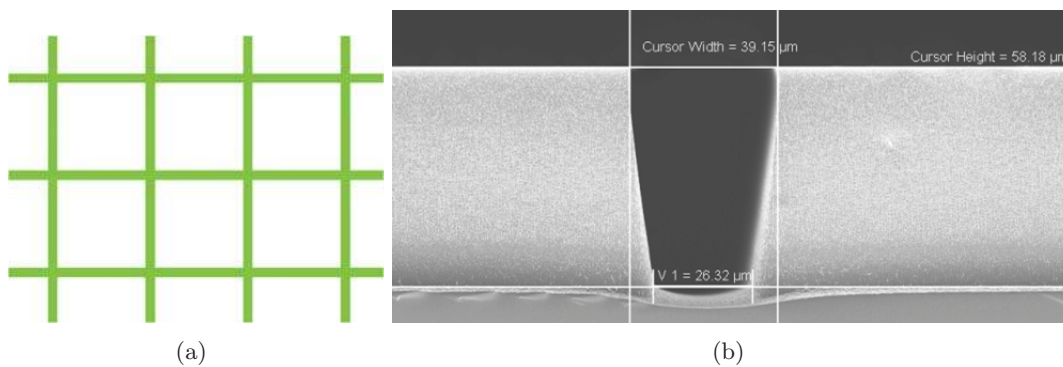


Figure 4.12: The figure shows a mask design and a SEM image of a silicon wafer etched with the continuous DRIE process. a) the mask design consists of squares of 300  $\mu\text{m}$  by 300  $\mu\text{m}$ . b) shows a cross-sectional view of a wafer broken along one of the etch lines.

design consisting of squares of  $300\ \mu\text{m}$  by  $300\ \mu\text{m}$ . Figure 4.12(b) shows a cross-sectional view of a wafer broken along one of the etch lines. The depth of the etch is  $58\ \mu\text{m}$  with a width at the top of  $39\ \mu\text{m}$  and a width at the bottom of  $26\ \mu\text{m}$ . If vertical is considered  $90^\circ$  and a positive slope is less than  $90^\circ$ , the slope of the sidewall in figure 4.12(b) is around  $77\text{-}78^\circ$ .

## 4.7 summary

Processes for the fabrication of stamps in SU-8, silicon and nickel have been presented. SU-8 is found to be suited for fast prototyping with the shortest fabrication time of the three materials, while nickel by far is the most durable and the preferred material for stamps used for extensive experiments. The only drawback of the nickel stamp compared to the SU-8 and silicon is the more time consuming fabrication process. The fabricated silicon stamps performed poorly and are not recommended for experiments similar to the ones performed in this project. It is believed that the brittle nature of silicon is the main cause for concern. DRIE processes producing sloped sidewalls for better release of stamps are developed. It is found that the slope of the sidewalls can be controlled by varying the pressure and platen power.



## Chapter 5

# Micro containers

This chapter covers the different micro containers fabricated in this project. First, the SU-8 container fabrication is described along with examples of different container designs. A short review of possible fabrication technologies is given along with arguments of why technologies are chosen or discarded. Then the micro containers fabricated in the FDA approved biopolymers polycaprolactone and polylactide acid [70] are described along with the hot embossing process used to do so.

### 5.1 SU-8 micro containers

The first prototypes of the micro containers are fabricated in the photosensitive epoxy resist SU-8. The process resembles the one described for the fabrication of SU-8 stamps in section 4.2. Figure 5.1 shows the fabrication process. A layer of SU-8 is spin coated on a silicon wafer and baked. The layer is then patterned by photolithography. The thickness of this layer defines the bottom thickness of the micro containers. A second layer of SU-8 is spin coated and patterned by photolithography. The thickness of this layer defines the height of the micro container walls. The patterning of the container in the two SU-8 layers is now complete and the SU-8 is developed in propylene glycol methyl ether acetate. The development removes the non exposed SU-8 leaving behind the micro containers on a silicon wafer. The exact process details for the containers are described in appendix F. Micro containers with different design parameters are fabricated to meet experiment criteria and to showcase different possibilities. The most used design is containers with an outer diameter of  $300\ \mu\text{m}$  and an inner diameter of  $200\text{-}260$ , thus varying the wall thickness from  $20\text{-}50\ \mu\text{m}$ . The height of the fabricated containers is varied as well and containers with a total height ranging  $85\text{-}300\ \mu\text{m}$  are realized. The SU-8 micro container process is a very flexible process and various geometries can be fabricated with it. Figure 5.2 shows some of the possibilities of the process. Figure 5.2(a) shows micro containers with four different diameters of  $50, 100, 150, 300\ \mu\text{m}$  and multiple compartments in the case of the squared containers with compartments sizes of  $20, 40, 60, 120\ \mu\text{m}$ . As seen in the figure the three largest container sizes are mechanically stable, while the smallest container is leaning a bit. Figure 5.2(b) shows containers with a diameter of  $300\ \mu\text{m}$  and varying wall

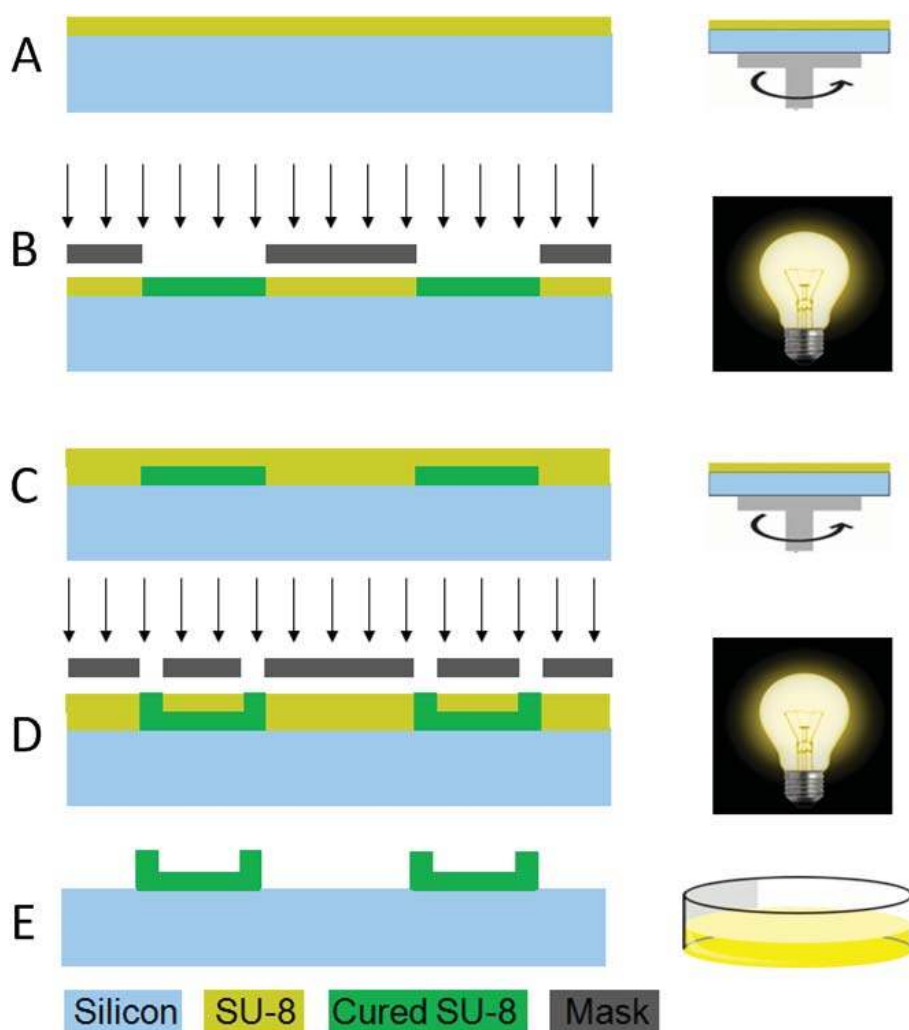


Figure 5.1: Schematic showing the five major steps for the fabrication of SU-8 micro containers. A, a layer of SU-8 is spin coated on a silicon wafer. B, the bottom container layer is exposed. C, another layer of SU-8 is spin coated. D, the container sidewalls are exposed. E, the redundant SU-8 is removed in propylene glycol methyl ether acetate.

thickness. The wall thickness needs to be thicker than  $5 \mu\text{m}$  for a container to maintain its stability and avoid buckling. Figure 5.3 shows the typical micro container design with an outer diameter of  $300 \mu\text{m}$ . The wall thickness of the containers shown is  $40 \mu\text{m}$  by design although the actual size is slightly larger. The SU-8 prototype containers are mainly used by collaborators to test various drug delivery aspects involving filling of micro containers and spacial confinement of drugs [71] [72]. In this work, SU-8 micro containers are used to test wafer scale filling of micro containers with a solid polymer drug matrix by embossing. This method enables filling of thousands of micro containers in one process and is described in section 6.1 and appendix A.



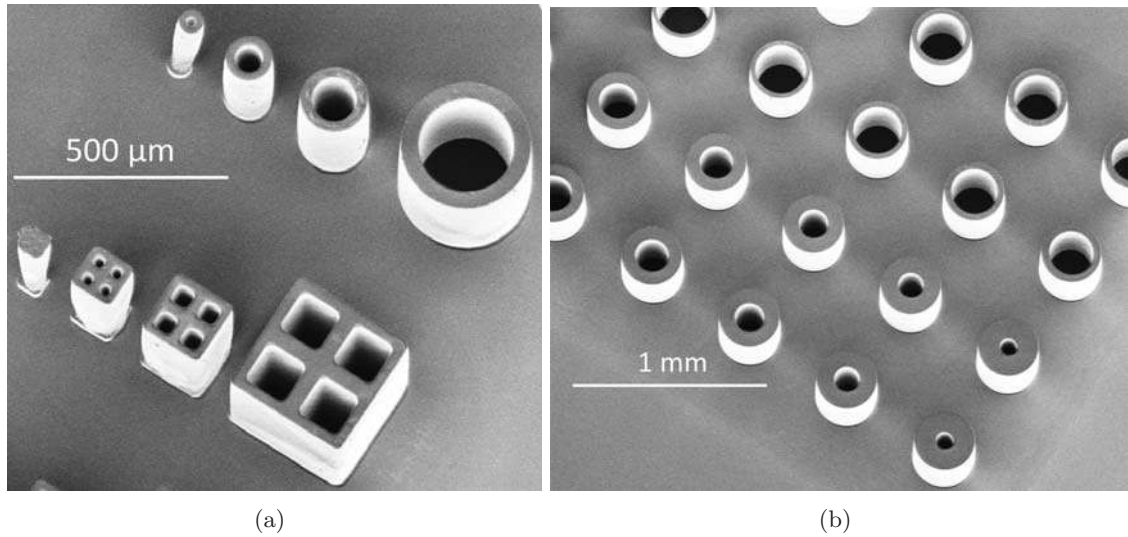


Figure 5.2: The figure shows some of the possibilities of fabricating a variety of different designs with the SU-8 micro container process. a) multiple micro containers with different sizes and design, providing an idea of what is possible. b) circular micro containers with an outer diameter of  $300\ \mu\text{m}$  with varying wall thickness.

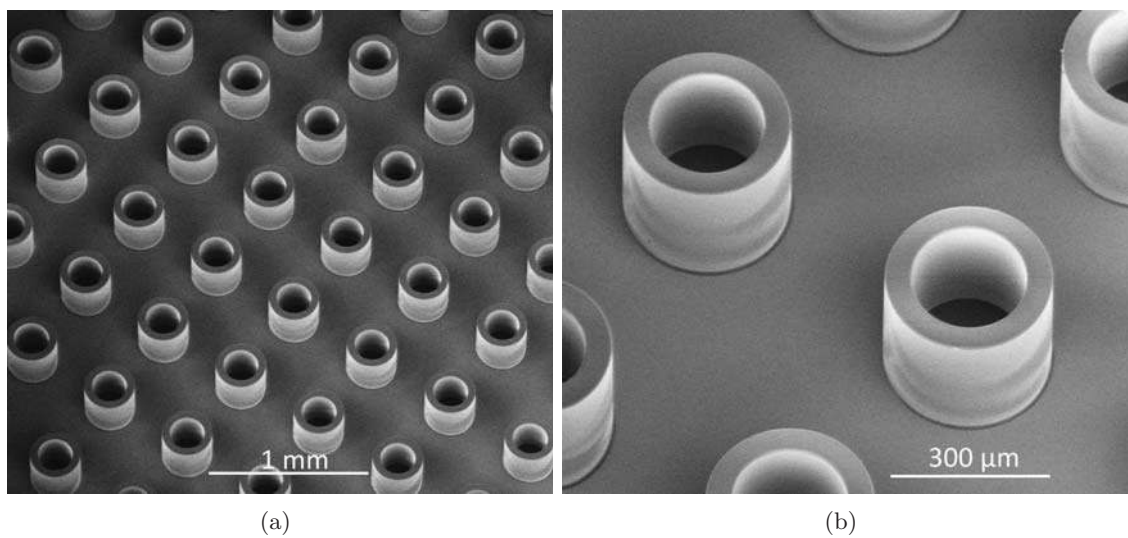


Figure 5.3: The figure shows the typical SU-8 micro container design. a) overview of micro containers with an outer diameter of  $300\ \mu\text{m}$ . b) close up view of the containers seen in a).



## 5.2 Biodegradable polymer containers

Micro fabrication in FDA approved biopolymers presents a challenge compared with conventional micro fabrication where often photo-resists are used to pattern materials via different methods of pattern transfer or the resist itself is used to create structures. An example of this is the SU-8 micro container fabrication presented above or the stamp fabrication presented in chapter 4. No commercial FDA approved biodegradable polymer resins exist on the market today and thus the use of photolithography to fabricate micro containers directly is not possible. Researchers are looking into developing such materials i.e. Åkesson et al. study resins based on lactic acid and soybeans [73], while Pulkkinen et al. study cross linking of PCL based resins [74] [75]. A short review of possible fabrication technologies is given below. An introduction to hot embossing is given as this is the most used technique for container fabrication. Containers fabricated in PLLA and PCL are presented along with the challenges faced in the fabrication processes.

## 5.3 Fabrication technologies

Many fabrication techniques for structuring polymers exist today such as thermoforming, extrusion, molding and casting. Different techniques for polymer micro structuring exist, such as micro milling, injection molding, etching, three dimensional printing, laser cutting, two photon laser writing and embossing. The different techniques all have their strengths and weaknesses and a short review of these are given in the following paragraphs.

**Micro milling** In micro milling fine tools are used to remove material in a film or a sheet. Tools with a typical feature sizes of 100  $\mu\text{m}$  are commercially available and structures with feature sizes of roughly 100  $\mu\text{m}$  can be fabricated. Tools with a width of tens of microns have been used in recent years, thus pushing the limits for fabrication[76]. The technique is good for prototyping and it is not suitable for mass production as each part needs to be milled.

**Two photon laser writing** Two photon laser writing is used in micro- and nano technology for fabricating three dimensional structures for several different applications such as scaffolds, tissue engineering, molds etc [77]. The technique is very good for fabrication of true three dimensional structures and there are basically no limitations to the design. The drawbacks are that a limited number of resin materials are available for this techniques and that the process requires long writing times.

**Injection molding** Injection molding is a very common method for fabrication of polymer structures. Well know products made this way are the lego<sup>TM</sup> toys. The technique is great for mass fabrication though the drawback is that it is difficult to fabricate structures with thin features like the walls and the bottom of the micro containers. A batch of containers is fabricated by injection molding in polypropylene at collaborators at DTU Mechanics. Figure 5.4 shows some of the injection molded structures lined up next to each

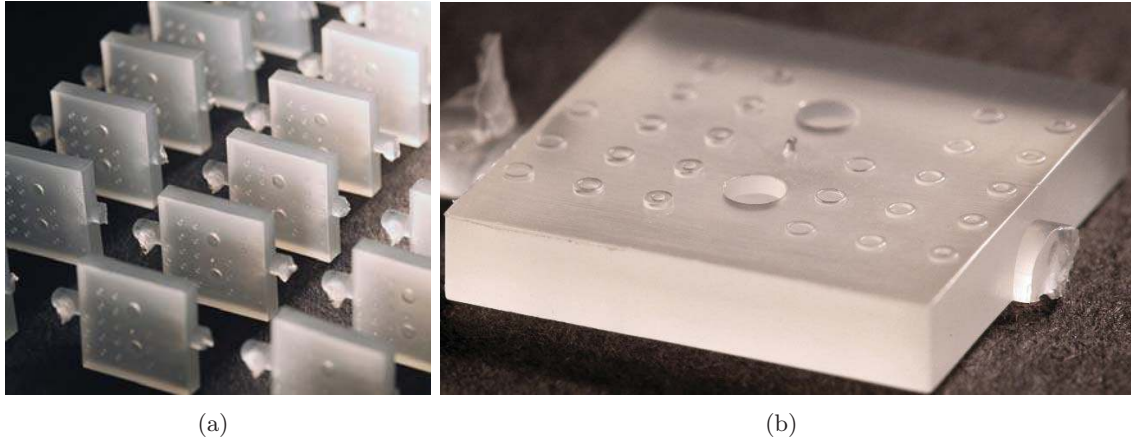


Figure 5.4: The figure shows two images of the injection molded micro containers. It is seen that the containers consist of a thick bottom layer with ring structures on top.

other as well as a close up. The injection molded structures form a thick base with ring structures of varying sizes on top. The diameter of the ring structures are roughly  $500\ \mu\text{m}$ . The fabrication showed that injection molding is not suitable for container fabrication but it can be used for a model system with a thick bottom layer.

**Etching** Etching as a fabrication method for containers is considered and initial steps are taken to develop this method. Specifically DRIE processes are in development and these are used in the project for different purposes. The advantage of using etching as fabrication method is that many containers can be made at once. Drawbacks include loss of precision, rough surfaces, need for masking methods.

**Laser cutting** Laser cutting of polymers is used in the project for cutting out polymer films and for initial experiments on container fabrication in PLLA film. Figure 5.5 shows a micro container fabricated in a PLLA film. The advantages of laser cutting are that the process is fast, it is very flexible and allows for fast design changes. Drawbacks include local heating of material and possible generation of radicals during the processing.

**Hot embossing** Hot embossing is an old and well known technique for patterning of polymers i.e. a wax seal. In micro and nanotechnology the similar process of nano imprint lithography is used for fabrication of structures ranging from nm to  $\mu\text{m}$ . The advantages of hot embossing are that high precision can be obtained and that large surfaces can be structured in one process. The disadvantages include a residual layer that needs to be removed afterwards for separation of structures and the need for a stamp. The technique is useful for 2.5d structures with the restraint that the stamp needs to be removed.

**Roll to roll** The roll to roll technique is well known and used for many different purposes such as electrodes [78] and polymer solar cells [79]. The technique is very good for mass

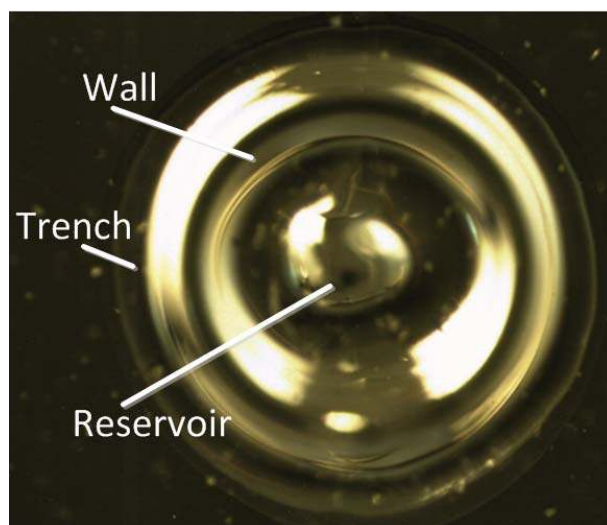


Figure 5.5: Optical image of a micro container made by laser cutting of a PLLA film. The image show the light reflecting of the sloped sidewalls of the container.

production and a good candidate for commercialization of micro containers. The drawback is that large quantities of material are required for the development of a working process.

## 5.4 Comparison of methods

When deciding which fabrication method to go with it is important to keep in mind what the potential volume of containers is and what requirements one has to the dimensions of the containers. In the case of the model drug furosemide, a dose of 20 mg - 40 mg is common for the treatment of edema. If a 20 mg furosemide dose is to fit inside containers without any excipient the following amount of containers are needed, assuming a cylindrical shape with an inner diameter of 200  $\mu\text{m}$  and a height of 100  $\mu\text{m}$ .

$$\# \text{ containers} = \frac{0.020\text{g} \cdot 1.6 \frac{\text{g}}{\text{cm}^3}}{\pi \cdot (0.01\text{cm})^2 \cdot 0.01\text{cm}} \approx 10000 \text{ containers} \quad (5.1)$$

With a need for thousands of containers some of the fabrication methods can be eliminated. Two photon laser writing as well as micro milling do not offer an acceptable volume production. Etching could be possible though several aspect of this technique remain uncertain. As for laser writing and embossing, both techniques offer medium volume production and are possible condidates. Roll to roll and injection molding are both high volume production techniques. Roll to roll facilities are not accessible to the Nanoprobes group and thus this technique has not been explored. Injection molding is possible though initial experiments showed extensive challenges to overcome with respect to size and precision of container production and thus this method is discarded. This leaves embossing and laser cutting as candidates. Embossing is chosen as the main fabrication method as this technique offers medium production and high precision fabrication. Laser cutting

equipment in form of CO<sub>2</sub>-lasers are accessible and experiments using this to fabricate containers have been performed. The experiments showed that a fast output is possible though with very limited precision and with possible issues with high temperature processing. For these reasons hot embossing serves as the main fabrication method of biodegradable micro containers. For future fabrication, roll to roll is definitely a possibility as well as laser writing in terms of recent development within laser machining in transparent materials [80].

## 5.5 Hot embossing

The hot embossing technique utilizes a drop in material stiffness when exceeding what is known as the glass transition temperature ( $T_g$ ). Figure 5.6 shows a schematic of the embossing process. Figure 5.6(a) shows a curve explaining the effect of young's modulus as a function of temperature for polymers. Below the  $T_g$  the polymer is stiff and remains in its current configuration. Once the temperature passes the  $T_g$ , the polymer chains can move with respect to each other. With the ability of chain movement the material becomes softer and rubber like. If the temperature is increased further the melting point  $T_m$  is reached and the polymer becomes molten allowing free flow of the polymer chains. The plateau between  $T_g$  and  $T_m$  is known as the rubbery state of the polymer. In this state it is possible to shape the polymer by applying pressure on it. The hot embossing technique utilizes this material characteristics. A stamp is brought in contact with the polymer. The polymer is then heated above the glass transition temperature, going from 1 to 2 in figure 5.6(a). Pressure is then applied to the stamp, forcing it into the polymer. Once the stamp is fully pressed into the polymer, the polymer is cooled below the  $T_g$ , going from 2 to 1 in figure 5.6(a). In this way the polymer stiffens while retaining its current shape. The stamp is finally separated from the polymer. Figure 5.6(b) shows

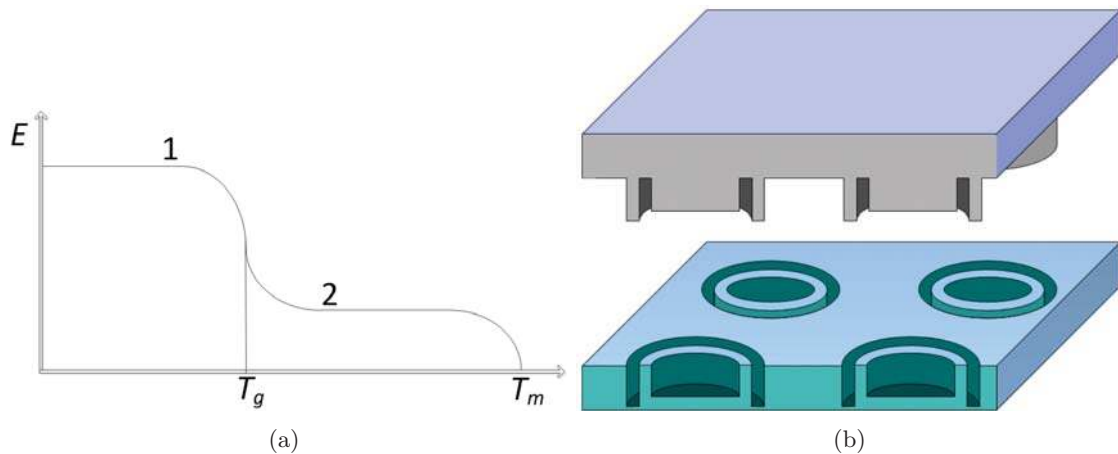


Figure 5.6: The figure shows a graphics of the young's modulus as a function of temperature and a graphics showing the component of a hot embossing process after a stamp is release from a polymer film.

an illustration of a stamp after embossing and separation of the stamp from the polymer layer. The structures on the stamp can either stick out of the surface or be grooved in the surface. In this case the structures are sticking out of the surface. The reason is that less materials needs to be move in the embossing process. The less material that needs to be displaced in order to obtain the wanted shape, the quicker the embossing will be. The entire process is often run in vacuum to avoid trapping of air bubbles, which can result in poor pattern transfer. For theory on hot embossing the reader is referred to [67].

## 5.6 PLLA containers

For the fabrication of the PLLA containers embossing as described above is used. The  $T_g$  of PLLA is around  $60\text{ }^\circ\text{C}$ , see table 2.2, and thus embossing is carried out above this temperature. Figure 5.7 shows the result of an experiment where embossing at  $80$ ,  $100$  and  $120\text{ }^\circ\text{C}$  is carried out. For the experiment, SU-8 stamps are used and similar results are observed for the nickel stamps. Other embossing parameters such as time, pressure and ramping are kept constant at 1 hour,  $1.9\text{ MPa}$ ,  $10\text{ }^\circ\text{C}/\text{min}$ . The graph shows the measured container wall height after embossing and the corresponding stamp height. The figure shows that embossing with these parameters results in partial pattern transfer for  $80$  and  $100\text{ }^\circ\text{C}$  while a good pattern transfer is obtained at  $120\text{ }^\circ\text{C}$ . The study is published in Microelectronic Engineering and can be found in appendix B. Figure 5.8 shows a PLLA

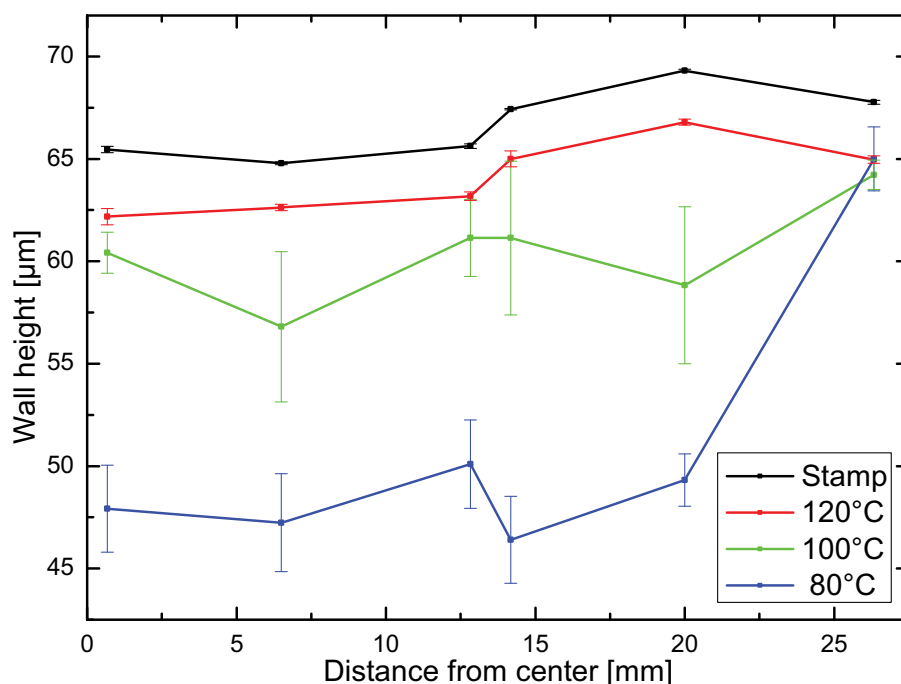


Figure 5.7: The figure shows the measured wall height after embossing in PLLA polymer film. The blue, green and red curves show the results of embossing at  $80$ ,  $100$  and  $120\text{ }^\circ\text{C}$  respectively. The black line shows the corresponding stamp height.

container after embossing and a schematic with a cross sectional view of a container. The container is covered with a thin layer of gold for better SEM imaging. The embossing

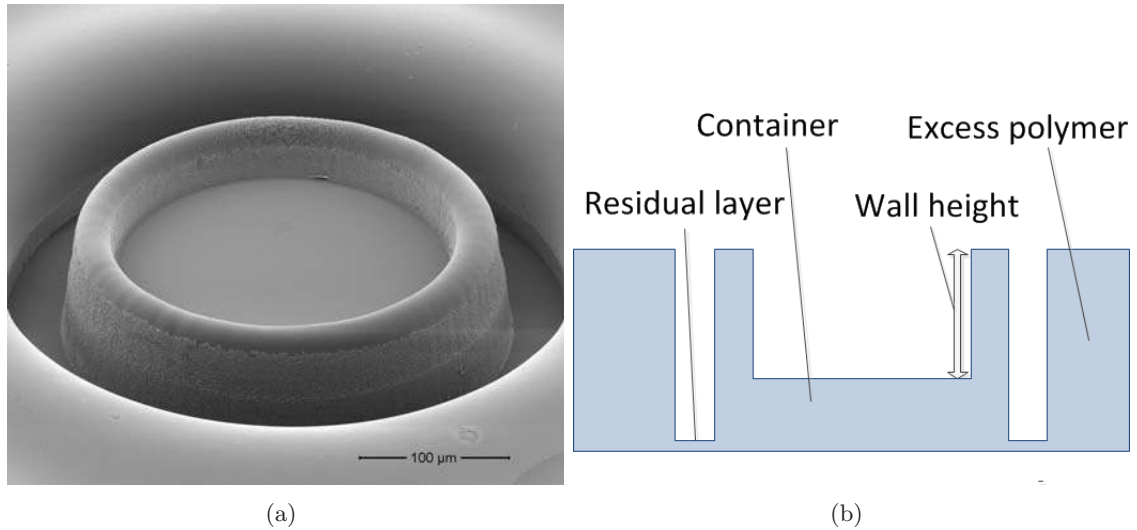


Figure 5.8: Hot embossed micro container in PLLA with gold thin film for SEM imaging and a schematic of the cross sectional view of a container. The dimensions of the micro-container are; Outer diameter of 300  $\mu\text{m}$ , inner diameter of 240  $\mu\text{m}$ , height of 100  $\mu\text{m}$ , wall height of 65  $\mu\text{m}$ .

process leaves a residual layer behind connecting the container to the redundant polymer film. To release the containers from the polymer film it needs to be removed or broken. It is desirable to release all of the containers from the polymer film in one process. A possible solution is to etch the residual layer with an oxygen plasma [81]. In collaboration with Danchip investigations on polymer etching are conducted. The etching is performed in a DRIE machine though less than optimal results are achieved for the structured containers. During the etching the PLLA is only partially removed and meshes of residues are left behind. Furthermore, the etching process primarily attacks the top of the PLLA structure and thus the bottom of the separation trench is not attacked as strongly. The longer the etching is sustained the more pronounced the effect become. Figure 5.9 shows the result of prolonged etching for 24 minutes. It is clear that the etching is non uniform and that it is not an anisotropic etch, which would be the ideal scenario. Development of DRIE for polymers such as PLLA and PCL is an ongoing task at Danchip and could be a solution in the future. As of now the process is not working as intended.

Besides the removal of the residual layer the polymer needs to be separated from the wafer. This can be done in several ways. The adhesion can be tuned in the spin coating process and thus enable the polymer film to be peeled off. Another trick is to put water at the edge of the wafer. Once the water comes in contact with both the polymer and the wafer, it is drawn in between the polymer and wafer, due to capillary forces. The water effectively separates the polymer film from the wafer. Another and similar approach used in the project is to spin coat a thin layer of PAA before spin coating the PLLA on top.



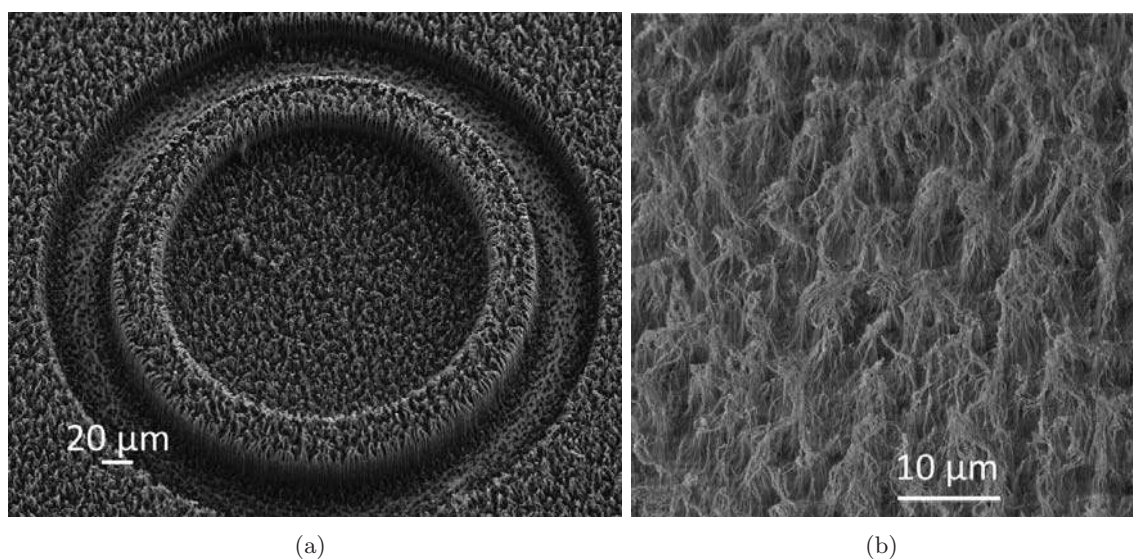


Figure 5.9: PLLA micro container etched for 24 min and a zoom of that surface.

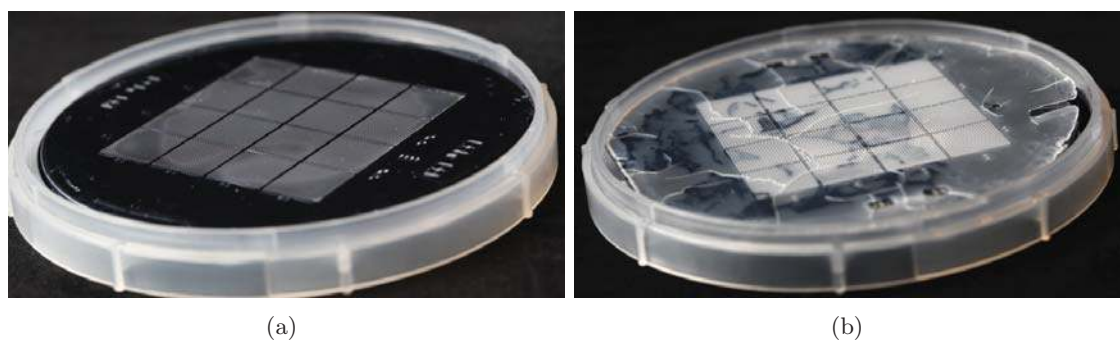


Figure 5.10: Pictures showing the long term effect of crystallization during the hot embossing process if the film containing the micro containers is kept on the silicon substrates. a) PLLA film embossed at 100 °C. b) PLLA film embossed at 120 °C.

The PAA is water soluble and dipping the wafer in water after the embossing results in a lift-off of the polymer film. The same approach is successful with the use of dextran and other researchers have used this technique with a variety of materials [82]. A side effect of the embossing process is that the PLLA increases its crystallinity. The growth in crystallinity happens when the polymer is heated to 120-160 °C according to Abe et al. [83]. Figure 5.10 shows two wafers with containers in PLLA, one embossed at 100 °C and one at 120 °C. The wafers have been stored in the Danchip cleanroom at a constant temperature of 20 °C and relative humidity of 45 % for six months. The sample embossed at 100 °C retains good adhesion to the wafer and show no polymer cracking. The sample embossed at 120 °C is delaminated and cracks have propagated throughout the polymer film. The cracking of the embossed PLLA film can be avoided by releasing the film from

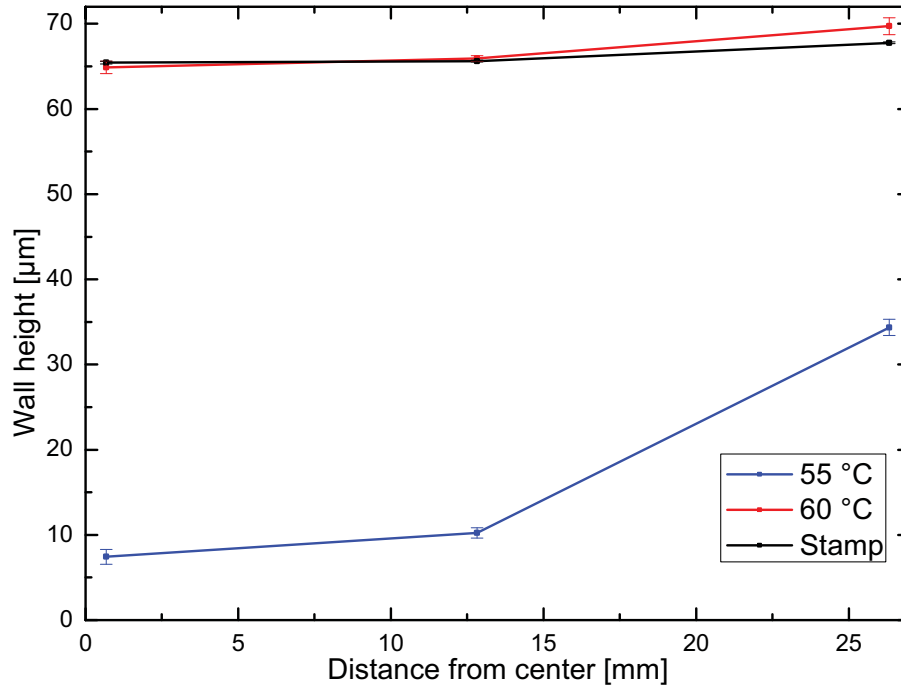


Figure 5.11: The figure shows the measured wall height after embossing in PCL polymer film. The red and the blue line shows the results of embossing at 60 and 55 °C respectively. The black line shows the corresponding stamp height.

the substrate within a few weeks of fabrication. The methods described above are used for the release and once the film is lifted from the substrate, no cracking is observed for prolonged storage times at room temperature.

## 5.7 PCL containers

Embossing in PCL is a special case since the  $T_g$  is  $-60$  °C and the  $T_m$  is  $60$  °C. PCL is "rubbery" at room temperature and thus embossing at room temperature should be possible. The material however is difficult to emboss and with the embossing tool available at DTU danchip it is not possible to go above 1.9 MPa in pressure. At this pressure it is not possible to perform embossing at room temperature and little to no deformation of PCL appears. Therefore it is decided to emboss at a temperature just below the melting point as this should lead to a lower Young's modulus of the PCL. Figure 5.11 shows the container wall height at three points between the center and the edge of the stamp. The black line shows the corresponding height of the stamp and the red and blue lines show the container wall height for embossing experiments done at 55 and 60 °C for 1 hour at maximum pressure of 1.9 MPa. It is seen that embossing at 60 °C results in a good pattern transfer matching the stamp dimensions. Embossing at 55 °C results in a partial pattern transfer where the wall height is significantly lower than the stamp



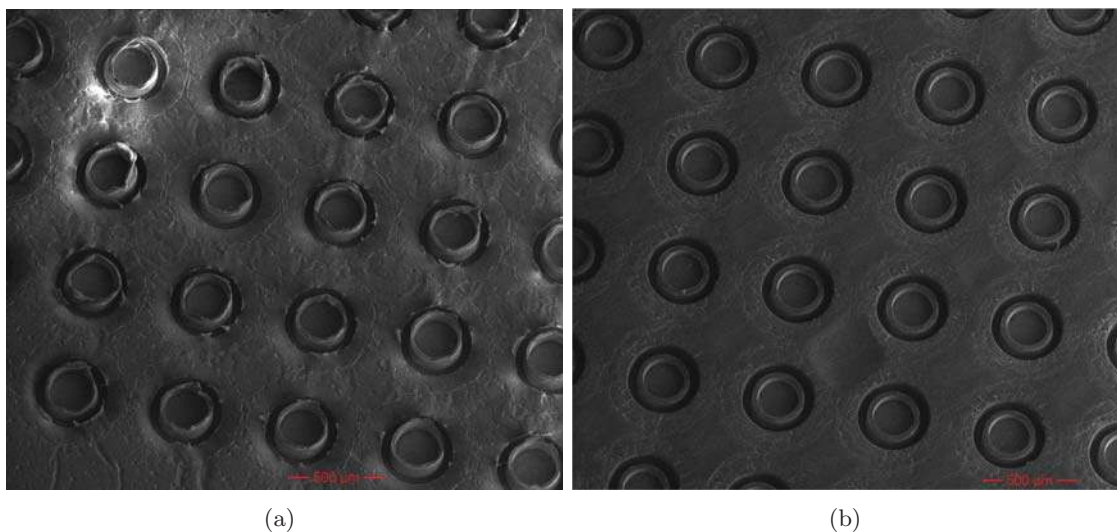


Figure 5.12: PCL hot embossed micro containers. a) Embossed at 60 °C with a ramping of 10 °C / min. The embossing results in a difficult separation of the stamp and the PCL film. The separation tears the container walls apart. b) Successful pattern transfer achieved at 60 °C with a ramping 5 °C / min. The temperature does not overshoot and melt the PCL film and an easy separation of the stamp and the film ensures a good pattern transfer.

dimensions. The ramping of temperature for the embossing process is very important due to the close proximity of the embossing temperature to the melting point. If the ramping is fast the temperature can overshoot and cause the PCL to melt or partly melt before the temperature stabilizes at 60 °C. If that happens the PCL is either completely stuck to the stamp or the PCL is torn during separation of the stamp. Figure 5.12 shows PCL containers embossed at 60 °C after stamp separation. In figure 5.12(a) the ramping is 10 °C/min while it is only 5 °C/min in figure 5.12(b). It is clear that the container walls are elongated in the stamp separation process in figure 5.12(a) when compared to the successful pattern transfer observed in figure 5.12(b). Thus for a successful embossing in PCL, the ramping should not exceed 5 °C/min. To remove the residual layer in the case of PCL containers, similar approaches and unfortunately similar results as for the PLLA are observed. Alternatively, the containers can be released by laser cutting although the current setup of laser cutters does not support alignment.

## 5.8 Summary

Micro containers in SU-8, PCL and PLLA have been fabricated. The SU-8 containers are realized by a photolithography process while the PCL and PLLA containers are realized by hot embossing in spin coated PCL and PLLA films. Embossing tests showed that a good pattern transfer is obtained at 120 °C for PLLA and at 60 °C for PCL. Residual

polymer layer left after the embossing process is difficult to remove in an efficient manner and development is needed to successfully achieve this task.



## Chapter 6

# Container filling

In this chapter three experiments dealing with filling of micro containers are described. First, a hot embossing process for filling of micro containers is shown. This method is used in the project to fill micro containers in SU-8. This work was presented at the 16<sup>th</sup> international conference on miniaturized systems for chemistry and life sciences,  $\mu$ TAS 2012 and a three page conference proceeding can be found in appendix A. Second, a method using a simple form of screen printing for filling of micro containers is described. This method was used in the project to fill micro containers of the biodegradable polymers PLLA and PCL. Third, solvent casting is described as a possible filling method. This method is in development and has so far not been used for further micro container experiments. Other methods, such as inkjet printing and CO<sub>2</sub> impregnation, are investigated in the NAMEC project by colleagues and will not be covered here.

### 6.1 Embossing

This section describes a method developed in order to fill micro containers on wafer scale with a solid polymer drug matrix. For the experiment, SU-8 micro containers as the ones shown in section 5.1 are used. As solid polymer drug matrix, the films described in section 3.2 are used.

#### 6.1.1 Process

Figure 6.1 shows a graphical representation of the process while figure 6.2 shows SEM images after the major process steps. The two starting components are the SU-8 containers shown in figure 6.2(a) and the polymer drug matrix, see section 3.2, on a silicon wafer substrate coated with a fluorocarbon anti-sticking coating [62]. The polymer-drug film is embossed into the micro containers at a temperature of 60 °C and a pressure of 1.9 MPa for 1 hour, figure 2.1. Embossing at 60 °C, which is just below the melting point of PCL, ensures an optimal hot embossing and pattern transfer. The system is then cooled to 20 °C and the silicon wafer initially holding the drug matrix is removed, as shown in figure 6.2(b). The anti-sticking coating ensures that separation takes place between the coating and the polymer-drug film. A deep reactive ion etch is used to separate

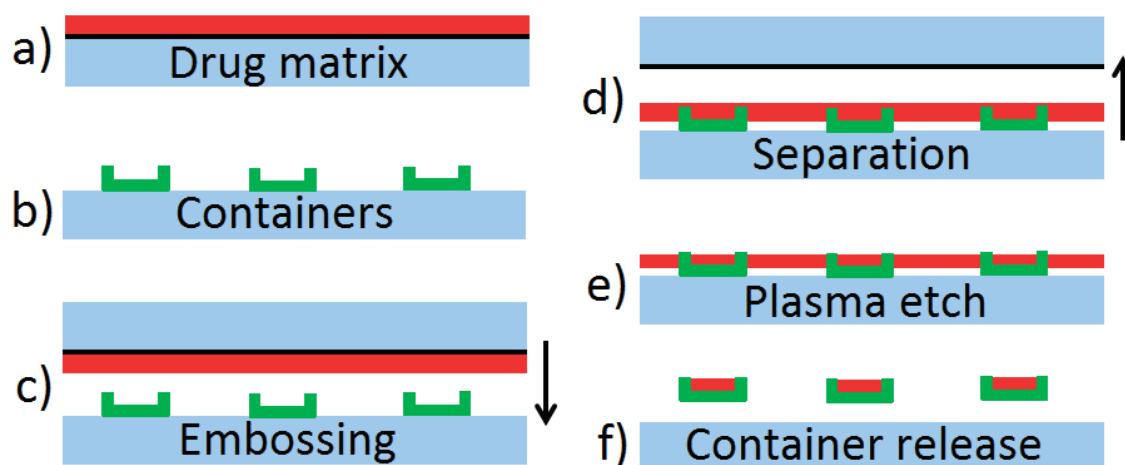


Figure 6.1: Schematic of the micro container filling process using hot embossing of a polymer drug matrix. The starting point are micro containers on a silicon substrate and a polymer drug matrix on a silicon substrate with an anti-sticking coating, a) and b). The polymer drug matrix is embossed into the containers and the following separation occurs between the anti-sticking coating and the polymer drug matrix, c) and d). A deep reactive ion etch is performed to trim down the polymer drug matrix. This separate the drug matrix in the containers from that outside the containers e). The containers are released from the substrate by peeling the redundant drug matrix and mechanically removing the containers, f).

the micro containers from the excess polymer-drug matrix, shown in figure 6.2(c). The etching is performed with an advanced silicon etcher using the following parameters for an anisotropic etch.  $O_2$  flow of 20 sccm, Ar flow 20 sccm, platen power 150 W, coil power 600 W, pressure 4 mTorr, temperature 10 °C and time 12 min. The etching process has been developed in collaboration with Danchip personnel. The process uses an oxygen plasma coupled with a high platen and coil power to remove the polymer. The high power results in some sputtering of the drug matrix. However the high power is needed for the process to remove significant amount of material. Finally, the containers are mechanically released, as shown in figure 6.2(d). The containers can be lifted from the substrate by scraping or with tweezers. The adhesion of the containers to the substrate is very poor, probably due to the heating and cooling involved in the etching process.

### 6.1.2 Result & discussion

The result of the embossing process is SU-8 micro containers filled with a film consisting of polycaprolactone and furosemide, as shown in figure 6.2. The method is demonstrated to work on wafer scale level with 4 inch wafers. The containers can be lifted from the substrate by scraping or with a pair of tweezers. It is however very difficult to handle the individual containers and subsequently place them. The release of the containers is a delicate process as they tend to stick to anything they come in contact with. Figure 6.3 shows some of

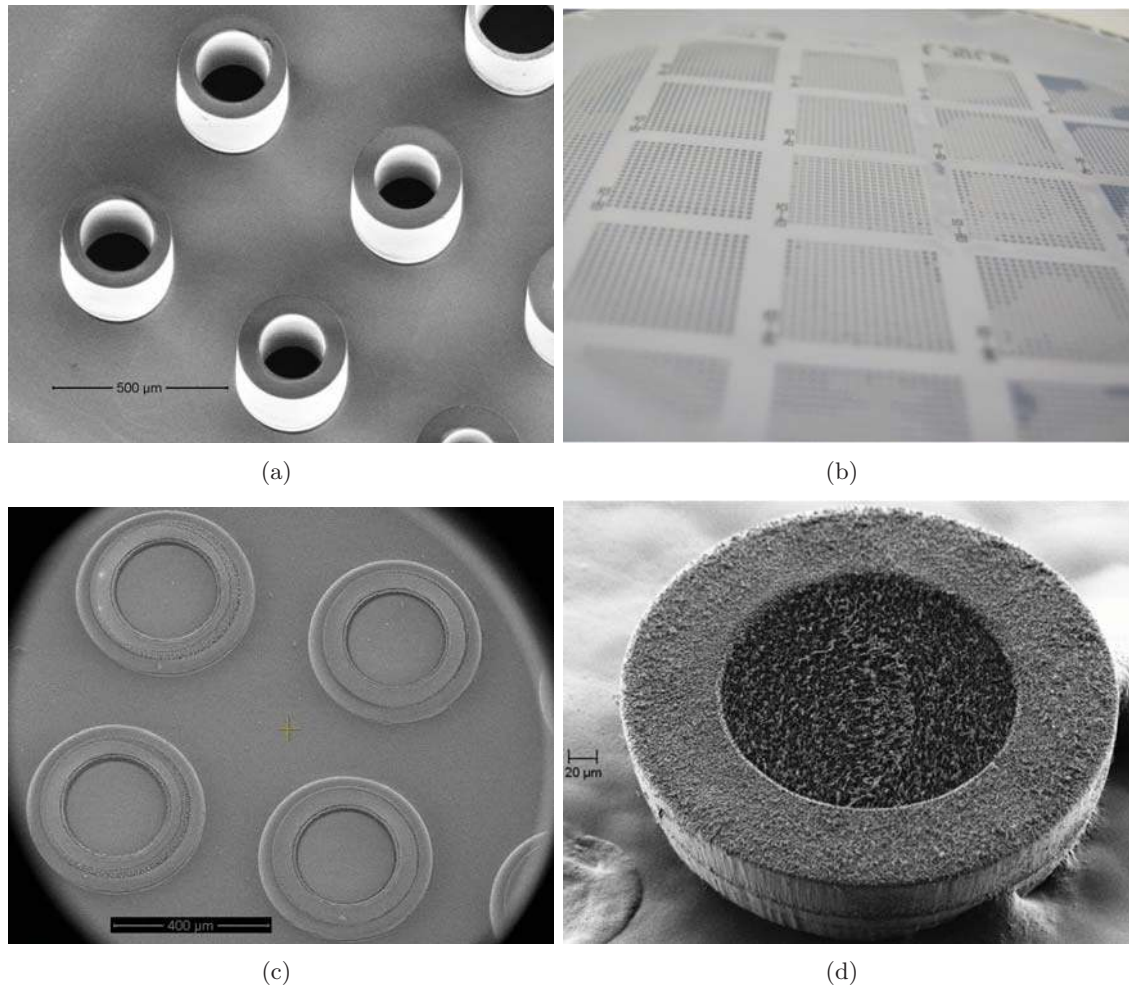


Figure 6.2: The figure shows images before, during and after the filling process shown in figure 6.1. a) SU-8 micro containers before the process. b) Polymer drug matrix after embossing and separation from the substrate. c) Filled micro containers after the polymer drug matrix is trimmed down by DRIE. d) Filled SU-8 container with the polymer drug matrix after release from the substrate.

the released containers collected in a capsule. The method for filling containers with a drug matrix can be applied to different systems following a few fabrication requirements. The  $T_g$  of the polymer drug matrix must be lower than the one of the micro container material. The embossing temperature should be in-between the  $T_g$  of the polymer drug matrix material and the  $T_g$  of the micro container material. This ensures a reflow of the polymer drug matrix without affecting the structural stability of the micro containers. Furthermore, the embossing temperature should not exceed  $T_m$  of the components to allow separation of the embossed stack after the cooling process. The experiment is done with SU-8 containers as they stick out of the surface and thus present a favorable embossing



Figure 6.3: The image shows released micro containers collected in a capsule.

case where minimal material needs to be deformed. If the process is to be performed on the biodegradable polymer containers the situation is very different. These containers are in plane with the redundant polymer. Embossing a film into the biodegradable containers means that the majority of the polymer drug matrix needs to be transferred into the small voids of the containers. For this to work, the biodegradable containers need to be separated from the redundant film. The separation of biodegradable containers is a process under development, but for future applications this method could be a possibility since the temperature needed to emboss PLLA is higher than the 60 °C used for the embossing of the PCL furosemide film.

## 6.2 Screen printing

This section describes a filling method for containers inspired by traditional screen printing technique. Screen printing is a technique utilizing a woven mesh in combination with a stencil mask to form open areas in the woven mesh [84]. A squeegee is used to press a paste or an ink through the mesh resulting in the stencil pattern being transferred to a substrate.

### 6.2.1 Experiment

In this work a simple version of the screen printing technique is applied. A flexible stencil is fabricated in transparent foil by laser machining and used without the woven mesh. The laser machining is done with a CO<sub>2</sub>-laser and the exact process parameters can be found in appendix J. The design of the stencil is made such that it contains holes matching the inner diameter of the micro containers with a few microns in variation. A graphical

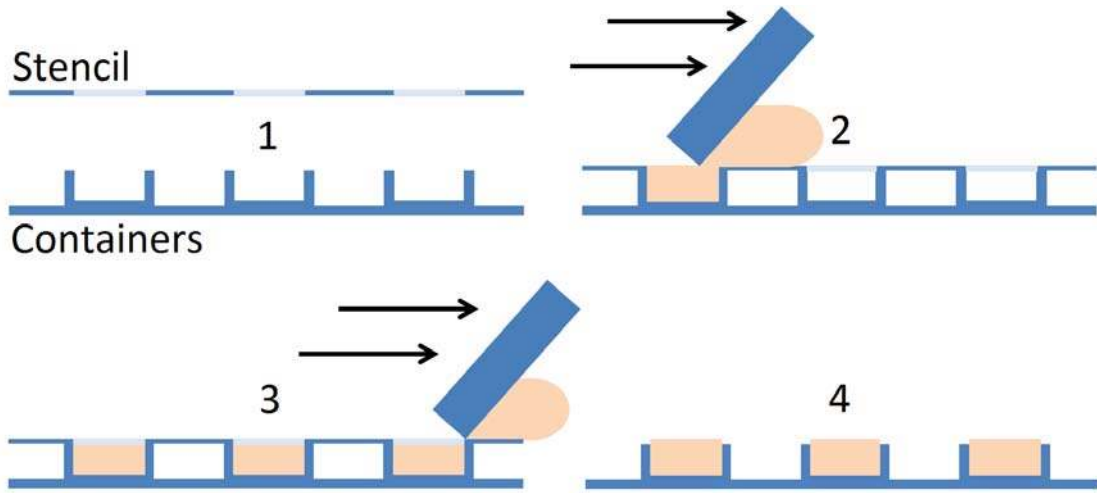


Figure 6.4: Graphics showing the filling process using screen printing, 1 stencil is aligned to containers, 2-3 furosemide powder is pressed into the containers, 4 stencil is removed.

representation of the filling process using screen printing is shown in figure 6.4. First, the stencil is aligned to the micro containers with an optical microscope (Figure 6.4.1). Then furosemide powder is pressed through the stencil (Figure 6.4.2, Figure 6.4.3). Finally the stencil is removed together with any excess powder (Figure 6.4.4).

### 6.2.2 Result & discussion

Figure 6.5 shows optical images of micro containers in PLLA filled with furosemide powder using the technique depicted in figure 6.4. Figure 6.5(a) shows a single container filled with furosemide. A small amount of furosemide resides on top and outside the container wall. The image is a good representation of how most containers look like in a successful process. Figure 6.5(b) shows an overview of a process with a slight mismatch in alignment. It is seen that some furosemide is deposited beside the containers while others have a good filling without furosemide beside them. Due to the very flexible transparent foil and fabrication variations in the stencil it is difficult to achieve a perfect alignment of the stencil to the containers. This is the cause for the variation in deposition of furosemide powder. Taking these factors into consideration the method performs quite well with respect to filling and it is used in the project for filling of micro containers with furosemide powder. If the process is optimized, it is believed that filling of micro containers without misplaced material is possible. Introducing a self aligned stencil [85] and a magnetic stencil ensuring a good clamping of the stencil to the containers [86], perfect filling of the containers should be possible. The strength of the process is that the technique can be applied to any of the micro containers presented in this thesis.



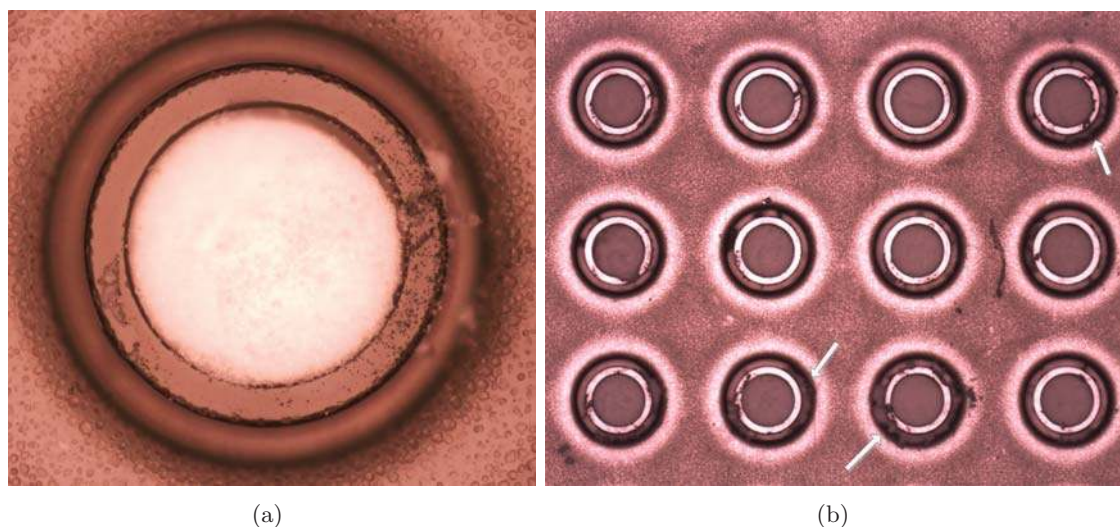


Figure 6.5: Micro containers made in PLLA by embossing filled with furosemide powder. a) Micro container with 300  $\mu\text{m}$  diameter filled with furosemide powder. b) Array of micro containers filled with furosemide by screen printing. Arrows point at the furosemide deposited beside the containers.

### 6.3 Solvent casting

This section deals with the idea of using solvent casting in combination with surface tension to fill micro containers. In the field of microfluidics, surface tension is a well know property used to manipulate fluids [87]. Due to the micrometer size of the containers the idea is to test if surface tension can be used to fill the containers. The aim is to have solution stay in the micro container while excess solution can be removed by tilting the substrate. Figure 6.6 shows a schematic of the idea. Solution is dispensed on the containers and the substrate is then tilted. The tilting allows excess solution to run off the substrate while surface tension keeps the containers filled. The tricky part is to get the tilting angle right. The tilting angle should be large enough that excess solution runs off the substrate and yet small enough so that solution stays in the micro containers. Ideally, the solution should act as water on a super hydrophobic surface, allowing the solution to run off while not leaving anything behind.

#### 6.3.1 Experiment

For the experiments micro containers in PCL are tested as PCL is known for its hydrophobic properties [88] [89]. A solution of furosemide and PAA in DMSO is used in the experiment. The weight ratio of PAA to furosemide is 2:1 and the total wt% of the solution is 13.6. DMSO is used as it has a high boiling point and thus a slow evaporation allowing time to manipulate the solution on the PCL container sample. The solution is dispensed on the samples. The sample is carefully manipulated so that the solution covers the entire array of containers. By tilting the sample the solution starts flowing off the

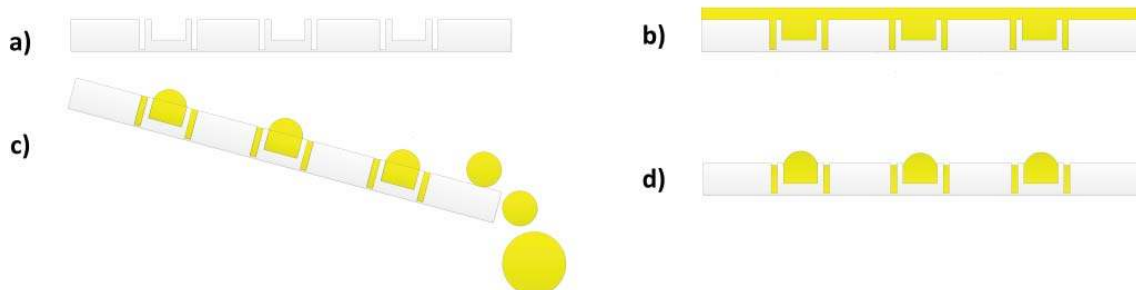


Figure 6.6: Schematic of the solvent casting idea. a) and b) solution of PAA and furosemide is deposited. c) and d) excess solution runs off the substrate while surface tension keeps solution in place in the containers.

substrate and the residual solution is collected in a beaker. Small droplets of solution remain for the majority of the container locations.

### 6.3.2 Result & discussion

Figure 6.7 shows the results of the experiment. Figures 6.7(a) and 6.7(c) show the containers before the experiment and figures 6.7(b) and 6.7(d) show the containers after the experiment. It is seen that the containers are indeed filled by this method. Furthermore, the surface area between the containers is changed, which likely means that some solution is deposited there as well. Comparing figures 6.7(a) and 6.7(b) it is seen that only small amounts of polymer and drug reside in the trench next to the container. The containers are still well defined and they seem to be completely filled. To investigate the filling further the sample is measured with a Dektak 8 stylus profilometer. Figure 6.8 shows representative profilometer scans of containers after the experiment. Figure 6.8(a) shows a case where the container is almost filled. A small difference in height of 5-10  $\mu\text{m}$  between the container wall and reservoir of the container is observed. With a total container height around 100  $\mu\text{m}$  and a reservoir depth of roughly 65  $\mu\text{m}$ . It can be conclude that around 90 % of the container volume has been filled. Unfortunately, it is not possible to measure the depth of the separation trench due to the aspect ratio (narrow and deep) and thus the shape of the profilometer tip is imaged at the trench "bottom". What can be said about the trench filling is that it is significantly less than the container filling though an exact measurement is not obtained. The fact that the trench is not filled to the same level as the containers suggests that either the solution only partially enters the trench or the solution easily escapes the trench in the tilting process. Based on the observations from the experiment the latter seems to be the most likely scenario. Figure 6.8(b) shows a case where two containers and the excess polymer film between them are profiled. It is seen that the containers are almost completely filled, with a difference in height of only a couple of  $\mu\text{m}$  between the wall and the reservoir. It is seen that the excess polymer film between the containers are roughly 10  $\mu\text{m}$  higher than the containers. This measurement supports the observations on figure 6.7 that the surface between the containers is altered.

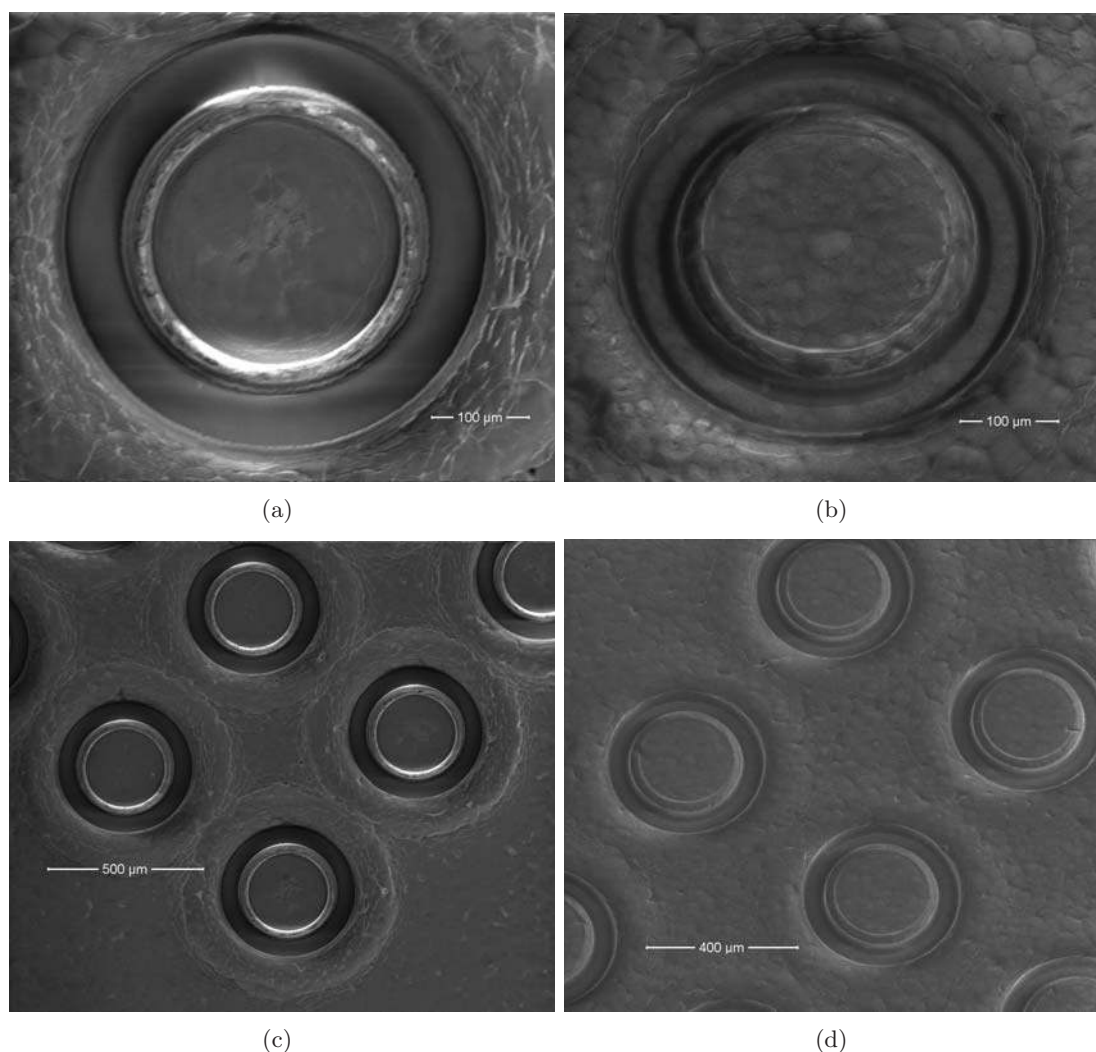


Figure 6.7: The figure shows SEM images before and after filling of containers using solvent casting. a) and c) shows empty PCL containers. b) and d) shows filled PCL containers. It is seen that surface in between the containers is altered. It is likely that a thin polymer drug layer is deposited.

It is likely that a layer of PAA and furosemide is deposited. While the results show that this method can be used to fill containers, it also shows that a polymer drug film is deposited everywhere. The fact that the PAA furosemide film is both inside and outside the containers can be solved in different ways. If a coating is applied to the containers and not to the surrounding areas, the excess PAA and furosemide might be washed away while the coating protects the container with the PAA furosemide inside. This could i.e. be done by spray coating through a shadow mask [86], a process that is in development by a colleague in the Nanoprobes group. The solvent casting process might be optimized by introducing

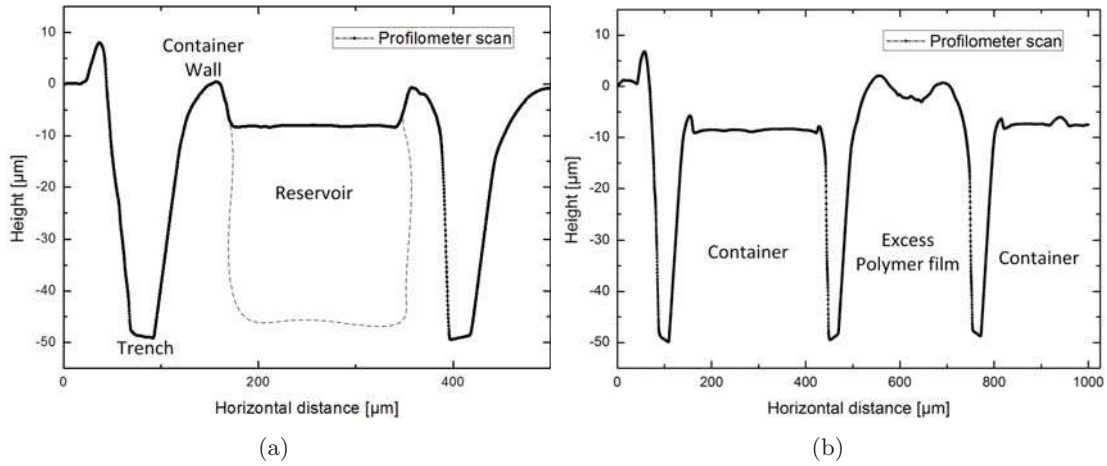


Figure 6.8: The figures shows two profilometer scan of containers after the solvent casting deposition process. It is seen that the containers are filled with the solvent casting process.

a partly patterned surface. Altering of the surface can be done by chemical modification [90] or deposition of material. i.e. spray coating. If the surface altering process is done with a masking material or stencil, specific areas such as the containers or the areas in between the containers can be targeted. If the surface is tuned in this manner, it might be possible to reduce the amount of material deposited in unwanted places.

## 6.4 Comparison

The three filling methods described in this chapter have their strengths and weaknesses. The embossing method is good for filling a large amount of containers in one process. This is an important aspect as thousands of containers are needed for a dose of furosemide. The downside of the method is that it requires the micro containers to be placed on a surface like the SU-8 containers presented in section 5.1 and that the polymer drug matrix only contains 20 % drug (at its current stage). The amount of drug might be increased with further development of the polymer drug matrix or with the use of other polymers and drugs. The method is not limited to the SU-8 containers and might be feasible if biodegradable containers are fabricated in a manner that leaves them protruding on top of a substrate. The PLLA used in this project matches the material conditions described in the embossing process for a successful filling process with respect to  $T_g$  and  $T_m$ . The screen printing method is used to fill the biodegradable containers. This method is very versatile as it only requires alignment of the stencil to the containers. Thus the container material is not important and the process can be used regardless of material preference. The process provides a high filling level and completely filled containers are obtained. The process is demonstrated on squares with 400 containers. The screen printing process is up scalable and it is possible to do wafer scale deposition with high precision in the tens of μm range [91]. The downside of the process is the need for alignment to the containers. The

Table 6.1: Comparison of the three filling methods described in the chapter. The table shows the type of container the three filling methods have been used for. The level of filling obtained and the process level.

Method	Container type	Filling	Process level
Embossing	SU-8	80% PCL 20% Furosemide	Wafer scale
Screen printing	PLLA / PCL	up to 100% Furosemide	400 container square upscalable process
Solvent casting	PCL	66% PAA 33% Furosemide	Wafer scale

solvent casting method presents a simple filling method for a large amount of containers. The filling level of the containers depends on the solution used. In the experiments a blend of 33 % furosemide and 66 % PAA is used. The process works well on a wafer scale, though polymer and drug is deposited outside the containers. The container filling is not limited to a certain material, however the choice of material is likely to affect the behavior of the solution. The three methods are summarized in their current development stage in table 6.1 The table lists the container type for which the processes are developed, the level of container filling and the scale of the process. Of the three processes the screen printing method is the most versatile process as it can be applied to any container shape and the potential filling level is 100 %. With further development, as suggested in section 6.2.2, the screen printing method provides a robust method for filling of micro containers. The embossing process is a viable alternative to the screen printing process, though with certain limitations to the filling level and requirements to container structure. The solvent casting method needs further development for it to be effective.

## 6.5 Summary

In this chapter it is shown that it is possible to integrate filling of micro containers as part of the fabrication on a wafer scale level through hot embossing of a polymer drug matrix in SU-8 containers. Filling of micro containers using a screen printing method is shown to work with furosemide powders, thus utilizing the container volume to its fullest in respect to the amount of active pharmaceutical ingredient. The method is demonstrated on PLLA containers, though the method is applicable to SU-8 containers as well. Last, a method based on surface tension for filling of the containers is investigated. Filling of containers is successful however redundant polymer medicine solution is deposited outside the containers.



## Chapter 7

# Drug delivery

This chapter covers the method used to test drug release, the results of drug release from the drug matrix described in chapter 3 and drug release from micro containers described in chapter 5 are shown. First, a description of the Pion  $\mu$ DISS profiler<sup>TM</sup> used to test drug release is given along with standard procedures used for the drug release experiments. Once the test method is established, the release data for the drug matrix and the micro containers are presented. Finally, an experiment using UV imaging to validate drug release from the micro containers in real time is shown.

### 7.1 Dissolution

This section covers the test setup used for dissolution testing of the different drug delivery systems developed. To test release of drug a Pion  $\mu$ DISS profiler<sup>TM</sup> is used. Figure 7.1 shows the Pion  $\mu$ DISS profiler used for the dissolution measurements. The machine is capable of conducting six release tests simultaneously. The profiler is controlled with a computer which is also used for data collection. Figure 7.2 shows a close up view of the test setup. It shows the beakers used and the tip of the UV probes. The device uses UV spectroscopy to measure concentration of a solution over time. The UV probes measure absorption of the UV light as it passes through solution. The travel distance of the UV light is twice the distance from the UV probe to the mirror. The longer the travel length is, the more UV light is absorbed. To avoid full absorption at specific wavelengths, the distance from the UV probe to the mirror is adjustable. The beaker contains a combined magnetic stirrer and sample holder. The magnetic stirrer ensures a good mixing of the solution. The entire setup is placed inside a water bath to control the temperature of the solutions. In order to measure the concentration of a compound, standard curves are made with known concentrations of the compound and the UV absorption is measured. In this way a correlation between the UV spectrum and the concentration of the solution is obtained. For the case of the drug matrix and the micro patches the following conditions are used. The drug release is performed using biorelevant dissolution media, Fasted State Simulated Intestinal Fluid (FaSSIF), to simulate the gastrointestinal fluids. The FaSSIF is pH adjusted to pH 6.5 before the release experiments are conducted in beakers contain-



Figure 7.1: The image shows the Pion  $\mu$ DISS profiler used for dissolution experiments. It is seen that the machine has six separate testing setups consisting of a UV probe that is inserted in a beaker with solution. The beaker has a sample holder at the bottom which at the same time functions as a magnetic stirrer.

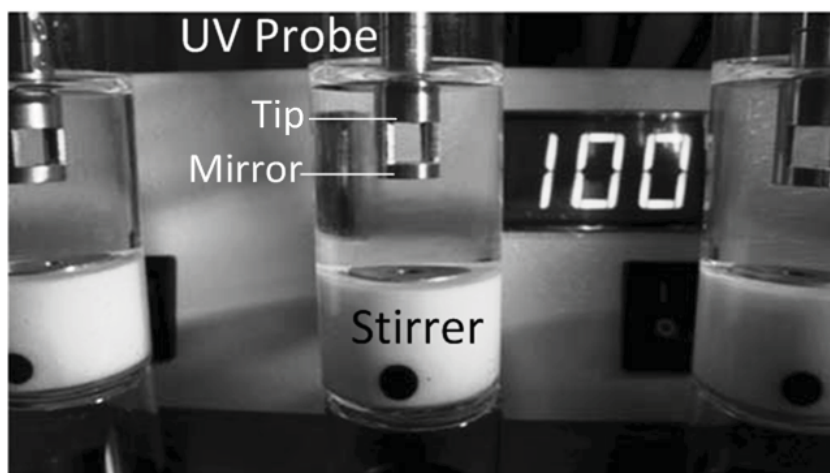


Figure 7.2: The image shows a close up of the Pion  $\mu$ DISS profiler setup. It shows the tip of the UV probe, the mirror and the beakers with the stirrer in a solution. The stirrer functions as a sample holder at the same time.



ing 10 ml FaSSIF media kept at a temperature of 37 °C. The magnetic stirrer is set to 100 RPM. In case of the micro containers similar conditions as above are used with the exception, that dissolution tests at different pH are conducted to test the effectiveness of enteric coatings. For this purpose a combination of Fasted State Simulated Gastric Fluid (FaSSGF) with a pH of 1.5 and FaSSIF pH 6.5 are used. First, the containers are kept for 120 minutes in FaSSGF media, and then the media is changed to the FaSSIF in which the containers are kept for 180 minutes.

### 7.1.1 Measurement uncertainties

In the dissolution experiments PLLA and PCL polymers are used in connection with the furosemide model drug. Control experiment with PCL and PLLA are conducted to investigate whether or not the polymers affect the dissolution tests. Films of pure PCL and PLLA are tested against the standard curves used for the furosemide dissolution experiments to see if "furosemide is released" from the pure polymer films. Figure 7.3 shows the dissolution results for PCL and PLLA films. It is seen that both polymers show "release". The effect of the PCL is higher than that of the PLLA. It can be concluded that both polymers contribute to the release concentration measured.

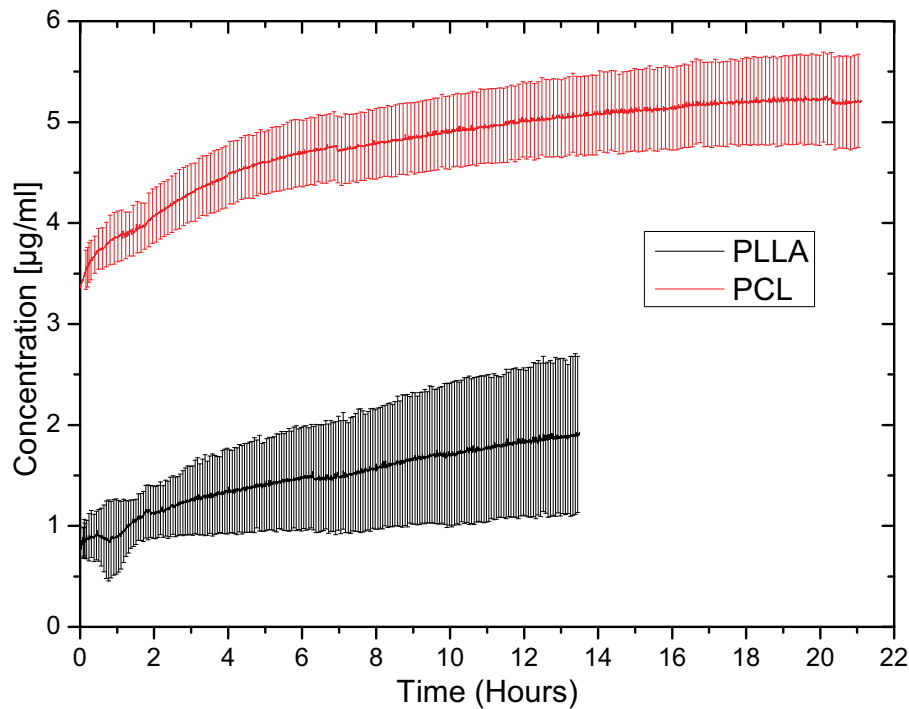


Figure 7.3: Graph showing the release signal from PCL and PLLA.

## 7.2 Drug matrix

This section covers the drug release from the drug matrix described in chapter 3. Dissolution tests are performed on seven different drug matrix batches; samples with a film thickness of 15 and 39  $\mu\text{m}$ , heat treated; 60 °C for 10, 30, 60 min and 100 °C for 60 min, embossed at 60 °C for 60 min at 1.9MPa are tested.

### 7.2.1 Release results & discussion

Figure 7.4 shows dissolution curves for drug matrices with a thickness of 15 and 39  $\mu\text{m}$ . It is seen that the thin drug matrix releases furosemide faster than the thicker film, but the thicker film releases more furosemide. The 15  $\mu\text{m}$  thick films release most of the furosemide within 1 hour and then the concentration stabilizes while the 39  $\mu\text{m}$  thick films release furosemide for the duration of the dissolution test. The rate of furosemide release decreases with time. The concentration approaches a stable level at the end of the dissolution test. In order to determine how much drug is released from the films, the films are weighed before dissolution tests. The weight of the 15  $\mu\text{m}$  thick film is 1 mg and the weight of the 39  $\mu\text{m}$  thick films is 3.2 mg. With a blend of 20 % furosemide to PCL, the amount of furosemide in the 15  $\mu\text{m}$  thick films is 0.2 mg and 0.6 mg for the 39  $\mu\text{m}$  thick film. Calculating the amount of released furosemide at the end point of the graphs shown in figure 7.4 with respect to the total amount of furosemide in the films gives:

$$\frac{10\text{ml} \cdot 17.1 \frac{\mu\text{g}}{\text{ml}}}{0.2\text{mg}} 100\% = 85.5\% \quad ; \quad \frac{10\text{ml} \cdot 49.1 \frac{\mu\text{g}}{\text{ml}}}{0.604\text{mg}} 100\% = 81.3\% \quad (7.1)$$

The calculation shows that 81-85 % of the furosemide is released from the drug matrix. Figure 7.5 shows the cumulative release curves for three samples; the non treated, the embossed and the 60 °C, 1 hour heat treated. Furthermore, it shows the release curves for two furosemide discs, one consisting of amorphous furosemide and one consisting of crystalline furosemide. It is seen that the embossed and the heat treated samples release all of the furosemide while the non treated sample only releases about 80-85 % furosemide as calculated. The fact that the samples go above 100 % release of the furosemide can be explained by the contribution from the PCL, as observed in figure 7.3. Furthermore, there is some uncertainty in weighing samples with such a small weight. An analytical laboratory balance is used with a precision of  $\pm 0.1$  mg. The lack of precision can account for as much as 10% uncertainty as the total weight of the samples varies from 1-3.2 mg. This uncertainty is not included in the error bars. The graph shows that the release from the drug matrix is fast and that all the furosemide is released within 30 minutes for the embossed and heat-treated samples while it takes an hour for the non treated sample. The release from the drug matrix resembles the quick release observed from the amorphous furosemide disc, while the release from the crystalline disc is very slow. The embossed and the heat treated samples have similar release characteristic and thus pressure treatment does not seem to affect the drug release. Figure 7.6 shows the cumulative release curves for all the heat treated samples with the non treated sample as reference. It is seen that the samples with short heating at 60 °C and the sample heated at 100 °C have a faster

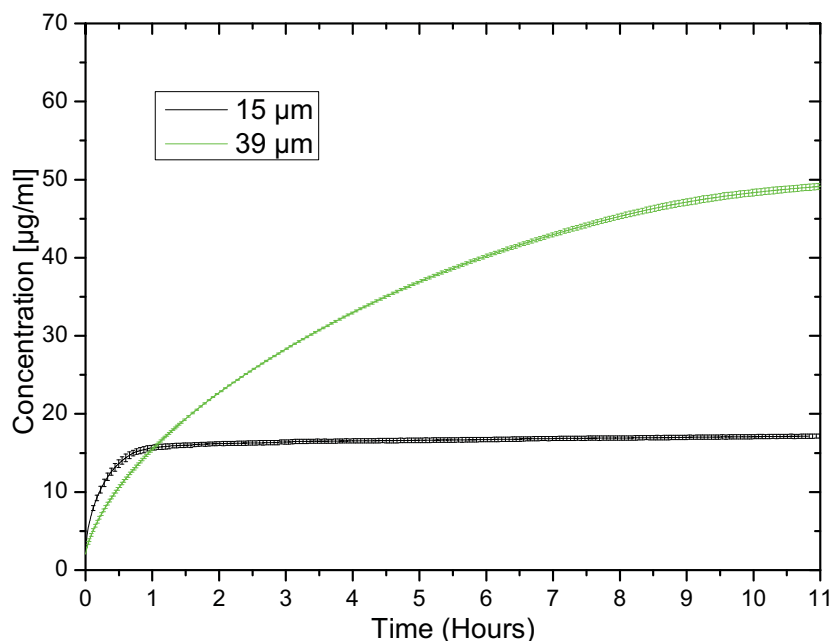


Figure 7.4: Graph showing the release curves for two different thicknesses of the PCL furosemide drug matrix.

release than the sample heated for 1 hour at 60 °C. The fact that the drug release increases from roughly 80 % to 100 % when the drug matrix is heated is yet to be explained. It can be concluded that heating results in similar drug release characteristics, whether it be 10 minutes at 60 °C or 1 hour at either 60 or 100 °C. The spin coating process, which the drug matrix is fabricated by, resembles a quench cooling of the polymer. It could be that the quenching traps some of the furosemide in the PCL in such a way that it is not able to diffuse out of the polymer drug matrix. Heating of the drug matrix should increase the crystallinity of both PCL and furosemide. It is likely that the heating allows the trapped furosemide to rearrange itself in the drug matrix making it available for release or that it is forced out by crystal growth. The exact process involved in releasing the trapped furosemide is unknown at this point. The drug release results show that PCL as a matrix for furosemide works very well and that it is possible to get all of the furosemide released from the matrix. Heating and pressure in form of embossing does not hinder release of furosemide, if anything it enhances the release. This behavior enables the drug matrix to be processed and thus provides a versatile polymer drug film that can be used in various applications.

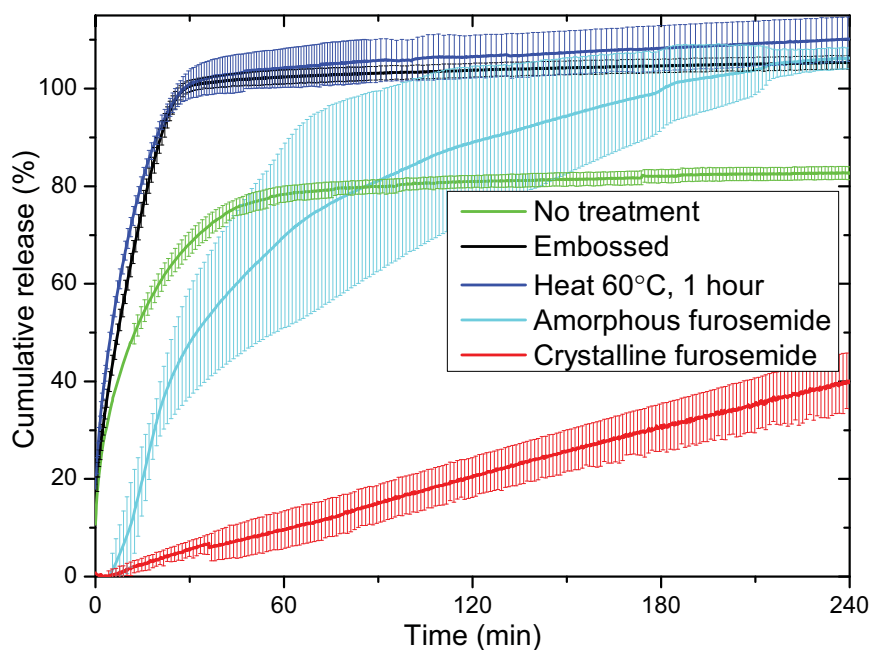


Figure 7.5: Graph showing the cumulative release curves for; the embossed, the non treated and the 60 °C 1 hour treated samples. For comparison release curves for discs made of crystalline and amorphous furosemide are plotted.

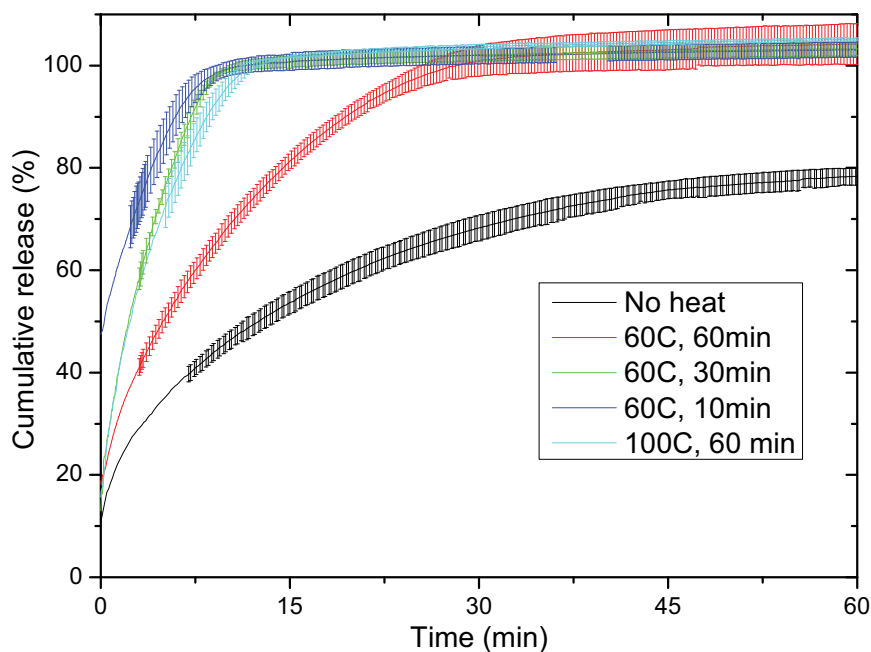


Figure 7.6: Graph showing the release of the samples with different heat treatments

## 7.3 Micro containers

This section describes the drug release from the micro containers prepared as summarized in figure 7.7. It shows the micro containers at three different stages; container shaping by embossing, filling by screen printing and coating by spray coating.

### 7.3.1 Experiments

Two different sets of experiments are conducted. One, PLLA containers filled with crystalline furosemide powder are tested. This corresponds to the situation shown in figure 7.7(e). The samples used for the experiment are squares of 400 containers. The experiment is conducted as described in section 7.1. Two, release from coated containers is tested,

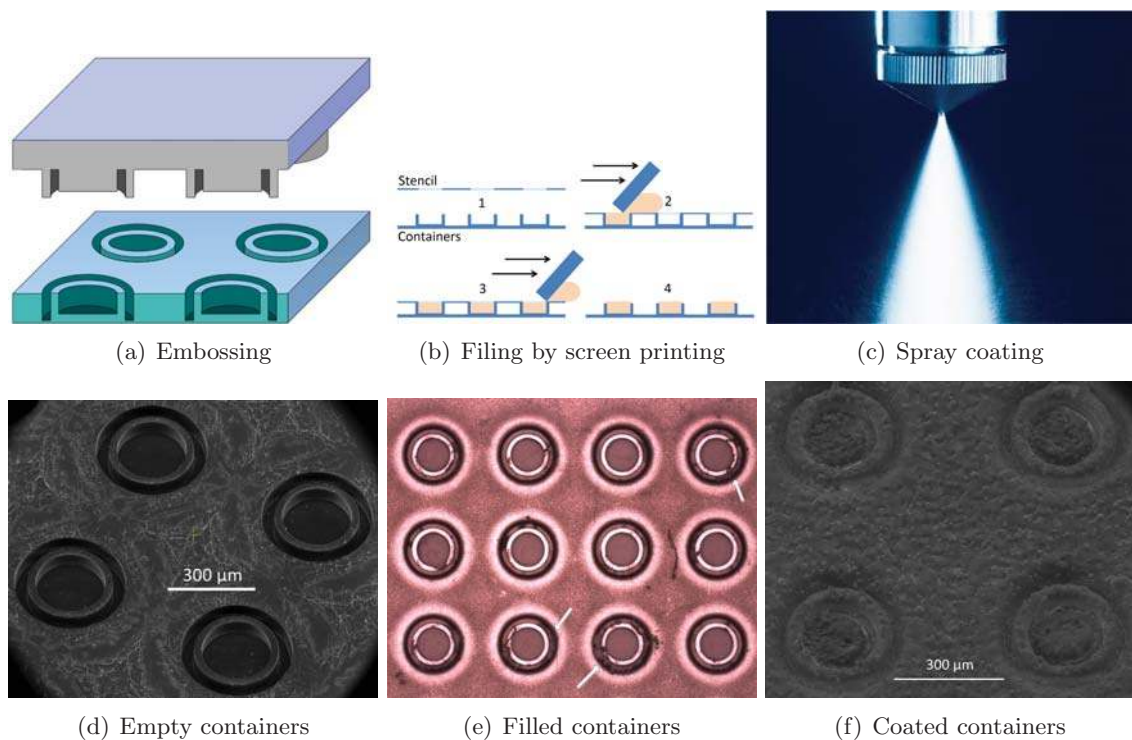


Figure 7.7: PLLA containers at different stages.

this corresponds to the sample shown in figure 7.7(f). Spray dried amorphous furosemide is used for the experiment. The dissolution tests for the second experiment and the preparation of the spray dried amorphous furosemide powder are performed by PhD student Line Hagner Nielsen at the Department of Pharmaceutics and Analytical Chemistry at the University of Copenhagen. For this experiment FaSSGF media of pH 1.5 and FaSSIF media of pH 6.5 are used to test the effectiveness of an enteric coating made by spray coating of Eudragit<sup>®</sup> L100 (Evonik industries) on the PLLA containers. The Eudragit<sup>®</sup> L100 is a polymer used by the pharmaceutical industry for coating of tablets. It does not dissolve in acidic solutions, such as the stomach environment, but it dissolves at higher

pH present in the intestine. The deposition is made with an ExactaCoat system from Sono-Tak.

### 7.3.2 Release results & discussion

First, the results of experiment one are presented, then the results of experiment two are presented. The results of the first dissolution test is shown in figure 7.8. It is seen that the furosemide is dissolved fast and a stable concentration level is reached after 5-7 minutes. After dissolution tests the containers are inspected by microscope. The inspection shows that no furosemide is left in the containers. The containers are weighed before and after filling and the difference is found to be 2 mg. The graph shows that 180  $\mu\text{g}/\text{ml}$  is released from the containers, corresponding to 1.8 mg released furosemide. A possible explanation for the difference in furosemide is loss of furosemide during handling of the samples before the experiment. The containers are not coated and thus the furosemide is lying loosely in the containers. The results from the second dissolution experiment with Eudragit coated

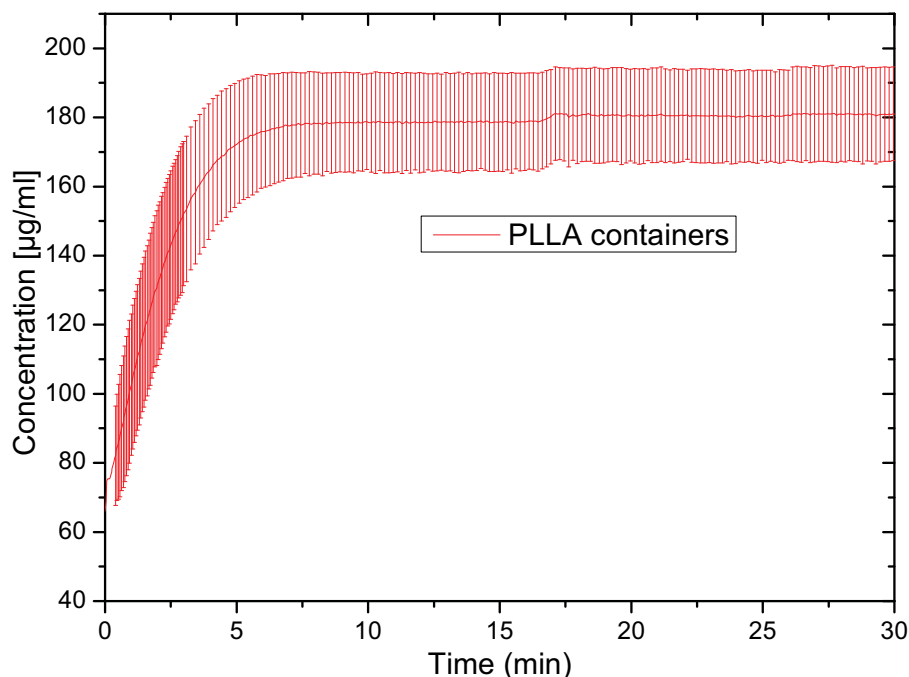


Figure 7.8: Graph showing the release of crystalline furosemide powder from PLLA containers.

PLLA containers are shown in figure 7.9. It is seen that the release of furosemide is neglectable for the first 120 minutes where the containers are immersed in FaSSGF media with a pH of 1.5. Once the media is changed to FaSSIF pH 6.5, the furosemide is released swiftly. The release curve indicates that the Eudragit coating withstands the FaSSGF media, while it is dissolved by the FaSSIF media, resulting in release of furosemide. The containers are inspected after dissolution tests and no furosemide is found to reside on the

PLLA after the experiment. It is seen that the release curve does not equate to 100 % dissolution of furosemide. A possible explanation for this is that some of the furosemide is blown away during the spray coating of Eudragit. The Eudragit polymer is deposited onto the surface of the containers by a stream of nitrogen gas. The furosemide powder consists of particles with a size down to 5  $\mu\text{m}$ . It is likely that these particles can be redistributed by the nitrogen gas stream, either redepositing on the container surface or removed from sample entirely. Another possibility is that some of the furosemide diffuses into the PLLA instead of dissolving in the FaSSIF media. Based on the HSP data for PLLA and furosemide presented in table 3.1 the two compounds are not alike. Thus it is unlikely that furosemide diffuses into the PLLA. Finally, the furosemide could enter the solution as particles, though not dissolve and thus not contribute to the concentration of the solution. The drug release results from the micro containers show that it is possible

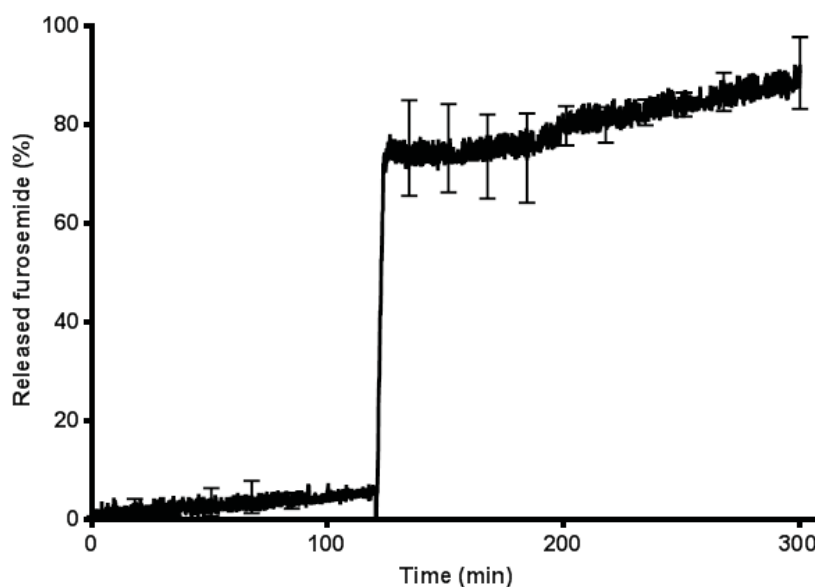


Figure 7.9: Graph showing release curve of furosemide from Eudragit-coated PLLA micro containers in biorelevant media at pH 1.5 for 120 min and at pH 6.5 for 180 min. Data represent  $n=3\pm\text{SD}$

to control the release of drug by pH sensitive polymers. It shows that most of the drug if not all is released from the containers and that the drug release happens within a few minutes.

## 7.4 UV imager experiment

This section describes an experiment conducted on PLLA containers that have been filled by screen printing and spray coated with an enteric coating of Eudragit L100. The experiment is performed to verify the observation from the dissolution tests. For the experiment



a test setup (UV imager) available at the Department of Pharmaceutics and Analytical Chemistry at the University of Copenhagen is used. The UV imager experiment and data analysis is performed by Post doc. Sarah Gordon.

### 7.4.1 Experiment

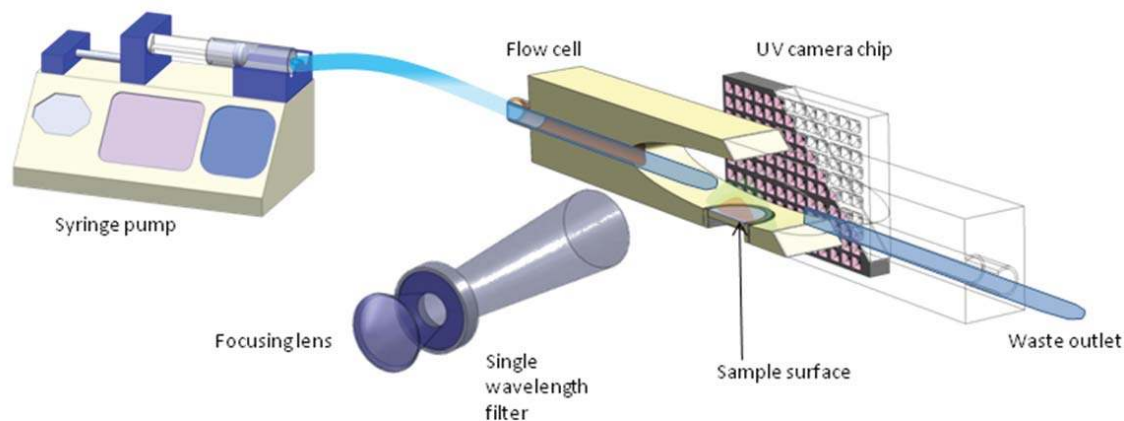


Figure 7.10: Schematic showing the UV imager setup used by Sarah Gordon for the experiment. [92]

For the experiment, a sample with four containers PLLA containers is cut out by laser to match a cylindric holder with an inner diameter of 1.5 mm. Figure 7.10 shows a schematic of the test setup. The setup consists of a syringe pump system, where the syringes are connected to a flow cell via tubes. A sample holder is located at the bottom of the flow cell. Around the flow cell, a setup consisting of a pulsed Xenon lamp in connection with a band pass filter is located on one side and a UV camera chip is located on the other side to record UV images. The setup allows for real time imaging of release from the sample holder in the flow cell. For a more detailed explanation of the measurement setup the reader is referred to [92, 93]. First, gastric media with pH 1.5 is passed through the flow cell for 5 minutes to test the enteric coating. Then, intestinal media with pH 6.5 is passed through the cell until the drug release is complete. The flow rate of both media is 0.2 mL/min.

### 7.4.2 Results & discussion

The result of the experiment is shown in figure 7.11, where four images taken at different times are shown. Figure 7.11(a) shows an image after 5 minutes of gastric media. No release from the containers is observed. Figure 7.11(b) shows an image after 1 minute of flow with intestinal media. It is seen that furosemide is released from the containers. This is the starting point of the release. Figure 7.11(c) shows an image after 5 minutes of flow with intestinal media. At this point the release of furosemide is at its peak. Figure 7.11(d) shows an image after 15 minute of flow with intestinal media. At this point, the release

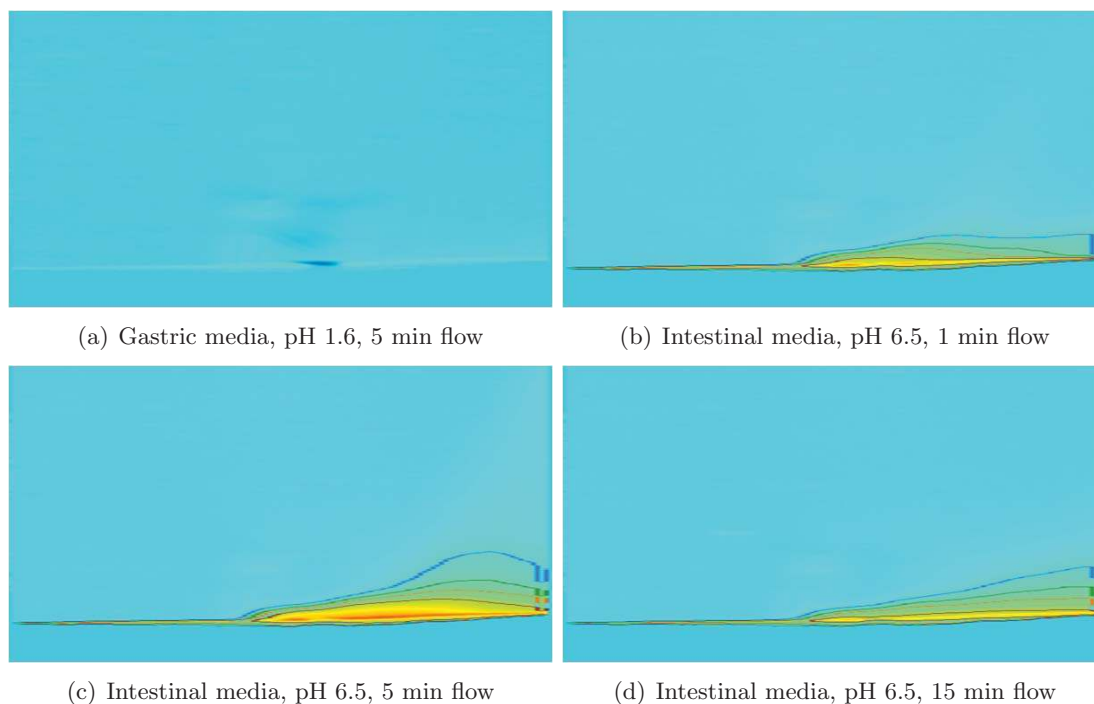


Figure 7.11: The figure shows images at specific times for the UV imager experiment. The sample is placed in the bottom center of the images. Contour Lines: dark blue = 100 mAU, green = 150 mAU, orange = 200 mAU, light blue = 250 mAU, brown = 300 mAU. mAU = milli-absorbance units.

from the containers is almost complete. The series of images illustrates the drug release from four containers coated with Eudragit L100. It is observed that it takes less than a minute for the Eudragit to be dissolved by the intestinal media and that the peak of the release happens after 5 minutes. At this point the release diminishes and the majority of the drug is released after 15 minutes. The experiment supports the observations from the dissolution experiments. The enteric Eudragit coating is dissolved by the FaSSIF media shortly after it is introduced in the flow cell. The release of the furosemide from the containers occurs quickly, peaking after 5 minutes whereupon the release slowly decreases.

## 7.5 Summary

In this chapter methods for characterising drug release from the drug matrix and the containers are described; dissolution tests using a Pion  $\mu$ DISS profiler<sup>®</sup> and a setup utilizing a flow cell in combination with UV imaging equipment. It is found that the drug matrix releases 80% of the total furosemide contained within the matrix in its initial state. If the drug matrix is heat treated at 60- or 100 °C, the drug matrix releases 100%. Furthermore, the release time is shortened by the heat treatment. For the micro container drug delivery systems, the drug release occurs within a few minutes. The release from the container

system can be controlled by enteric coatings. Experiments show that an Eudragit L100 polymer coating can prevent drug release in acidic media, FaSSGF pH 1.5. Changing the media to FaSSIF pH 6.5 dissolves the coating and drug release from the container system is observed. The experiments show that it is possible to tune the release of drug through coatings.

## Chapter 8

# Conclusion

The goal of this project has been to develop techniques for micro fabrication in biodegradable polymer and to use these techniques to realize biodegradable micro containers for oral drug delivery. This has successfully been achieved by fabrication of micro containers for drug delivery by hot embossing in biodegradable polymer films made of PLLA and PCL.

Polymer solutions have been developed using the theory of Hansen's solubility parameters. The solutions are used to deposit films which are used in the fabrication of the micro container. The films are made by spin coating and experiments have shown that it is possible to fabricate uniform and homogeneous PCL and PLLA films with a thickness up to 110  $\mu\text{m}$ . While it is possible to realize thicker films, the thickness variation increases drastically as the film thickness increases.

It is found that the adhesion of the PCL and PLLA films to silicon substrates can be tuned by heat treatment following the spin coating process. If a strong adhesion is desired the heat treatment should exceed the melting temperature of the polymer. Following the heat treatment, the polymer should be cooled slowly to room temperature to avoid stress caused by differences in thermal expansion of polymer and substrate. This procedure can be used to remove potential bubbles in the polymer films. A poor adhesion is obtained by heat treatment below the melting point or no treatment at all.

Solutions consisting of both polymer and pharmaceuticals have been developed using the Hansen's solubility parameters. Drug matrices have been fabricated by spin coating these solutions. It is found that organic solvents should have similar boiling points and thus similar evaporation rates if more than one solvent is used. If the evaporation rates differ, the solvent composition changes with time which can result in precipitation of either polymer or pharmaceutical. Homogenous drug matrices are obtained with solvents having a low boiling point and thus a fast evaporation rate. A drug matrix consisting of PCL and furosemide has been developed. It is found that the highest weight ratio of furosemide to PCL is 1:4 to achieve homogenous films. A blend of DCM and Acetone is used in a volume ratio of 1:2 to dissolve both compounds. Microscopy characterization of the PCL furosemide matrix has shown that the matrix contains porous structures with a size of

5-10  $\mu\text{m}$ . Experiments have shown that the porous structures can be removed by heating above the melting temperature of the polymer or by performing an embossing at 1.9 MPa above the  $T_g$ . The morphology of the drug matrix has been studied by X-ray diffraction and experiments show that furosemide is amorphous after spin coating. Experiments show that the furosemide remains amorphous after the drug matrix is heat treated at 60°C and after embossing at 1.9 MPa at 60 °C. If the drug matrix is heat treated at 100°C, the furosemide starts to crystallize. The experiments show that the PCL remains semi crystalline for all kinds of treatment. Drug release from the drug matrix is tested by dissolution. Experiments show that the drug matrix releases 80% of the total furosemide contained within the matrix. If the drug matrix is heat treated at 60 °C or 100 °C, the drug matrix releases 100% and the drug release is shortened. Pressure such as the one applied during embossing has no effect on the drug release.

Hot embossing processes have been developed for fabrication of micro containers with the biodegradable polymers PCL and PLLA. A stamp is pressed into a spin coated polymer film of PCL or PLLA. A successful pattern transfer from stamp to polymer film is achieved at 60 °C and a pressure of 1.9 MPa for 1 hour for the PCL films. For the PLLA, a successful pattern transfer is obtained at 120 °C and a pressure of 1.9 MPa for 1 hour. Embossing experiments show that a residual layer connects the micro containers to the surrounding polymer film after embossing and that the residual layer is difficult to remove in an efficient manner. Crystallization of PLLA is observed during the embossing and to avoid cracking of the PLLA film it should be lifted from the substrate after embossing. No cracking is observed for the PCL film.

For the embossing process, stamps in three different materials have been fabricated. SU-8 stamps have been fabricated by a two step photo lithography process. Silicon stamps have been fabricated by a two step DRIE process. Nickel stamps have been fabricated by a two step DRIE process followed by an electroplating process. Both silicon and SU-8 stamps have shown limited durability, with SU-8 having the better performance of the two. The brittle nature of silicon causes severe damage to the stamps during embossing. For the SU-8, the lack of durability is believed to be caused by a lack of material strength. The nickel stamps have shown impeccable durability and are recommended for further work. DRIE processes capable of producing positively sloped side walls have been developed. It is found that by varying the chamber pressure and platen power, the slope of the sidewalls can be controlled. The sloped sidewalls enable an easy release of stamps from polymer films.

Besides the micro containers fabricated in the biodegradable polymers PCL and PLLA, micro containers have been fabricated in SU-8. The containers are made by a two step photo lithography process. The SU-8 micro containers serve as a model system for testing filling methods for micro containers and initial studies on micro containers as drug delivery devices.

Three different ways of filling micro containers with drug have been tested; embossing

of polymer drug matrix, solvent casting and screen printing. The embossing of polymer drug matrix to fill micro containers has been tested on SU-8 containers. The filling method has been shown to work on a wafer scale. The method is not limited to the SU-8 containers and might be feasible as filling method for the biodegradable containers, if they are fabricated in a manner that leaves them sitting out of plane with the polymer film. The drug loading is related to the ratio of drug to polymer used in the drug matrix. At its current state, this means a filling level of 20 %. Solvent casting is another method used to fill micro containers. The method works on a wafer level, although polymer and drug is deposited outside the micro containers as well as inside. In the experiments a blend of 33 % furosemide and 66 % PAA was used and thus a filling level of 33 % is currently possible. Screen printing is another method used to fill micro container and this method is the one used for drug release experiments carried out with the micro containers. The method utilizes a stencil fabricated by laser cutting of a transparent foil. The foil is aligned to the micro containers whereafter the containers are filled by scraping drug across the stencil. The foil is removed along with excess drug. If pure drug powder is used, the method allows for up to 100 % filling level. The method is tested on squares containing 400 biodegradable micro containers. The method is not limited to the biodegradable containers and can be used for the SU-8 containers as well. The method is up scalable and is recommended for filling of micro containers.

Drug release experiments with furosemide showed that release from the micro containers take place within a few minutes and that most of the furosemide is able to exit the container and dissolve in simulated intestinal media. It is shown that the drug release of the containers can be controlled by adding polymeric coatings. Experiments show that an Eudragit L100 polymer coating prevents drug release in simulated gastric media, pH 1.5 while it dissolves in simulated intestinal media, pH 6.5 and enables drug release from the containers.

In conclusion micro systems for drug delivery have been developed. To achieve this, polymer films have been fabricated by spin coating of solutions consisting of PCL and PLLA in organic solvents. Defining of micro structures by hot embossing processes has been developed. The processes enable large scale fabrication of micro containers in biodegradable polymers. Large scale filling methods have been developed for the biodegradable micro containers. Enclosed micro container drug delivery devices capable of releasing drug by change in pH have been demonstrated by spray coating of enteric coatings. A drug matrix has been developed by spin coating solutions consisting of both polymer and drug.





## Chapter 9

# Outlook

Micro containers present progress towards the vision described in section 1.1 further improvements are needed. Separating containers and handling of individual devices has proven to be difficult. Therefore imminent improvements within these areas are needed. A possibility is to use laser machining equipment to fabricate the entire device or to cut out the micro containers after embossing. Another option is to introduce a sacrificial layer on which the micro containers can be fabricated. The sacrificial layer can then be cut into pieces containing a desired amount of containers needed for a dose. Once the containers need to be released, this can be done by dissolving the sacrificial layer. One possibility is to use a water soluble polymer layer, like the PAA used in this work.

At this stage, the drug matrix consists of a polymer and a drug that are not alike according to HSP. The principle of the HSP is that "like dissolve like", thus it could be interesting to match polymers and drugs by HSP values. This could be a way to increase the amount of drug that can be homogeneously distributed in the polymer film. Another possibility is to investigate if the introduction of surfactants to the drug matrix could increase the drug loading.

A lot of research has been put into the development of micro devices for oral drug delivery, as detailed in section 1.5 and in this work. It has shown that a large number of devices, thousands to hundred thousands, are needed for the delivery of a dose. Thus, fabrication of these devices needs to be up scaled to accommodate this. It means that fabrication techniques capable of fabricating millions, if not billions are needed. Additionally, the micro devices have to be able to compete with other drug delivery systems such as conventional tablets and pills. This means that the fabrication must be cheap. These factors point in the direction of mass production.

The state of art of micro devices for oral drug delivery is as follows; proof of concept has been shown for; protection of drug by container and outer layers, mucoadhesion by surface chemistry modification or polymeric coatings, controlled release by enteric coatings and unidirectional release by design. To advance the concept of micro devices for oral

drug delivery the following needs to be accomplished; clinical trials where micro devices are used for treatment and where features (drug protection, mucoadhesion, unidirectional release) of micro devices proves critical for the success of the treatment. Furthermore, fabrication techniques enabling mass production of devices are crucial; large amounts of devices are needed for a dose and many doses are needed in order to conduct clinical trials.

# Bibliography

- [1] F.J. Martin and C. Grove. Microfabricated drug delivery systems: concepts to improve clinical benefit. *Biomedical Microdevices*, 3(2):97–108, 2001.
- [2] X. Zhang, H. He, C. Yen, W. Ho, and L.J. Lee. A biodegradable, immunoprotective, dual nanoporous capsule for cell-based therapies. *Biomaterials*, 29(31):4253–4259, 2008.
- [3] H. Takeuchi, J. Thongborisute, Y. Matsui, H. Sugihara, H. Yamamoto, and Y. Kawashima. Novel mucoadhesion tests for polymers and polymer-coated particles to design optimal mucoadhesive drug delivery systems. *Advanced drug delivery reviews*, 57(11):1583–1594, 2005.
- [4] A. Ahmed, C. Bonner, and T.A. Desai. Bioadhesive microdevices with multiple reservoirs: a new platform for oral drug delivery. *Journal of Controlled Release*, 81(3):291–306, 2002.
- [5] C.J.H. Porter, N.L. Trevaskis, and W.N. Charman. Lipids and lipid-based formulations: optimizing the oral delivery of lipophilic drugs. *Nature Reviews Drug Discovery*, 6(3):231–248, 2007.
- [6] J. Brouwers, M.E. Brewster, and P. Augustijns. Supersaturating drug delivery systems: The answer to solubility-limited oral bioavailability? *Journal of pharmaceutical sciences*, 98(8):2549–2572, 2009.
- [7] T. Vasconcelos, B. Sarmiento, and P. Costa. Solid dispersions as strategy to improve oral bioavailability of poor water soluble drugs. *Drug discovery today*, 12(23):1068–1075, 2007.
- [8] C. Leuner and J. Dressman. Improving drug solubility for oral delivery using solid dispersions. *European Journal of Pharmaceutics and Biopharmaceutics*, 50(1):47–60, 2000.
- [9] G.G. Liversidge and K.C. Cundy. Particle size reduction for improvement of oral bioavailability of hydrophobic drugs: I. absolute oral bioavailability of nanocrystalline danazol in beagle dogs. *International journal of pharmaceutics*, 125(1):91–97, 1995.

- [10] L. Engelen, R.A. de Wijk, A. van der Bilt, J.F. Prinz, A.M. Janssen, and F. Bosman. Relating particles and texture perception. *Physiology & behavior*, 86(1):111–117, 2005.
- [11] J. Guan, H. He, L.J. Lee, and D.J. Hansford. Fabrication of particulate reservoir-containing, capsulelike, and self-folding polymer microstructures for drug delivery. *small*, 3(3):412–418, 2007.
- [12] HV Chavda, CN Patel, IS Anand, et al. Biopharmaceutics classification system. *Systematic Reviews in Pharmacy*, 1(1):62, 2010.
- [13] S. Stegemann, F. Leveiller, D. Franchi, H. De Jong, and H. Lindén. When poor solubility becomes an issue: from early stage to proof of concept. *European journal of pharmaceutical sciences*, 31(5):249–261, 2007.
- [14] Furosemid, pro.medicin.dk @online jan 2013. <http://pro.medicin.dk/Medicin/Praeparater/4004>.
- [15] Furosemide at www.drugs.com @online jan 2013. <http://www.drugs.com/furosemide.html>.
- [16] M.H. Cohen, K. Melnik, A.A. Boiarski, M. Ferrari, and F.J. Martin. Microfabrication of silicon-based nanoporous particulates for medical applications. *Biomedical Microdevices*, 5(3):253–259, 2003.
- [17] A.B. Foraker, R.J. Walczak, M.H. Cohen, T.A. Boiarski, C.F. Grove, and P.W. Swaan. Microfabricated porous silicon particles enhance paracellular delivery of insulin across intestinal caco-2 cell monolayers. *Pharmaceutical research*, 20(1):110–116, 2003.
- [18] S.L. Tao and T.A. Desai. Gastrointestinal patch systems for oral drug delivery. *Drug discovery today*, 10(13):909–915, 2005.
- [19] S. Sant, S.L. Tao, O. Fisher, Q. Xu, N.A. Peppas, and A. Khademhosseini. Microfabrication technologies for oral drug delivery. *Advanced drug delivery reviews*, 2011.
- [20] P. Colombo, F. Sonvico, G. Colombo, and R. Bettini. Novel platforms for oral drug delivery. *Pharmaceutical research*, 26(3):601–611, 2009.
- [21] H.D. Chirra and T.A. Desai. Emerging microtechnologies for the development of oral drug delivery devices. *Advanced Drug Delivery Reviews*, 2012.
- [22] D. Teutonico and G. Ponchel. Patches for improving gastrointestinal absorption: an overview. *Drug discovery today*, 16(21):991–997, 2011.
- [23] H.D. Chirra and T.A. Desai. Multi-reservoir bioadhesive microdevices for independent rate-controlled delivery of multiple drugs. *Small*, 2012.

- [24] D.A. Canelas, K.P. Herlihy, and J.M. DeSimone. Top-down particle fabrication: control of size and shape for diagnostic imaging and drug delivery. *Wiley Interdisciplinary Reviews: Nanomedicine and Nanobiotechnology*, 1(4):391–404, 2009.
- [25] N. Venkatesan, K. Uchino, K. Amagase, Y. Ito, N. Shibata, and K. Takada. Gastrointestinal patch system for the delivery of erythropoietin. *Journal of controlled release*, 111(1):19–26, 2006.
- [26] A. Ahmed, C. Bonner, and T.A. Desai. Bioadhesive microdevices for drug delivery: a feasibility study. *Biomedical Microdevices*, 3(2):89–96, 2001.
- [27] S.L. Tao, M.W. Lubeley, and T.A. Desai. Bioadhesive poly (methyl methacrylate) microdevices for controlled drug delivery. *Journal of controlled release*, 88(2):215–228, 2003.
- [28] S.L. Tao and T.A. Desai. Microfabrication of multilayer, asymmetric, polymeric devices for drug delivery. *Advanced Materials*, 17(13):1625–1630, 2005.
- [29] K.M. Ainslie, C.M. Kraning, and T.A. Desai. Microfabrication of an asymmetric, multi-layered microdevice for controlled release of orally delivered therapeutics. *Lab Chip*, 8(7):1042–1047, 2008.
- [30] K.M. Ainslie, R.D. Lowe, T.T. Beaudette, L. Petty, E.M. Bachelder, and T.A. Desai. Microfabricated devices for enhanced bioadhesive drug delivery: Attachment to and small-molecule release through a cell monolayer under flow. *Small*, 5(24):2857–2863, 2009.
- [31] S.E.A. Gratton, P.D. Pohlhaus, J. Lee, J. Guo, M.J. Cho, and J.M. DeSimone. Nanofabricated particles for engineered drug therapies: A preliminary biodistribution study of print nanoparticles. *Journal of Controlled Release*, 121(1):10–18, 2007.
- [32] S.E.A. Gratton, S.S. Williams, M.E. Napier, P.D. Pohlhaus, Z. Zhou, K.B. Wiles, B.W. Maynor, C. Shen, T. Olafsen, E.T. Samulski, et al. The pursuit of a scalable nanofabrication platform for use in material and life science applications. *Accounts of chemical research*, 41(12):1685–1695, 2008.
- [33] A. Garcia, P. Mack, S. Williams, C. Fromen, T. Shen, J. Tully, J. Pillai, P. Kuehl, M. Napier, J.M. DeSimone, et al. Microfabricated engineered particle systems for respiratory drug delivery and other pharmaceutical applications. *Journal of Drug Delivery*, 2012, 2012.
- [34] S. Eiamtrakarn, Y. Itoh, J. Kishimoto, Y. Yoshikawa, N. Shibata, M. Murakami, and K. Takada. Gastrointestinal mucoadhesive patch system (gi-maps) for oral administration of g-csf, a model protein. *Biomaterials*, 23(1):145–152, 2002.
- [35] S. Eaimtrakarn, YV Rama Prasad, S.P. Puthli, Y. Yoshikawa, N. Shibata, and K. Takada. Possibility of a patch system as a new oral delivery system. *International journal of pharmaceuticals*, 250(1):111–117, 2003.

- [36] Y. Ito, Y. Ochiai, K. Fukushima, N. Sugioka, and K. Takada. Three-layered microcapsules as a long-term sustained release injection preparation. *International journal of pharmaceuticals*, 384(1):53–59, 2010.
- [37] J. Guan, H. He, D.J. Hansford, and L.J. Lee. Self-folding of three-dimensional hydrogel microstructures. *The Journal of Physical Chemistry B*, 109(49):23134–23137, 2005.
- [38] J. Guan, N. Ferrell, L. James Lee, and D.J. Hansford. Fabrication of polymeric microparticles for drug delivery by soft lithography. *Biomaterials*, 27(21):4034–4041, 2006.
- [39] H. He, V. Grignol, V. Karpa, C. Yen, K. LaPerle, X. Zhang, N.B. Jones, M.I. Liang, G.B. Lesinski, WS Ho, and L.J. Lee. Use of a nanoporous biodegradable miniature device to regulate cytokine release for cancer treatment. *Journal of Controlled Release*, 151(3):239–245, 2011.
- [40] H. He, X. Cao, and L.J. Lee. Design of a novel hydrogel-based intelligent system for controlled drug release. *Journal of controlled release*, 95(3):391–402, 2004.
- [41] Gert R. Strobl. *The physics of polymers: concepts for understanding their structures and behavior*. Springer, 1997.
- [42] Charles m. hansen ::: The official hansen solubility parameters website. <http://www.hansen-solubility.com/index.php?id=25>.
- [43] Charles M. Hansen. *Hansens solubility parameters: a user's handbook*, volume 2007. CRC Press, second edition edition, jun 2007.
- [44] D.W Van Krevelen. *Properties of polymers*, volume 1990. Elsevier, third edition edition, 1990.
- [45] Charles m. hansen ::: The official hansen solubility parameters website. <http://www.hansen-solubility.com/index.php?id=25>.
- [46] European bioplastics organization, fact sheets, bioplastics @online dec 2012. <http://en.european-bioplastics.org/multimedia/>.
- [47] N. Umeki, T. Sato, M. Harada, J. Takeda, S. Saito, Y. Iwao, and S. Itai. Preparation and evaluation of biodegradable films containing the potent osteogenic compound bfb0261 for localized delivery. *International journal of pharmaceuticals*, 404(1):10–18, 2011.
- [48] R. Shi and H.M. Burt. Amphiphilic dextran-graft-poly  $\epsilon$ -caprolactone) films for the controlled release of paclitaxel. *International journal of pharmaceuticals*, 271(1):167–179, 2004.

- [49] ZG Tang, RA Black, JM Curran, JA Hunt, NP Rhodes, and DF Williams. Surface properties and biocompatibility of solvent-cast poly  $\epsilon$ -caprolactone] films. *Biomaterials*, 25(19):4741–4748, 2004.
- [50] T.K. Dash and V.B. Konkimalla. Poly- $\epsilon$ -caprolactone based formulations for drug delivery and tissue engineering: A review. *Journal of Controlled Release*, 158(1):15–33, 2012.
- [51] RRM Bos, FB Rozema, G. Boering, AJ Nijenhuis, AJ Pennings, AB Verwey, P. Nieuwenhuis, and HWB Jansen. Degradation of and tissue reaction to biodegradable poly (l-lactide) for use as internal fixation of fractures: a study in rats. *Biomaterials*, 12(1):32–36, 1991.
- [52] K. Van de Velde and P. Kiekens. Biopolymers: overview of several properties and consequences on their applications. *Polymer Testing*, 21(4):433–442, 2002.
- [53] NG Semaltianos. Spin-coated pmma films. *Microelectronics journal*, 38(6):754–761, 2007.
- [54] Stephan Keller. *Fabrication of an autonomous surface stress sensor with the polymer SU-8*. PhD thesis, Technical University of Denmark, 2008.
- [55] C. Mack. *Fundamental principles of optical lithography: the science of microfabrication*. Wiley, 2011.
- [56] G.S. May and S.M. Sze. *Fundamentals of semiconductor fabrication*. Wiley, 2004.
- [57] PSI. Paul scherrer institut, materials group @ONLINE dec, 2012. [http://materials.web.psi.ch/Research/Thin\\_Films/Methods/Spin.htm](http://materials.web.psi.ch/Research/Thin_Films/Methods/Spin.htm).
- [58] M.M. Crowley, F. Zhang, M.A. Repka, S. Thumma, S.B. Upadhye, S. Kumar Battu, J.W. McGinity, and C. Martin. Pharmaceutical applications of hot-melt extrusion: part i. *Drug development and industrial pharmacy*, 33(9):909–926, 2007.
- [59] M.A. Repka, S.K. Battu, S.B. Upadhye, S. Thumma, M.M. Crowley, F. Zhang, C. Martin, and J.W. McGinity. Pharmaceutical applications of hot-melt extrusion: Part ii. *Drug development and industrial pharmacy*, 33(10):1043–1057, 2007.
- [60] M. Belmares, M. Blanco, WA Goddard, RB Ross, G. Caldwell, S.H. Chou, J. Pham, PM Olofson, and C. Thomas. Hildebrand and hansen solubility parameters from molecular dynamics with applications to electronic nose polymer sensors. *Journal of computational chemistry*, 25(15):1814–1826, 2004.
- [61] S.C. Shin and J. Kim. Physicochemical characterization of solid dispersion of furosemide with tpgs. *International journal of pharmaceuticals*, 251(1):79–84, 2003.
- [62] S. Keller, D. Haefliger, and A. Boisen. Optimized plasma-deposited fluorocarbon coating for dry release and passivation of thin su-8 cantilevers. *Journal of Vacuum Science & Technology B: Microelectronics and Nanometer Structures*, 25(6):1903–1908, 2007.



- [63] Y. MATSUDA, M. OTSUKA, M. ONOE, and E. TATSUMI. Amorphism and physicochemical stability of spray-dried frusemide. *Journal of pharmacy and pharmacology*, 44(8):627–633, 1992.
- [64] BC Ng, HY Wong, KW Chew, and Z. Osman. Development and characterization of poly- $\epsilon$ -caprolactone-based polymer electrolyte for lithium rechargeable battery. *Int. J. Electrochem. Sci*, 6:4355–4364, 2011.
- [65] M.J. Madou. *Fundamentals of microfabrication: the science of miniaturization*. CRC, 2002.
- [66] Anders Greve. *Fabrication of polymer microcantilevers by nanoimprint lithography*. PhD thesis, Technical University of Denmark, 2009.
- [67] M. Worgull. *Hot embossing: theory and technology of microreplication*. William Andrew Pub, 2009.
- [68] J.D. Gelorme, R.J. Cox, and S.A.R. Gutierrez. Photoresist composition and printed circuit boards and packages made therewith, November 21 1989. US Patent 4,882,245.
- [69] R. Li, Y. Lamy, WFA Besling, F. Roozeboom, and PM Sarro. Continuous deep reactive ion etching of tapered via holes for three-dimensional integration. *Journal of Micromechanics and Microengineering*, 18(12):125023, 2008.
- [70] R.C. Rowe, P.J. Sheskey, and S.C. Owen. *Handbook of pharmaceutical excipients*. Pharmaceutical press London, 2006.
- [71] L.H. Nielsen, S.S. Keller, K.C. Gordon, A. Boisen, T. Rades, and A. Müllertz. Spatial confinement can lead to increased stability of amorphous indomethacin. *European Journal of Pharmaceutics and Biopharmaceutics*, 2012.
- [72] Paolo Marizza. Inkjet printing as a technique for filling of micro-wells with biocompatible polymers. Submitted to *Journal of Microelectronic Engineering*, 2012.
- [73] D. Åkesson, M. Skrifvars, S. Lv, W. Shi, K. Adekunle, J. Seppälä, and M. Turunen. Preparation of nanocomposites from biobased thermoset resins by uv-curing. *Progress in Organic Coatings*, 67(3):281–286, 2010.
- [74] M. Pulkkinen, M. Malin, T. Tarvainen, T. Saarimäki, J. Seppälä, and K. Järvinen. Effects of block length on the enzymatic degradation and erosion of oxazoline linked poly- $\epsilon$ -caprolactone. *European journal of pharmaceutical sciences*, 31(2):119–128, 2007.
- [75] M. Pulkkinen, M. Malin, J. Böhm, T. Tarvainen, T. Wirth, J. Seppälä, and K. Järvinen. *in vivo* implantation of 2, 2'-bis (oxazoline)-linked poly- $\epsilon$ -caprolactone: Proof for enzyme sensitive surface erosion and biocompatibility. *European Journal of Pharmaceutical Sciences*, 36(2):310–319, 2009.

- [76] J. Wang, Y. Gong, G. Abba, J. Cao, J. Shi, and G. Cai. Micro milling technologies for mems. In *Perspective Technologies and Methods in MEMS Design, 2007. MEMSTECH 2007. International Conference on*, pages 86–95. IEEE, 2007.
- [77] A.M. Greiner, B. Richter, and M. Bastmeyer. Micro-engineered 3d scaffolds for cell culture studies. *Macromolecular Bioscience*, 2012.
- [78] S. Bae, H. Kim, Y. Lee, X. Xu, J.S. Park, Y. Zheng, J. Balakrishnan, T. Lei, H.R. Kim, Y.I. Song, et al. Roll-to-roll production of 30-inch graphene films for transparent electrodes. *Nature nanotechnology*, 5(8):574–578, 2010.
- [79] F.C. Krebs, T. Tromholt, and M. Jørgensen. Upscaling of polymer solar cell fabrication using full roll-to-roll processing. *Nanoscale*, 2(6):873–886, 2010.
- [80] R.R. Gattass and E. Mazur. Femtosecond laser micromachining in transparent materials. *Nature Photonics*, 2(4):219–225, 2008.
- [81] S.S. Keller, N. Feidenhans'l, N. Fisker-Bødker, D. Soulat, A. Greve, D.V. Plackett, and A. Boisen. Fabrication of biopolymer cantilevers using nanoimprint lithography. *Microelectronic Engineering*, 88(8):2294–2296, 2011.
- [82] V. Linder, B.D. Gates, D. Ryan, B.A. Parviz, and G.M. Whitesides. Water-soluble sacrificial layers for surface micromachining. *Small*, 1(7):730–736, 2005.
- [83] H. Abe, Y. Kikkawa, Y. Inoue, and Y. Doi. Morphological and kinetic analyses of regime transition for poly [(s)-lactide] crystal growth. *Biomacromolecules*, 2(3):1007–1014, 2001.
- [84] A. Stromquist. *Simple screenprinting: basic techniques & creative projects*. Lark Books, 2005.
- [85] Gyuman Kim, Beomjoon Kim, and Jürgen Brugger. All-photoplastic microstencil with self-alignment for multiple layer shadow-mask patterning. *Sensors and Actuators A: Physical*, 107(2):132–136, 2003.
- [86] A. Boisen S.S. Keller, F.G. Bosco. Ferromagnetic shadow mask for spray coating of polymer patterns. Submitted to Journal of Microelectronic Engineering, 2012.
- [87] H. Bruus. *Theoretical microfluidics*, volume 18. Oxford University Press, USA, 2007.
- [88] AK Bassi, JE Gough, M. Zakikhani, and S. Downes. The chemical and physical properties of poly ( $\epsilon$ -caprolactone) scaffolds functionalised with poly (vinyl phosphonic acid-co-acrylic acid). *Journal of tissue engineering*, 2(1), 2011.
- [89] ZG Tang, RA Black, JM Curran, JA Hunt, NP Rhodes, and DF Williams. Surface properties and biocompatibility of solvent-cast poly  $\epsilon$ -caprolactone films. *Biomaterials*, 25(19):4741–4748, 2004.

- [90] T.I. Croll, A.J. O'Connor, G.W. Stevens, and J.J. Cooper-White. Controllable surface modification of poly (lactic-co-glycolic acid)(plga) by hydrolysis or aminolysis i: Physical, chemical, and theoretical aspects. *Biomacromolecules*, 5(2):463–473, 2004.
- [91] S. Pranonsatit and S. Lucyszyn. Micromachined screen printing (masprint) technology for rf mems applications. In *High Frequency Postgraduate Student Colloquium, 2005*, pages 3–6. IEEE, 2005.
- [92] J. Østergaard, E. Meng-Lund, S.W. Larsen, C. Larsen, K. Petersson, J. Lenke, and H. Jensen. Real-time uv imaging of nicotine release from transdermal patch. *Pharmaceutical research*, 27(12):2614–2623, 2010.
- [93] S. Gordon, K. Naelapää, J. Rantanen, A. Selen, A. Müllertz, and J. Østergaard. Real-time dissolution behavior of furosemide in biorelevant media as determined by uv imaging. *Pharmaceutical Development and Technology*, (00):1–10, 2012.

## List of scientific contributions

This appendix lists the scientific contributions presented during the PhD study. First oral presentation are listed, the poster presentations and lastly published works is listed.

### Oral presentations

The 3rd Biomaterials Symposium "Biointerfaces", "3D microstructuring of biopolymers" at iNANO, Aarhus University, November 4th, 2010.

38th International Micro and Nano Engineering Conference, "Micro containers with solid polymer drug matrix for oral drug delivery", Toulouse, 2012.

### Poster presentations

36th International Micro and Nano Engineering Conference, "3D Microstructuring of biodegradable polymers", Genoa, 2010.

48th Nordic Polymer Days, "Biopolymer micro wells", Stockholm, KTH, Royal Institute of Technology, 2011.

American Association of Pharmaceutical Scientists Annual Meeting and Exposition 2012, "Spin coated films for use in micro patch drug delivery system", Chicago, 2012.

16th International Conference on Miniaturized Systems for Chemistry and Life Sciences, "Micro Containers with Solid Polymer Drug Matrix for Oral Drug Delivery" Japan 2012.

### Publications

"3D microstructuring of biodegradable polymers", J. Nagstrup, S. S. Keller, K. Almdal, A. Boisen, *Journal of Microelectronic Engineering*, volume 88, 2342-2344, 2011.

"Micro containers with solid polymer drug matrix for oral drug delivery" J. Nagstrup, S. S. Keller, A. Müllertz and A. Boisen, 16th International Conference on Miniaturized Systems for Chemistry and Life Sciences, 978-0-9798064-5-2/ $\mu$ TAS 2012/\$20@12CBMS-0001, (2012)



# Appendix A

# MICRO CONTAINERS WITH SOLID POLYMER DRUG MATRIX FOR ORAL DRUG DELIVERY

Johan Nagstrup<sup>1</sup>, Stephan Sylvest Keller<sup>1</sup>, Anette Müllertz<sup>2</sup> and Anja Boisen<sup>1</sup>

<sup>1</sup>Technical University of Denmark, DTU Nanotech, Denmark

<sup>2</sup>University of Copenhagen, Department of Pharmacy, Denmark

## ABSTRACT

In this work, we present micro containers for drug delivery and a method for wafer scale filling utilizing hot embossing. Hot embossing of a polymer drug matrix followed by a deep reactive ion etch (DRIE) enables filling and release of individual micro containers. Finally, drug release from the embossed polymer drug matrix is shown.

**KEYWORDS** Drug delivery, Hot embossing, micro container.

## INTRODUCTION

Advances in microtechnology and pharmaceutical engineering have led to the proposition of micro containers as carriers for oral drug delivery [1] [2] [3]. Micro containers can be used for oral administration and are able to protect drug from degradation during transit of the gastro-intestinal tract. Further they will enable one-directional drug release at the site of absorption and can thereby enhance the bioavailability of drugs.

Traditionally, micro containers are filled by micro spotting or microinjection [2]. The techniques require liquid solutions and are time consuming. Alternatively, micro containers are filled using hydrogels, a batch method involving several process steps such as deposition, cross-linking, washing, and swelling [2] [3]. Our method enables an easy integration of filling of solid drug formulations into micro container during the fabrication process.

## THEORY

Hot embossing is a technique by which an amorphous or semi-crystalline material is molded with a stamp to achieve a wanted shape. Hot embossing is possible due to lowering of the Young's moduli of materials when the temperature approaches the melting point,  $T_m$ . The point where the softening sets is known as the glass transition temperature,  $T_g$ . The glass transition is a reversible transition from a hard state into a molten state. Hot embossing takes advantage of that reversible process by molding the material above the  $T_g$  and below the  $T_m$ . A stamp is used to mold the material in the desired shape by pressing the stamp in the material. Once the stamp is filled with material, the system is cooled below the  $T_g$ , thus hardening the material before the stamp is withdrawn.

## EXPERIMENTAL

The micro containers are fabricated in SU-8 by a two step photolithography process using a silicon wafer as substrate, as shown in figure 1. The micro containers have an outer diameter of 300  $\mu\text{m}$  and an inner diameter of 200-250 (design variation). The total height is measured to be  $105 \pm 5 \mu\text{m}$  with a container depth of  $60 \pm 5 \mu\text{m}$ . The polymer-drug film is fabricated by spin coating of a solution of polycaprolactone (PCL) and furosemide (furosemide is a diuretic drug used for the treatment of e.g. edema) on a silicon wafer with a fluorocarbon anti-sticking coating [4]. The solution consists of 20 ml dichloromethane, 40 ml acetone, 8 g PCL, 2 g furosemide. The spin coating parameters are 1000 rpm for 60 s with a ramp of 2000 rpm/s. The resulting film is 15  $\mu\text{m}$  thick. To achieve the desired thickness of 45  $\mu\text{m}$ , the spin coating procedure is performed 3 times.

Figure 2 shows the major process steps in the micro container filling. First, the polymer-drug film is embossed into the micro containers at a temperature of 60 °C and a force of 15 kN for 1 hour, figure 2.1. Embossing at 60 °C, which is just below the melting point of PCL, ensures an optimal hot embossing and pattern transfer [4]. The system is then cooled to 20 °C and the silicon wafer is removed, as shown in figure 2.2 and figure 3. The anti-sticking coating ensures that separation takes place between the coating and the polymer-drug film. The next process step is a deep reactive ion etch (DRIE) that separates the micro containers from the excess polymer-drug film, figure 2.3 and figure 4. The etching is performed with a DRIE using the following parameters for an anisotropic etch: O<sub>2</sub> flow of 20 sccm, Ar flow 20 sccm, platen power 150 W, coil power 600, pressure of 4 mTorr, temperature of 10 °C and time of 12 min. Finally, the individual containers are detached from the carrier wafer mechanically, figure 2.4.

Drug release of the embossed polymer drug matrix is performed using a Pion  $\mu$ DISS profiler that utilizes UV spectroscopy to measure concentration over time. The drug release is performed using the biorelevant dissolution media Fasted State Simulated Intestinal Fluid (FaSSIF), to simulate the gastrointestinal fluids, and with a pH that is adjusted to pH 6.5 before the release. Experiments are conducted in beakers containing 10 ml FaSSIF media held at a temperature of 37 °C.



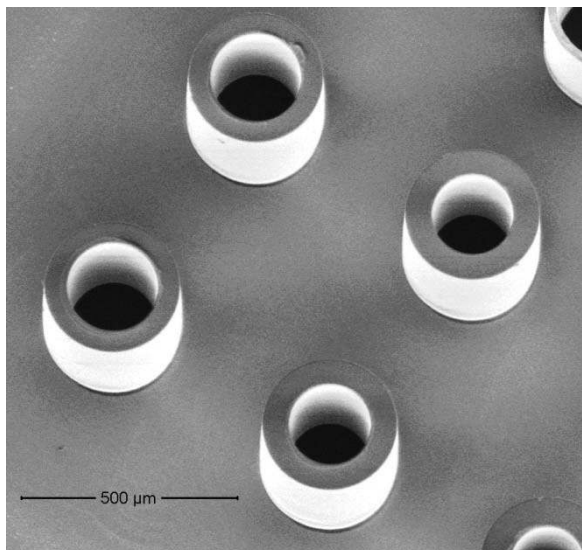


Figure 1. SEM image showing micro containers fabricated in SU-8 by a two step photolithography process

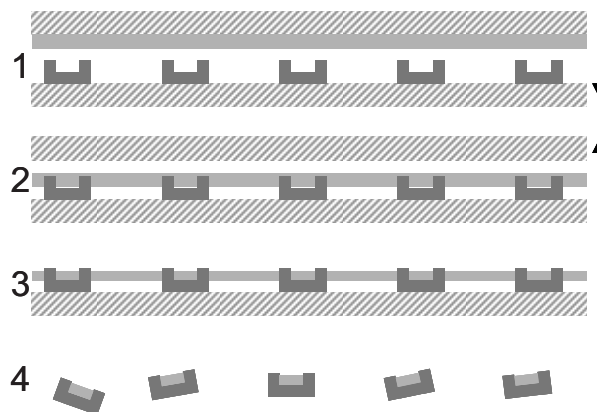


Figure 2. Micro container filling process. 1-2 Embossing polymer drug matrix into containers and removing the carrier wafer. 3 Etching of polymer drug matrix. 4 Mechanical release of containers

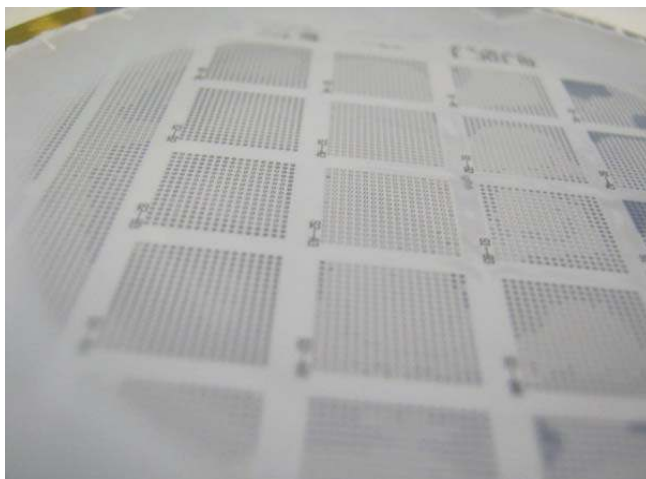


Figure 3. Wafer with micro containers after polymer drug matrix embossing.

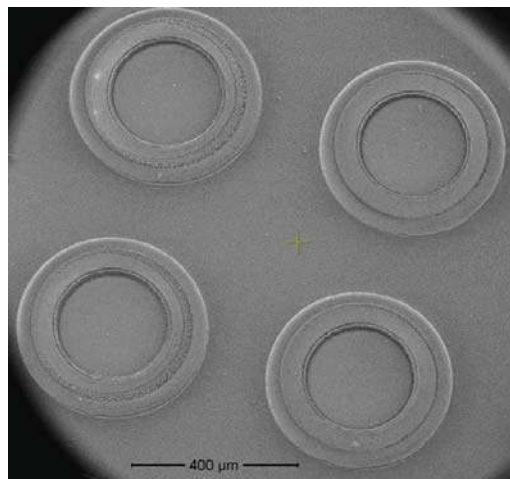


Figure 4. SEM image showing polymer drug matrix embossed into micro containers and etched by DRIE.

## RESULTS & DISCUSSION

The result of the fabrication process is SU-8 micro containers filled with a film consisting of polycaprolactone and furosemide, as shown in figure 5. The method is demonstrated to work on wafer scale level with 4 inch wafers. Our method for filling containers with a drug matrix can be applied to any polymeric drug that presents the following fabrication requirements. . The  $T_g$  of the polymer drug matrix must be lower than the one of the micro container material. The embossing temperature should be in-between the  $T_g$  polymer drug matrix material and the  $T_g$  of micro container material. This ensures a reflow of the polymer drug matrix without effect on the structural stability of the micro containers. Furthermore, the embossing temperature should not exceed  $T_m$  of the components to allow separation of the embossed stack following the cooling process.

Drug release test is performed on the embossed drug matrix, as shown in figure 6 together with the release curve for crystalline furosemide powder and an amorphous spray dried furosemide powder. For the embossed polymer drug matrix more than 95% of the furosemide is released within the first 30 minutes. The release of the embossed polymer matrix shows improved drug release compared with crystalline furosemide. The release resembles the fast release seen from the amorphous furosemide. It is known that amorphous furosemide dissolves faster than crystalline [6], thus the furosemide in the embossed film exhibits amorphous characteristics. X-ray diffraction spectroscopy confirms the morphology and shows that the PCL furosemide films are amorphous before and after the embossing.

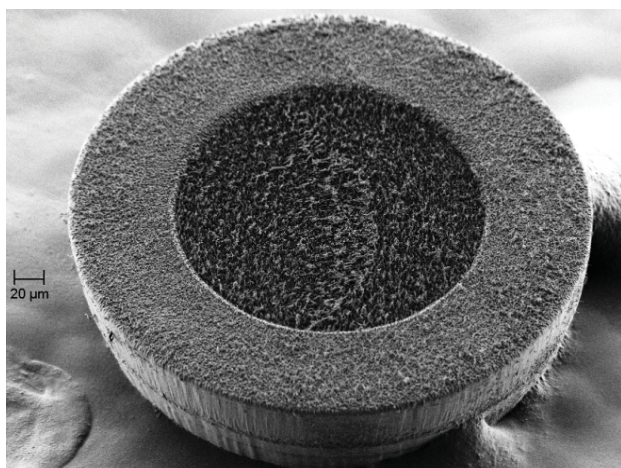


Figure 5. SEM image of released micro container filled with polymer drug matrix. The micro container is placed on carbon foil for ease of handling.

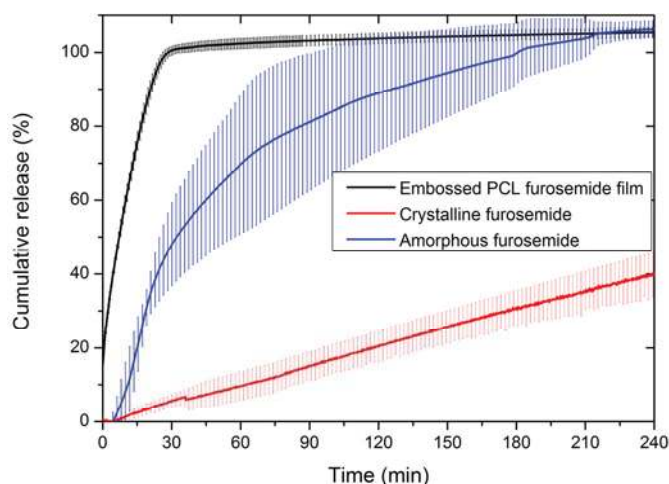


Figure 6. Release curve of embossed furosemide polycaprolactone matrix showing cumulative release. As a reference the cumulative release for an amorphous furosemide powder and a crystalline is plotted. Release test is performed with pion  $\mu$ disc profiler. Standard curve  $R^2$  value of 0.996.

## CONCLUSION

We have shown that it is possible to integrate filling of micro containers as part of the fabrication on a wafer scale level, thus enabling high volume production. The embossed PCL furosemide film shows fast drug release and the furosemide is found to be amorphous. Further development of micro containers for drug delivery includes the addition of a lid for controlled release and the exchange of SU-8 as container material with a biodegradable polymer

## ACKNOWLEDGEMENTS

This research was funded by the Villum Kann Rasmussen (centre of Excellence NAMEC). The authors would like to acknowledge Kristian Hagsted Rasmussen for his support in DRIE polymer etching.

## REFERENCES:

- [1] "Microfabricated drug delivery systems: Concepts to improve clinical benefit", F.J. Martin, C. Grove, Biomedical Microdevices 3:2 97-108 (2001).
- [2] "Bioadhesive microdevices with multiple reservoirs: a new platform for oral drug delivery", A. Ahmed, C. Bonner, T. A. Desai. Journal of Controlled Release 81, 291–306 (2002).
- [3] "Microfabrication technologies for oral drug delivery", S. Sant, S. L. Tao, O. Z. Fisher, Q. Xu, N. A. Peppas, A. Khademhosseini, Advanced Drug Delivery Reviews 64:6, 496-507 (2012).
- [4] "Optimized plasma-deposited fluorocarbon coating for dry release and passivation of thin SU-8 cantilevers" S. Keller, D. Haefliger, A. Boisen, Journal of Vacuum Science & Technology B, Vol. 25, 1903-1908 (2007).
- [5] "3D microstructuring of biodegradable polymers" J. Nagstrup, S. Keller, K. Almdal, A. Boisen, Microelectronic Engineering 88, 2342–2344 (2011).
- [6] "Mechanisms of dissolution of furosemide/PVP solid dispersions" C. Doherty and P. York, International Journal of Pharmaceutics, 34, pp. 197–205 (1987).

## CONTACT

Johan Nagstrup tel: +45 4525 5787 or email: [johan.nagstrup@nanotech.dtu.dk](mailto:johan.nagstrup@nanotech.dtu.dk)

# Appendix B



## 3D microstructuring of biodegradable polymers

Johan Nagstrup\*, Stephan Keller, Kristoffer Almdal, Anja Boisen

Department of Micro- and Nanotechnology, Technical University of Denmark, DTU Nanotech, Building 345 East, DK-2800 Kongens Lyngby, Denmark

### ARTICLE INFO

#### Article history:

Available online 13 December 2010

#### Keywords:

Biodegradable polymers  
Embossing  
Microstructures  
Spin coating  
Thick films

### ABSTRACT

Biopolymer films with a thickness of 100  $\mu\text{m}$  are prepared using spin coating technique with solutions consisting of 25 wt.% polycaprolactone or poly-L-lactide in dichloromethane. SU-8 stamps are fabricated using three photolithography steps. The stamps are used to emboss 3D microstructures in the biopolymer films. It is found that the best pattern transfer for the polycaprolactone films is achieved just below the melting point at 60  $^{\circ}\text{C}$ . For the poly-L-lactide films the best pattern transfer is achieved at 120  $^{\circ}\text{C}$ .

© 2010 Elsevier B.V. All rights reserved.

### 1. Introduction

Combining MEMS and NEMS with pharmaceutical research has led to propositions of a number of new medical solutions [1]. Examples of these are the use of micro tablets for enhanced drug delivery [2], and the fabrication of biodegradable polymer tubes for tissue engineering [3]. The next step in developing new medical solutions is to replace classical micro fabrication materials such as silicon and SU-8 with biodegradable polymers. In order to successfully do this, methods for fabricating 3D microstructures in biodegradable polymers need to be developed.

In this work, we present 3D microstructures fabricated in biodegradable polymer films with a thickness of 105  $\mu\text{m}$ . The polymer microstructures are fabricated using hot embossing. The fabricated structures have a shape like a well and could be used as drug containers following the concept presented by Ainslie and co-workers [2]. For the fabrication of the micro wells, thick films of biodegradable polymers in both polycaprolactone (PCL) and poly-L-lactide (PLLA) are fabricated. Both PCL and PLLA are approved by the food and drug administration (FDA) which makes them obvious candidates for biomedical applications. PCL and PLLA are new materials within the field of micro fabrication and previous work mainly revolves around mechanical property tests [4,5], degradation studies [6–8] and tissue engineering [3,7,8]. Food science is another area where biopolymers films are of interest [9].

### 2. General method

The technique used to microstructure PLLA and PCL films is hot embossing with a stack as shown in Fig. 1. It consists of a biopoly-

mer film on a silicon wafer and a SU-8 stamp on a silicon wafer. The stamp is pressed into the preheated substrate. Subsequently, substrate and stamp are cooled before separation.

### 3. Preparation of biopolymer films

For biopolymer thick film deposition by spin coating, PCL granulate from Sigma–Aldrich ( $M_n/(\text{kg}/\text{mol}) = 70\text{--}90$ ) and PLLA granulate from Nature Works LLC, 2002D are used. The biopolymer granulate is dissolved in dichloromethane (DCM) (25 wt.% polymer) facilitated by heating to 50  $^{\circ}\text{C}$ . The polymer solution is manually dispensed onto a silicon wafer followed by acceleration to the final spin-speed which is maintained for 50 s. The PCL films are baked on a hotplate (90  $^{\circ}\text{C}$ ; 1 h) to remove the solvent resulting in a flat and even film without bubbles. The PLLA films are degassed for 2 h before baking (220  $^{\circ}\text{C}$ ; 1 h) to avoid bubble formation. 220  $^{\circ}\text{C}$  is well above the melting point of PLLA which allow the polymer to reflow and to smoothen the surface.

The spin curves for both PCL and PLLA solutions are shown in Fig. 2. Polymer films are characterized by a profilometer and film thicknesses of 40–110  $\mu\text{m}$  are achieved. For the embossing experiments polymer films with a thickness of 100–110  $\mu\text{m}$  are used.

### 4. Stamp fabrication

The stamp for the hot embossing is fabricated in SU-8. The fabrication of the stamp is realized using a three step photolithography process. First, a 2  $\mu\text{m}$  thin SU-8 adhesion layer is spin coated and flood exposed with 250  $\text{mJ}/\text{cm}^2$ . The stamp structures are then defined with two subsequent thick SU-8 layers. A 40  $\mu\text{m}$  SU-8 layer is spincoated and softbaked for 2 h at 50  $^{\circ}\text{C}$ . The SU-8 is exposed with  $2 \times 250 \text{ mJ}/\text{cm}^2$  with a 30 s wait time and post-exposure-baked for 6 h at 50  $^{\circ}\text{C}$ . A second 65  $\mu\text{m}$  thick SU-8

\* Corresponding author.

E-mail address: [johan.nagstrup@nanotech.dtu.dk](mailto:johan.nagstrup@nanotech.dtu.dk) (J. Nagstrup).



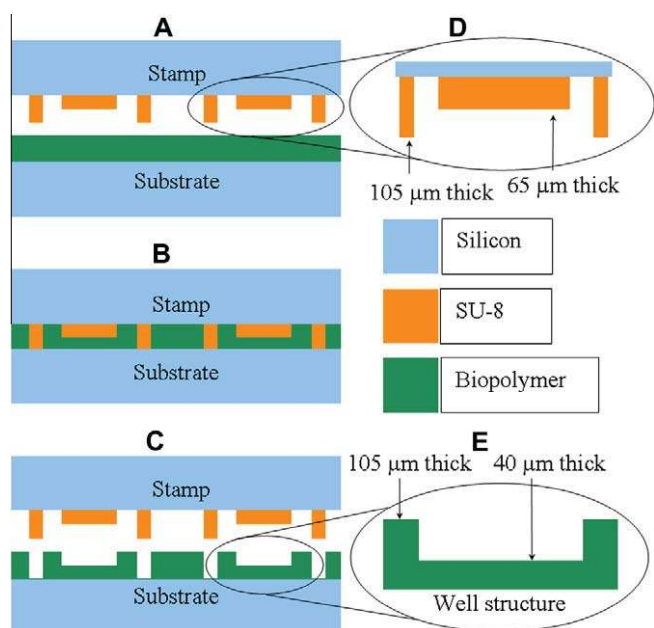


**Fig. 1.** Schematic of the hot embossing process. (A) Stamp and substrate are heated, (B) stamp pressed into substrate, (C) cooling followed by release, (D) cross sectional view of SU-8 structure and (E) cross sectional view of biopolymer well structure.

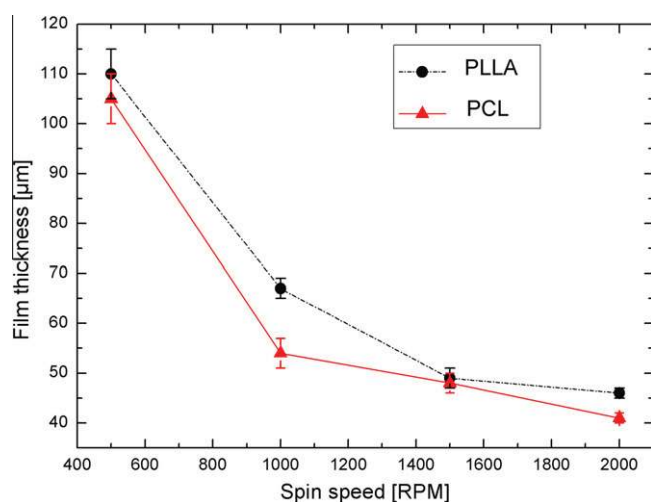


**Fig. 2.** Spin curves for PLLA and PCL solutions in DCM solvent. The weight percentage is 25% biopolymers to 75% DCM. The spin time is 50 s.

layer is spincoated and softbaked for 10 h at 50 °C, before it is exposed with  $2 \times 250 \text{ mJ/cm}^2$  and post-exposure-baked at 50 °C for 10 h. The SU-8 is developed in Propylene Glycol Methyl Ether Acetate (PGMEA) for 20 min.

The stamp consists of 16 square arrays with 400 inverse well structures as the one shown in Fig. 3. The outer ring is  $110 \pm 3 \mu\text{m}$  high with an inner diameter of 300  $\mu\text{m}$ . The inner disk is  $66 \pm 2 \mu\text{m}$  high with a diameter of 270  $\mu\text{m}$ .

## 5. Embossing experiments

Preliminary experiments showed that adhesion between stamp and PLLA is critical, as reuse of the stamp results in the SU-8 cracking and minor pieces breaking off the stamp. Coating the stamp with a hydrophobic FDTS anti-stiction layer [11] did not improve the release of the SU-8 stamp. Deposition of a 140 nm fluorocarbon

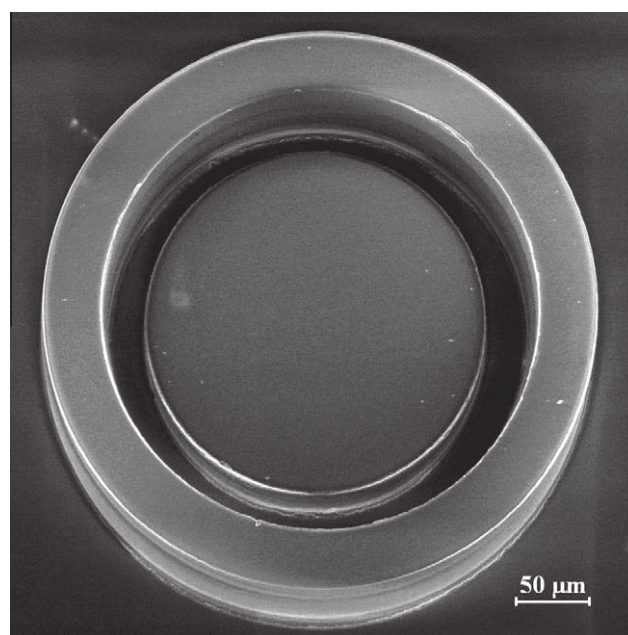


**Fig. 3.** Stamp structure shaped as an inverse well. The inner disk is 40  $\mu\text{m}$  high and the outer ring is 105  $\mu\text{m}$  high.

film on top of the biopolymer by plasma polymerization using a deep reactive ion etch device [12], results in a smooth separation of the stamp and biopolymer film, thus enhancing the durability of the stamps.

The embossing is performed with an EV Group 520 hot embosser capable of exerting a force of 15 kN. A series of experiments is conducted to optimize the pattern transfer from the SU-8 stamp into the PLLA and PCL films.

The hot embossing in PLLA is achieved by heating the substrate and stamp well above the glass transition temperature ( $T_g \sim 58 \text{ }^\circ\text{C}$  [10]). Force is then applied to press the stamp into the PLLA film. The sample is then cooled below  $T_g$  before the stamp is released from the PLLA. For the PLLA experiments, force and time is kept constant at 15 kN and 1 h respectively. The temperature is varied 80–140 °C with 20 °C intervals.

For the PCL, the hot embossing is carried out differently as  $T_g$  for PCL is  $\sim 60 \text{ }^\circ\text{C}$  [10]. The sample is heated just below the melting temperature at  $T_m = 65 \text{ }^\circ\text{C}$ , embossed and cooled to room temperature before the stamp is released.

Force and time are kept constant at 15 kN and 3 h respectively. Experiments are carried out at 25, 45, 55, 60, and 65 °C.

For characterization of the embossed structures the wall height is measured as this is the critical part of the well structure. The height of the walls should correspond to the height of the inner disk patterned in the second layer of SU-8 of the stamp, which is approximately 65–68  $\mu\text{m}$ .

## 6. Results and discussion

Successful embossing and easy stamp release are obtained for the PLLA film in the temperatures range 80–120 °C. At 140 °C, the PLLA film is very difficult to separate from the stamp. As a consequence, the stamp is partially destroyed with SU-8 structures remaining in the PLLA film. Fig. 4 shows a plot of the wall height versus the distance from the center of the wafer of embossed PLLA structures at 80, 100 and 120 °C and the corresponding stamp height. It is found that the thickness of the SU-8 layer is slightly thinner at the center of the wafer and increases towards the edge.

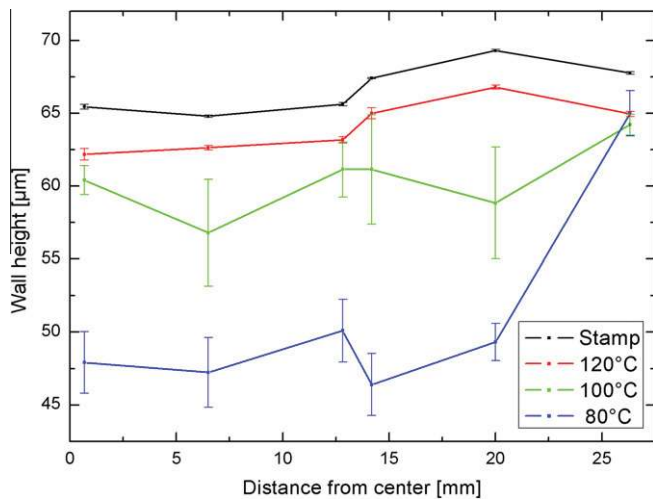


Fig. 4. Wall height of the embossed PLLA well structures as a function of the distance from the center of the wafer for three different embossing temperatures. The dashed line marks the nominal stamp height.

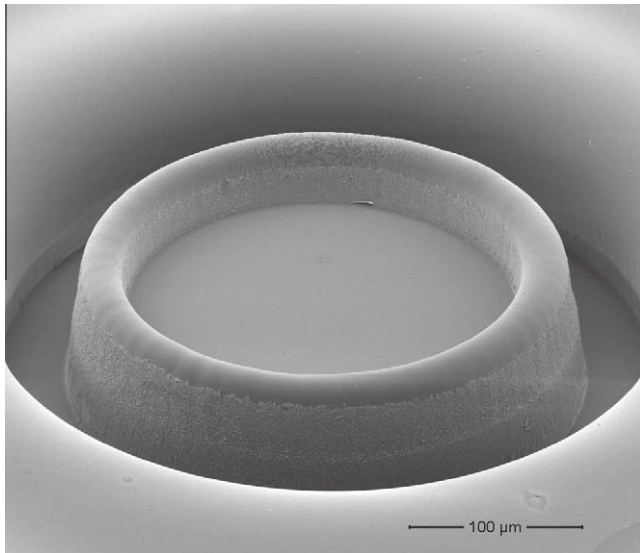


Fig. 5. SEM image of an embossed PLLA well structure. The well is 300 µm wide with 65 µm inner wall height.

Embossing at 80 and 100 °C yields a partial pattern transfer. It is seen that the contour of the embossing at 120 °C follows the contour of the stamp height with a high accuracy. This indicates a very good pattern transfer. The difference in height between the stamp and the 120 °C experiment could be caused by shrinkage in the

PLLA as it is cooled. Fig. 5 shows a SEM image of the well structure embossed in PLLA.

Embossing in PCL has proven more difficult than embossing in the PLLA films. For temperatures in the range from 25 to 45 °C, the pattern is not transferred and only minor indentation in the PCL polymer film is achieved. The experiments in the temperature range 55–60 °C show that it is possible to transfer the pattern from stamp to substrate. The results show that it is very important to control the temperature. At 55 °C pattern heights between 7 and 35 µm are obtained whereas film adhesion to the stamp occurs at 65 °C. This is probably due to the melting of the PCL film and strong adhesion to the stamp when it solidifies. 60 °C gives a good pattern transfer with pattern heights increasing from 65 µm at the center of the wafer to 68 µm at the edge of the wafer following the contour of the SU-8 stamp.

A residual biopolymer layer remain after the embossing, this layer can be removed with an oxygen plasma etch. The oxygen plasma etch will also remove the fluorocarbon layer used to enhance the durability of the stamps.

## 7. Conclusion

Biopolymer thick films in PCL and PLLA have successfully been deposited using spin coating. An SU-8 stamp has been fabricated and used for hot embossing in PCL and PLLA films. “The best pattern transfer in PLLA is achieved by embossing with a force of 15 kN for 1 h at a temperature of 120 °C”.

The PCL embossing experiments show that the embossing temperature is critical for a good pattern transfer and should be just below the melting point.

It was shown that it is possible to fabricate 3D microstructures in the FDA approved biopolymers, PCL and PLLA. The fabricated well structures in PCL and PLLA are suitable carriers for drugs and could be used as micro tablets.

## References

- [1] M. Staples, K. Daniel, M.J. Cima, R. Langer, *Pharmaceutical Research* 23 (5) (2006) 847–863.
- [2] K.M. Ainslie, R.D. Lowe, T.T. Beaudette, L. Petty, E.M. Bachelder, T.A. Desai, *Small* 5 (24) (2009) 2857–2863.
- [3] K. Seunarine, D.O. Meredith, M.O. Riehle, C.D.W. Wilkinson, N. Gadegaard, *Microelectronic Engineering* 85 (2008) 1350–1354.
- [4] M.F. Koenig, S.J. Huangt, *Polymer* 36 (9) (1995) 1877–1882.
- [5] N. Ogata, G. Jimenez, H. Kawai, T. Ogihara, *Journal of Polymer Science Part B: Polymer Physics* 35 (1997) 389–396.
- [6] D.R. Chen, J.Z. Bei, S.G. Wang, *Polymer Degradation Stability* 67 (2000) 455–459.
- [7] R.R.M. Bos, F.R. Rozema, G. Boering, A.J. Nijenhuis, A.J. Pennings, A.B. Verwey, P. Nieuwenhuis, H.W.B. Jansen, *Biomaterials* 12 (1991) 32–36.
- [8] H. Kweona, M.K. Yoob, I.K. Park, T.H. Kim, H.C. Lee, H. Lee, J. Oh, T. Akaike, C. Cho, *Biomaterials* 24 (2003) 801–808.
- [9] R.N. Tharanathan, *Trends in Food Science & Technology* 14 (2003) 71–78.
- [10] <http://biodeg.net/bioplasic.html>.
- [11] J. Moresco, C.H. Clausen, W. Svendsen, *Sensors and Actuators B* 145 (2010) 698–701.
- [12] S. Keller, D. Haefliger, A. Boisen, *Journal of Vacuum Science & Technology B* 25 (2007) 1903–1908.

## Appendix C

# Table of Polymers



## Polymers

Polymer	Biodegradable / inert	Solubility	Water soluble	Pharmaceutical used	Remarks
Aliphatic amine polymer	Inert		+	+	
Aliphatic polyesters	Biodegradable		Slightly soluble or insoluble	+	
Carboxymethylcellulose sodium		Insoluble in acetone, ethanol, ether, and toluene	+	+	
Carboxypolyethylene (carbomer)		Soluble in ethanol and glycerin	+	+	
Ethyl cellulose		Soluble in chloroform and alcohol	+	- (used in food products)	
Ethylhydroxyethylcellulose		Insoluble in acetone, ethanol, ether, toluene, and most organic solvents	+	+	
Eudragit® (polymethacrylates)	Biodegradable	Depends on the type	-	+	Different types, hence different properties
Hydroxypropylmethyl cellulose	Inert	Soluble in polar solvents. Insoluble in anhydrous alcohol, ether and chloroform.	Slowly soluble in cold water. Insoluble in hot water.		
Gelatin	Biodegradable	Soluble in polar solvents	Soluble in hot water	+	
Glyceryl monostearate	Biodegradable	Soluble in hot ethanol, ether, chloroform, acetone, oils	-	+	
Microcrystalline cellulose	Biodegradable	Slightly	-	+	

			soluble in 5% w/v sodium hydroxide solution				
Methyl cellulose			Insoluble in acetone, ethanol, ether, and toluene		Slowly soluble in water. Insoluble in hot water	+	
Pectinic acid	Biodegradable		Insoluble in ethanol and other organic solvents		+	+	
Poloxamer			Depends on the type		Depends on the type	+	Different types, hence different properties
Polydimethylsiloxane			Slightly soluble in ethanol		-	+	
Polyethylene glycol	Biodegradable		Soluble in methanol, benzene, dichloromethane, insoluble in diethyl ether hexane		+	+	
Poly (vinyl alcohol)			Slightly soluble in ethanol. Insoluble in organic solvents		+	+	
polyvinylpyrrolidone			Soluble in acids, chloroform, ethanol, and methanol		+	+	



## Appendix D

# PLLA datasheet

## For Fresh Food Packaging and Food Serviceware

Ingeo biopolymer 2003D, a NatureWorks LLC product, is a thermoplastic resin derived from annually renewable resources and is specifically designed for use in fresh food packaging and food serviceware applications. Ingeo biopolymer 2003D is a transparent general purpose extrusion grade that is used naturally or as part of a formulated blend. This is a high molecular weight biopolymer grade that processes easily on conventional extrusion equipment. Extruded roll stock is readily thermoformable. See table at right for properties.

Typical Material & Application Properties <sup>(1)</sup>		
Physical Properties	Ingeo 2003D	ASTM Method
Specific Gravity	1.24	D792
MFR, g/10 min (210°C, 2.16kg)	6	D1238
Clarity	Transparent	
Mechanical Properties		
Tensile Strength @ Break, psi (MPa)	7,700 (53)	D882
Tensile Yield Strength, psi (MPa)	8,700 (60)	D882
Tensile Modulus, kpsi (GPa)	500 (3.5)	D882
Tensile Elongation, %	6.0	D882
Notched Izod Impact, ft-lb/in (J/m)	0.3 (16)	D256
Shrinkage is similar to PET <sup>(2)</sup>		
Heat Distortion Temperature (°C)	55	E2092

(1) Typical properties; not to be construed as specifications.

(2) Refer to Ingeo biopolymer Sheet Extrusion Processing Guide

### Applications

Potential applications for Ingeo biopolymer 2003D include:

- Dairy containers
- Food serviceware
- Transparent food containers
- Hinged-ware
- Cold drink cups

### Processing Information

Ingeo biopolymer 2003D is easily processed on conventional extrusion equipment. The material is stable in the molten state, provided that the drying procedures are followed. More detailed recommendations and processing requirements are found in the Ingeo biopolymer sheet extrusion processing guide, the purging technical data sheet, and the drying and crystallizing processing guide, all of which can be found at [www.natureworkslc.com](http://www.natureworkslc.com).

### Machine Configuration

Ingeo biopolymer 2003D will process on conventional extrusion machinery with the following equipment: General purpose screw with L/D ratios from 24:1 to 32:1 and compression ratio of 2.5:1 to 3:1. Smooth barrels are recommended.

### Process Details

#### Startup and Shutdown

Ingeo biopolymer 2003D is not compatible with a wide variety of commodity resins, and special purging sequences should be followed:

1. Clean extruder and bring temperatures to steady state with low viscosity, general purpose polystyrene or polypropylene.
2. Vacuum out hopper system to avoid contamination.
3. Introduce Ingeo biopolymers into the extruder at the operating conditions used in Step 1.
4. Once Ingeo biopolymer has purged, reduce barrel temperatures to desired set points.
5. At shutdown, purge machine with high viscosity polystyrene or polypropylene.

be exposed to atmospheric conditions after drying. Keep the package sealed until ready to use and promptly reseal any unused material. Pellets that have been exposed to the atmosphere for extended time periods will require additional drying time. Amorphous regrind must be crystallized prior to

Processing Temperature Profile <sup>(1)</sup>		
Melt Temperature	410°F	210°C
Feed Throat	113°F	45°C
Feed Temperature	355°F	180°C
Compression Section	375°F	190°C
Metering Section	390°F	200°C
Adapter	390°F	200°C
Die	375°F	190°C
Screw Speed	20-100 rpm	

(1) These are starting points and may need to be optimized.

drying, to assure efficient and effective drying.

### Drying

In-line drying may be required. A moisture content of less than 0.025% (250 ppm) is recommended to prevent viscosity degradation. Typical drying conditions for crystallized granules are 2 hours at 195°F (90°C) or to a dew point of -40°F (-40°C), airflow rate of greater than 0.5 cfm/lbs per hour of resin throughput. The resin should not

## Compostability

Composting is a method of waste disposal that allows organic materials to be recycled into a product that can be used as a valuable soil amendment. Ingeo biopolymer is made of polylactic acid, a repeating chain of lactic acid, which undergoes a 2-step degradation process. First, the moisture and heat in the compost pile attack the polymer chains and split them apart, creating smaller polymers, and finally, lactic acid. Microorganisms in compost and soil consume the smaller polymer fragments and lactic acid as nutrients. Since lactic acid is widely found in nature, a large number of organisms metabolize lactic acid. At a minimum, fungi and bacteria participate in this degradation process. The end result of the process is carbon dioxide, water and also humus, a soil nutrient. This degradation process is temperature and humidity dependent. Regulatory guidelines and standards for composting revolve around four basic criteria: Material Characteristics, Biodegradation, Disintegration, and Ecotoxicity. Description of the requirements of these testing can be found in the appropriate geographical area: DIN V 54900-1 (Germany), EN 13432 (EU), ASTM D 6400 (USA), GreenPla (Japan). This grade of Ingeo biopolymer meets the requirements of these four standards with limitation of maximum thickness 3.2mm.

## Food Packaging Status

### U.S. Status

On January 3, 2002 FCN 000178 submitted by NatureWorks LLC to FDA became effective. This effective notification is part of list currently maintained on FDA's website at

<http://www.cfsan.fda.gov/~dms/opa-fcn.html>

This grade of Ingeo biopolymer may therefore be used in food packaging materials and, as such, is a permitted

component of such materials pursuant to section 201(s) of the Federal, Drug, and Cosmetic Act, and Parts 182, 184, and 186 of the Food Additive Regulations. All additives and adjuncts contained in the referenced Ingeo biopolymer formulation meet the applicable sections of the Federal Food, Drug, and Cosmetic Act. The finished polymer is approved for all food types and B-H use conditions. We urge all of our customers to perform GMP (Good Manufacturing Procedures) when constructing a package so that it is suitable for the end use. Again, for any application, should you need further clarification, please do not hesitate to contact NatureWorks LLC.

### European Status

This grade of Ingeo biopolymer complies with Commission Directive 2002/72/EC as amended by 2004/19/EC, 2005/79/EC, 2007/19/EC, 2008/39/EC, and 2009/975/EC. No SML's for the above referenced grade exist in Commission Directive 2002/72/EC or as amended by 2004/19/EC, 2005/79/EC, 2007/19/EC, 2008/39/EC, 2009/975/EC. NatureWorks LLC would like to draw your attention to the fact that the EU-Directive 2002/72/EC, which applies to all EU-Member States, includes a limit of 10 mg/dm<sup>2</sup> of the overall migration from finished plastic articles into food. In accordance with EU-Directive 2002/72/EC the migration should be measured on finished articles placed into contact with the foodstuff or appropriate food simulants for a period and at a temperature which are chosen by reference to the contact conditions in actual use, according to the rules laid down in EU-Directives 93/8/EEC (amending 82/711/EEC) and 85/572/EEC

Please note that it is the responsibility of both the manufacturers of finished food contact articles as well as the industrial food packers to make sure that these articles in their actual use are in compliance with the imposed

specific and overall migration requirements.

This grade as supplied meets European Parliament and Council Directive 94/62/EC of 20 December 1994 on packaging and packaging waste heavy metal content as described in Article 11. It is recoverable in the form of material recycling, energy recovery, composting, and biodegradable per Annex II point 3, subject to the standards of the local community. Again, for any application, should you need further clarification, please do not hesitate to contact NatureWorks LLC.

## Bulk Storage Recommendations

The resin silos recommended and used by NatureWorks LLC are designed to maintain dry air in the silo and to be isolated from the outside air. This design would be in contrast to an open, vented to atmosphere system that we understand to be a typical polystyrene resin silo. Key features that are added to a typical (example: polystyrene) resin silo to achieve this objective include a cyclone and rotary valve loading system and some pressure vessel relief valves. The dry air put to the system is sized to the resin flow rate out of the silo. Not too much dry air would be needed and there may be excess instrument air (-30°F dew point) available in the plant to meet the needs for dry air. Our estimate is 10 scfm for a 20,000 lb/hr rate resin usage. Typically, resin manufacturers specify aluminum or stainless steel silos for their own use and avoid epoxy-lined steel

## Safety and Handling Considerations

Material Safety Data (MSD) sheets for Ingeo biopolymers are available from NatureWorks LLC. MSD sheets are provided to help customers satisfy their own handling, safety, and disposal needs, and those that may be required by locally applicable health and safety regulations, such as OSHA (U.S.A.), MAK (Germany), or WHMIS (Canada). MSD sheets are updated regularly; therefore, please request and review the most current MSD sheets before handling or using any product.

The following comments apply only to Ingeo biopolymers; additives and processing aids used in fabrication and other materials used in finishing steps have their own safe-use profile and must be investigated separately.

## Hazards and Handling Precautions

Ingeo biopolymers have a very low degree of toxicity and, under normal conditions of use, should pose no unusual problems from incidental ingestion, or eye and skin contact. However, caution is advised when handling, storing, using, or disposing of these resins, and good housekeeping and controlling of dusts are necessary for safe handling of product. Workers should be protected from the possibility of contact with molten resin during fabrication. Handling and fabrication of resins can result in the generation of vapors and dusts that may cause irritation to eyes and the upper respiratory tract. In dusty atmospheres, use an approved dust respirator. Pellets or beads may present a slipping hazard. Good general ventilation of the polymer processing area is recommended. At temperatures exceeding the polymer melt temperature (typically 170°C), polymer can release fumes, which may contain fragments of the polymer, creating a potential to irritate eyes and mucous membranes. Good general ventilation should be sufficient for most conditions.

Local exhaust ventilation is recommended for melt operations. Use safety glasses if there is a potential for exposure to particles which could cause mechanical injury to the eye. If vapor exposure causes eye discomfort, use a full-face respirator. No other precautions other than clean, body-covering clothing should be needed for handling Ingeo biopolymers. Use gloves with insulation for thermal protection when exposure to the melt is localized.

## Combustibility

Ingeo biopolymers will burn. Clear to white smoke is produced when product burns. Toxic fumes are released under conditions of incomplete combustion. Do not permit dust to accumulate. Dust layers can be ignited by spontaneous combustion or other ignition sources. When suspended in air, dust can pose an explosion hazard. Firefighters should wear positive-pressure, self-contained breathing apparatuses and full protective equipment. Water or water fog is the preferred extinguishing medium. Foam, alcohol-resistant foam, carbon dioxide or dry chemicals may also be used. Soak thoroughly with water to cool and prevent re-ignition.

## Disposal

DO NOT DUMP INTO ANY SEWERS, ON THE GROUND, OR INTO ANY BODY OF WATER. For unused or uncontaminated material, the preferred options include recycling into the process or sending to an industrial composting facility, if available; otherwise, send to an incinerator or other thermal destruction device. For used or contaminated material, the disposal options remain the same, although additional evaluation is required. (For example, in the U.S.A., see 40 CFR, Part 261, "Identification and Listing of Hazardous Waste.") All disposal methods must be in compliance with Federal, State/Provincial, and local laws and regulations.

## Environmental Concerns

Generally speaking, lost pellets are not a problem in the environment except under unusual circumstances when they enter the marine environment. They are benign in terms of their physical environmental impact, but if ingested by waterfowl or aquatic life, they may mechanically cause adverse effects. Spills should be minimized, and they should be cleaned up when they happen. Plastics should not be discarded into the ocean or any other body of water.

## Product Stewardship

NatureWorks LLC has a fundamental duty to all those that make and use our products, and for the environment in which we live. This duty is the basis for our Product Stewardship philosophy, by which we assess the health and environmental information on our products and their intended use, then take appropriate steps to protect the environment and the health of our employees and the public.

## Customer Notice

NatureWorks LLC encourages its customers and potential users of its products to review their applications for such products from the standpoint of human health and environmental quality. To help ensure our products are not used in ways for which they were not intended or tested, our personnel will assist customers in dealing with ecological and product safety considerations. Your sales representative can arrange the proper contacts. NatureWorks LLC literature, including Material Safety Data sheets, should be consulted prior to the use of the company's products. These are available from your NatureWorks LLC representative.

**NOTICE:** No freedom from any patent owned by NatureWorks LLC or others is to be inferred. Because use conditions and applicable laws may differ from one location to another and may change with time, Customer is responsible for determining whether products and the information in this document are appropriate for Customer's use and for ensuring that Customer's workplace and disposal practices are in compliance with applicable laws and other governmental enactments. NatureWorks LLC assumes no obligation or liability for the information in this document. **NO WARRANTIES ARE GIVEN; ALL IMPLIED WARRANTIES OF MERCHANTABILITY OR FITNESS FOR A PARTICULAR USE ARE EXPRESSLY EXCLUDED.**

**NOTICE REGARDING PROHIBITED USE RESTRICTIONS:** NatureWorks LLC does not recommend any of its products, including samples, for use as: Components of, or packaging for, tobacco products; Components of products where the end product is intended for human or animal consumption; In any application that is intended for any internal contact with human body fluids or body tissues; As a critical component in any medical device that supports or sustains human life; In any product that is designed specifically for ingestion or internal use by pregnant women; and in any application designed specifically to promote or interfere with human reproduction.

For additional information please contact NatureWorks via our [website](#) on the tab called [FAQ's](#) or by clicking [here](#).



15305 Minnetonka Blvd., Minnetonka, MN 55345



## Appendix E

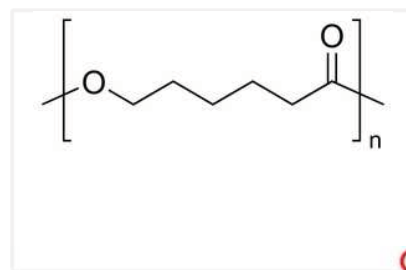
# PCL datasheet

Denmark Home 440744 - Polycaprolactone



440744 ALDRICH

## Polycaprolactone

M<sub>n</sub> 70,000-90,000 by GPC
[DOWNLOAD MSDS \(PDF\)](#)
Synonym: **2-Oxepanone homopolymer, 6-Caprolactone polymer**CAS Number **24980-41-4** | Linear Formula (C<sub>6</sub>H<sub>10</sub>O<sub>2</sub>)<sub>n</sub>
[POPULAR DOCUMENTS: SPECIFICATION SHEET \(PDF\) | FTIR \(PDF\)](#)


### Properties

Related Categories	<a href="#">Biodegradable Polymers</a> , <a href="#">Caprolactones</a> , <a href="#">Materials Science</a> , <a href="#">Polymer Science</a> , <a href="#">PolymersMore...</a>
form	pellets (~3 mm)
mol wt	M <sub>n</sub> 70,000-90,000 by GPC
total impurities	<1.0% water
mp	60 °C(lit.)
density	1.145 g/mL at 25 °C
M <sub>w</sub> /M <sub>n</sub>	<2

### Description

#### Features and Benefits

Biodegradable polymer

Non-toxic, biodegradable in soil, broad miscibility, mechanical compatibility with many polymers and good adhesion to a broad spectrum of substrates.

#### Packaging

250, 500 g in poly bottle

5 g in glass bottle

#### Application

Extrusion aid, die lubricant, mold release, pigment and filler dispersion aid and polyester segments in urethanes and block polyesters.

### Price and Availability

SKU-Pack Size	Availability	Price (EUR/DKK)	Quantity
440744-5G	Estimated Delivery 19.12.2012 - <a href="#">FROM</a>	<del>34.40</del> 223.91	<input type="text" value="0"/>
440744-250G	Estimated Delivery 19.12.2012 - <a href="#">FROM</a>	<del>408.50</del> 781.20	<input type="text" value="0"/>
440744-500G	Estimated Delivery 19.12.2012 - <a href="#">FROM</a>	<del>200.50</del> 1,443.59	<input type="text" value="0"/>

[Bulk orders?](#)


### Documents

[Bulk Quote-Order Product](#)  
[MSDS](#)  
[Specification Sheet](#)

### Safety Information

Personal Protective Equipment	<a href="#">Eyeshields, Gloves, type N95 (US), type P1 (EN143) respirator filter</a>
WGK Germany	3

### Certificate of Analysis

Enter Lot No.  Ser 

### Certificate of Origin

Enter Lot No.  Ser

## Appendix F

### SU-8 containers

**Project:** Fabrication of SU-8 micro-containers  
**Operator:** Johan  
**Last revision:** 01.02.2010  
**Substrates:** Silicon <100>, 100mm, 525µm, single side  
**Goal:** Initial test batch

Step N°	Description	Equipment	Program/Parameters	Target	Actual	Remarks
<b>1 WAFER PRE-CLEANING</b>						
1.1	Stock out					
1.2a	C4F8-passivation	Z2/ASE	dry_tef2 (120sccm, 300W, 0W, 5mTorr, 60s)			
1.2b	C4F8-passivation	Z2/ASE	wet_tef2 (120sccm, 350W, 0W, 60mTorr, 60s)			Lidt dårligere vedhæftning end dry
<b>2 SU-8 FIRST LAYER SPINNING</b>						
2.1a	SU-8 spin-coating	Z3/KS Spinner	1000rpm, 30s, 200rpm/s; 3000 rpm, 120s, 400rpm/s	34 µm		SU-8 2075; 6s; 42psi; Gyrset
2.1b	SU-8 spin-coating	Z3/KS Spinner	1000rpm, 30s, 200rpm/s; 5000 rpm, 120s, 500rpm/s	20 µm		SU-8 2075; 6s; 42psi; Gyrset
2.2a	SU-8 soft-bake	Z3/Hotplate	2h, 50°C, 2°C/min			
2.2b	SU-8 soft-bake	Z3/Hotplate	1h, 50°C, 2°C/min			
<b>3 SU-8 FIRST LAYER PHOTOLITHOGRAPHY</b>						
3.1a	SU-8 exposure	Z3/KS Aligner	4x250 mJ/cm2; soft contact			
3.1b	SU-8 exposure	Z3/KS Aligner	2x250 mJ/cm2; soft contact			
3.2a	Post-exposure bake	Z3/Hotplate	6h, 50°C, 2°C/min			
3.2b	Post-exposure bake	Z3/Hotplate	4h, 50°C, 2°C/min			
<b>4 SU-8 SECOND LAYER SPINNING</b>						
4.1a	SU-8 spin-coating	Z3/KS Spinner	1000rpm, 30s, 100rpm/s; 2000 rpm, 60s, 100rpm/s	65 µm		SU-8 2075; 6s; 42psi; Gyrset
4.1b	SU-8 spin-coating	Z3/KS Spinner	300rpm, 30s, 100rpm/s; 600 rpm, 60s, 100rpm/s	200 µm		SU-8 2075; 8s; 42psi; Gyrset
4.2	SU-8 soft-bake	Z3/Hotplate2	10h, 50°C, 2°C/min			over night
<b>5 SU-8 SECOND LAYER PHOTOLITHOGRAPHY</b>						
5.1a	SU-8 exposure	Z3/KS Aligner	4x250 mJ/cm2; soft contact			
5.1b	SU-8 exposure	Z3/KS Aligner	4x250mJ/cm2, sub 900µm, al 150µm, exp 100µm			GlobalWEC, Prox;
5.2	Post-exposure bake	Z3/Hotplate2	10h, 50°C, 2°C/min			over night
5.3a	SU-8 development	Z3/Developer	5min FIRST, 5min FINAL			PGMEA
5.3b	SU-8 development	Z3/Developer	20min FIRST, 20min FINAL			PGMEA
5.4	Rinse	Z3/Developer	Isopropanol, Air			
5.5	Thickness	Z9/Dektak				
5.6	SEM inspection	SEM-FEI				

**Remarks:** 1.2a C4F8-passivation Drug01/drug02 Coated with fluorocarbon  
 4.1a SU-8 spin-coating Drug02/drug04 Nominal thickness 65 µm  
 4.1b SU-8 spin-coating Drug01/drug03 Nominal thickness 200 µm

## Appendix G

### SU-8 stamps

**Project:** Fabrication of SU-8 stamps / containers

**Operator:** Johan Nagstrup

**Group:** Nanoprobes, DTU Nanotech

**Last revision:** 03.10.2011

**Substrates:** Silicon <100>, 100mm, 525µm, single side, amount=8

**Batch:** SU-8 stamp test, batch #2

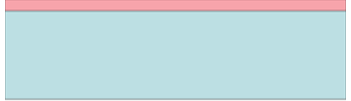


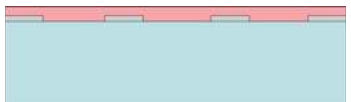
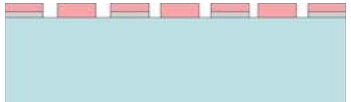
Step N	Description	Equipment	Program/Parameters	Target	Actual	Remarks	Date
0.1	Wafer bake out	Oven	120 °C, 1 h				
<b>1 Optional thin SU-8</b>							
1.1	SU-8 spin-coating	KS Spinner	1500rpm, 30 s, 5000 rpm/s	2 µm		SU-8 2002	
1.2	SU-8 soft-bake	Hotplate	2 mins, 50°C				
1.3	SU-8 exposure	KS Aligner	2*250mJ/cm2, Flood exposure				
	SU-8 exposure bake	Hotplate	1h, 50°C, 2°C/min				
<b>2 SU-8 FIRST LAYER SPINNING</b>							
2.1	SU-8 spin-coating	Z3/KS Spinner	1000rpm, 30s, 200rpm/s; 3000 rpm, 120s, 400rpm/s	34 µm		SU-8 2075; 6s; 42psi; Gyrset	
2.2	SU-8 soft-bake	Z3/Hotplate2	2h, 50°C, 2°C/min				
<b>3 SU-8 FIRST LAYER PHOTOLITHOGRAPHY</b>							
3.1a	SU-8 exposure	Z3/KS Aligner	2x250 mJ/cm2; soft contact				
3.2a	Post-exposure bake	Z3/Hotplate2	6h, 50°C, 2°C/min			over night	
<b>4 SU-8 SECOND LAYER SPINNING</b>							
4.1	SU-8 spin-coating	Z3/KS Spinner	1000rpm, 30s, 100rpm/s; 2000 rpm, 60s, 100rpm/s	65 µm		SU-8 2075; 6s; 42psi; Gyrset	
4.2	SU-8 soft-bake	Z3/Hotplate	10h, 50°C, 2°C/min			over night	
<b>5 SU-8 SECOND LAYER PHOTOLITHOGRAPHY</b>							
5.1a	SU-8 exposure	Z3/KS Aligner	2x250 mJ/cm2; soft contact				
5.2	Post-exposure bake	Z3/Hotplate	10h, 50°C, 2°C/min			over night	
5.3a	SU-8 development	Z3/Developer	10min FIRST, 10min FINAL			PGMEA	
5.4	Rinse	Z3/Developer	Isopropanol, Air				
<b>6 SU-8 stamp prep</b>							
6.1	SU-8 bake	120 °C oven	30 mins			Prep. Stamp for imprinting	
<b>7 Stamp characterization</b>							
7.1	Thickness	Z9/Dektak					
7.2	SEM inspection	SEM-FEI					

Notes: Step 1 is performed for half of the wafers. The purpose is to investigate if it is favorable to have pure SU-8 or SU-8 and silicon surfaces in the imprinting process. First mask used is called bottom container, second mask used is called container walls

## Appendix H

# Silicon stamps



Step	Process	Parameters/Machine	Illustration
1.1	PR for liftoff  SSE Spinner	Recipe: AZ4562-4inch-9.5um  PR: AZ4562 Thickness: 10 $\mu\text{m}$	 ■ Si
1.2	UV exposure KS aligner	Time: 2x50 s (30 s wait) Hard contact	
1.3	Developer Bond to a disk	AZ351b Time: 5 min.	-
1.4	Al deposition  50 nm	Wordentec	 ■ Al ■ Resist ■ Si
1.5	PR removal/liftoff  Acetone + ultrasound		 ■ Al ■ Si
1.6	PR for masking  SSE Spinner	Recipe: AZ4562-4inch-9.5um  PR: AZ4562 Thickness: 10 $\mu\text{m}$	 ■ Al ■ Resist ■ Si
1.7	UV exposure  KS aligner	Time: 2x50 s (30 s wait)  Hard contact	 ■ Al ■ Resist ■ Si

2.1	ASE/pegasus etch  Etch depth: 60-200 $\mu\text{m}$	Deep trench	
2.2	PR removal  Plasma Asher	O <sub>2</sub> flow: 300 mL/min  N <sub>2</sub> flow: 50 mL/min Time: 30 min Power 1000W	
2.3	ASE/pegasus etch  Etch depth: 60 $\mu\text{m}$	Deep trench	
2.4	Al removal H <sub>2</sub> O:H <sub>3</sub> PO <sub>4</sub> 1:2  Etch rate 100nm/min	50 °C  1 min etch time	
2.5	Oxidation wet1100 temp: 1100°C	Bohr-drive-in 50 min Thickness 600nm	
2.6	Oxide removal BHF etch rate : 75 nm/min	HF-dip 10 mins	
2.5	MVD coating		



## Appendix I

# Nikkel stamps

## Process for fabrication of Ni stamp

Johan Nagstrup

Group: Nanoprobes

Batch# 3d biopolymer

Revision nr: Rev #1

Wafer choise: Cheapest available

Esben Krirk Mikkelsen s082641

Saro Ulver Hierwagen s080297

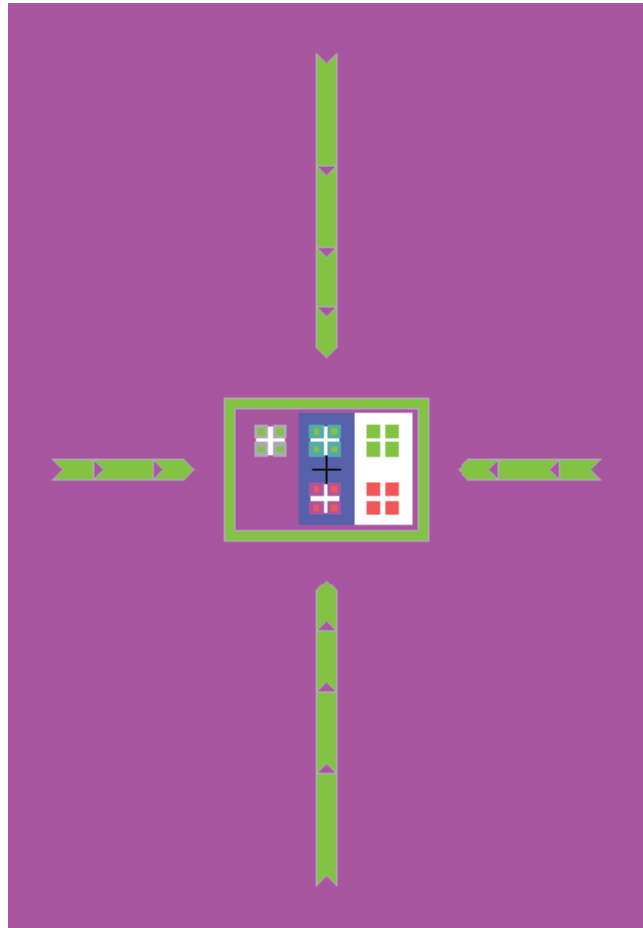


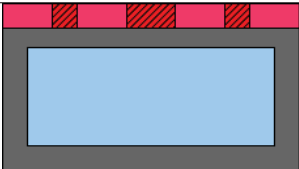
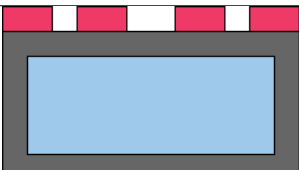
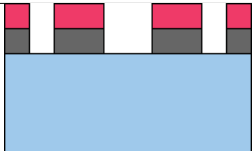
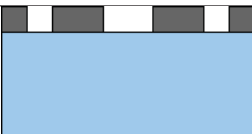
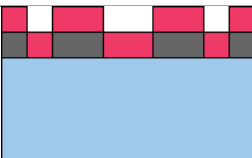


Figure 1: Alignment marks

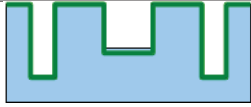
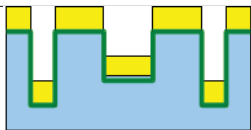
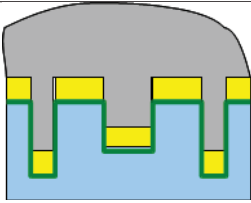
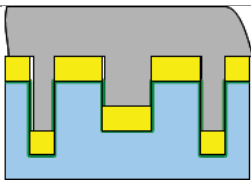
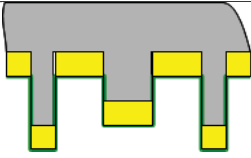
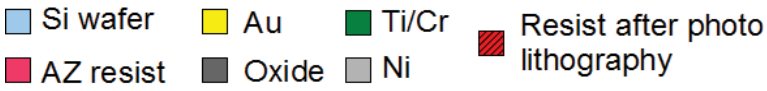
Step	Process	Parameter	Graphic	Note
1	Wet oxide	Bohr drive in wet oxide 1100 °C 500nm - 50 min		6 wafers
1.1	Oxide measurement	Filmtek Profileometer 5 points measurement		1 wafers
2	Spin coating AZ resist	1.5µm Track 1		HMDS 6 wafers
3	Positive photo lithography	Hard contact 3-5 sec		Mask: Container bottom 6 wafers
4	Develop	60sec		6 wafers
5	BHF	10min etch rate 75 nm/min. zero tolerance.		6 wafers
5.1	Dektak	Oxide thickness		1 wafers
6	Resist remove	Acetone Rough 1min Fine 1min		6 wafers
7	Spin coating AZ resist	1.5 µm Track 1		HMDS

■ Si wafer    ■ Au    ■ Ti/Cr    ▨ Resist after photo lithography  
■ AZ resist    ■ Oxide    ■ Ni

Step	Process	Parameter	Graphic	Note
8	Positive photo lithography	5-7 sec		Mask: Container walls
9	Develop	60 sec		2 wafers
10	Etch	Pegasus/Ase $20 \mu\text{m} \pm 2\mu\text{m}$		Mask: $1.5 \mu\text{m}$ resist
10.1	Dektak	Etch depth		1 wafers
11	Remove Resist plasma asher	Acetone		Mask: 100 nm Al
12	Etch	Pegasus $80 \mu\text{m} \pm 2\mu\text{m}$		
12.1	Dektak	Etch depth		1 wafers
13	Wet etch Oxide			Repeat step 8-12 with the rest of the wafers
14	SEM			1 wafer

Si wafer   
 Au   
 Ti/Cr   
 Resist after photo lithography  
 Oxide   
 Ni



Step	Process	Parameter	Graphic	Note
15	Optinoal oxide following SEM inspection	RCA cleaning WET oxide 1100 60 min		
16	Deposit Ti/Cr	Lesker		1 wafer Good coverage needed
17	Deposit Au	Lesker		Good coverage needed
18	Electro plating Ni			Process optimization with Mikkel Mar (step 18-20)
19	Rub down top of Ni			
20	Remove Si with KOH			
				



## Appendix J

# Stencil mask, CO2-laser parameters

Process parameters used in the fabrication of transparent foil stencil masks:

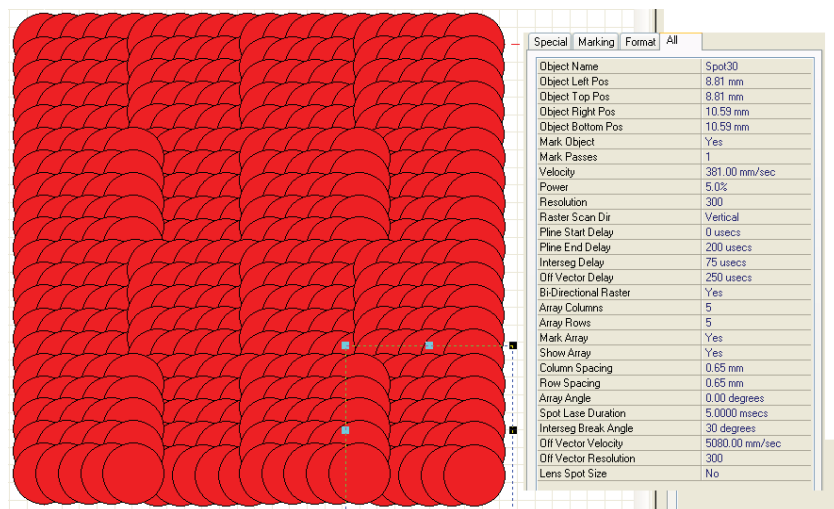


Figure J.1: For the design of the stencil, the spot tool is used along with the parameters shown to the left of the spots.